NASA Technical Memorandum 112208

Revised Simulation Model of the Control System, Displays, and Propulsion System for an ASTOVL Lift Fan Aircraft

James A. Franklin, Ames Research Center, Moffett Field, California

October 1997

National Aeronautics and
Space Administration

Ames Research Center
Moffett Field, California 94035-1000

Nomenclature

b	wing span, ft
c	mean aerodynamic chord, ft
C_D	drag coefficient
C_L	lift coefficient
C_{l_β}	rolling moment coefficient due to sideslip, rad^{-1}
C_{l_p}	rolling moment coefficient due to roll rate
C_{l_r}	rolling moment coefficient due to yaw rate
$C_{m_{GE}}$	pitching moment coefficient due to ground effect
C_{m_o}	pitching moment coefficient at zero angle of attack
C_{m_q}	pitching moment coefficient due to pitch rate
$C_m(\alpha)$	pitching moment coefficient as a function of angle of attack
C_{n_β}	yawing moment coefficient due to sideslip, rad^{-1}
C_{n_p}	yawing moment coefficient due to roll rate
C_{n_r}	yawing moment coefficient due to yaw rate
D	aerodynamic drag, lb
DLJEI	jet-induced lift factor due to lift fan and lift nozzles
DPMJEI	jet-induced pitching moment factor due to lift fan and lift nozzles
d_e	equivalent jet diameter, ft
F_{AI_X}	auxiliary inlet force along x body axis, lb
F_{AI_y}	auxiliary inlet force along y body axis, lb
F_{AI_Z}	auxiliary inlet force along z body axis, lb
F_{CN_x}	cruise nozzle force along x body axis, lb
F_{CN_z}	cruise nozzle force along z body axis, lb
F_{EX}	total propulsion system force along x body axis, lb
F_{EY}	total propulsion system force along y body axis, lb
F_{EZ}	total propulsion system force along z body axis, lb
F_{LF_x}	lift fan force along x body axis, lb
F_{LFIx}	lift fan inlet force along x body axis, lb
F_{LFIy}	lift fan inlet force along y body axis, lb
F_{LFIz}	lift fan inlet force along z body axis, lb
F_{LLN_x}	left lift nozzle force along x body axis, lb
F_{LN_x}	lift nozzle force along x body axis, lb
F_{LN_y}	lift nozzle force along y body axis, lb
F_{LN_z}	lift nozzle force along z body axis, lb
F_{PI_X}	primary inlet force along x body axis, lb
F_{PIy}	primary inlet force along y body axis, lb
F_{PI_Z}	primary inlet force along z body axis, lb
F_{RLN_X}	right lift nozzle force along x body axis, lb
g	acceleration due to gravity, ft/sec^2
h	altitude, ft
$\dot{h}$	vertical velocity, ft/sec
I_x	roll moment of inertia, $slug\text{-}ft^2$
I_y	pitch moment of inertia, $slug\text{-}ft^2$
I_z	yaw moment of inertia, $slug\text{-}ft^2$
I_{xz}	cross product of inertia, $slug\text{-}ft^2$
K	control system gain
K_{AUG}	lift fan augmentation ratio
K_{T_u}, K_{TL}	upper and lower thrust scaling for throttle
$K_{\gamma u}$, $K_{\gamma L}$	upper and lower flightpath command scaling
L	aerodynamic lift, lb
L_{CN}	cruise nozzle moment arm, ft
LFI	lift fan inlet
L_{LF}	lift fan moment arm, ft
L_{LN}	lift nozzle moment arm, ft
m	aircraft mass, slugs
$\dot{m}_{AI}$	auxiliary inlet mass flow rate, lbm/sec
$\dot{m}_e$	engine mass flow rate, slugs/sec
$\dot{m}_{LF}$	lift fan mass flow rate, lbm/sec

$\dot{m}_{PI}$	primary inlet mass flow rate, lbm/sec
PLA	power lever angle thrust command, percent of maximum
PLAp	past value of PLA, percent of maximum
p_B	body axis roll rate, rad/sec
q_B	body axis pitch rate, rad/sec
$\bar{q}$	dynamic pressure, lb/ft^2
r_B	body axis yaw rate, rad/sec
S	wing area, ft^2
T_{CN}	cruise nozzle thrust, lb
$T_{CN_{CMD}}$	cruise nozzle thrust command, lb
T_{EL}	propulsion system rolling moment, ft-lb
T_{EM}	propulsion system pitching moment, ft-lb
T_{EN}	propulsion system yawing moment, ft-lb
T_{LF}	lift fan thrust, lb
T_{LF_F}	lift fan thrust due to inlet guide vane authority, lb
T_{LF_S}	lift fan thrust due to fan rotational speed, lb
$T_{LF_{CMD}}$	lift fan thrust command, lb
T_{LLN}	left lift nozzle thrust, lb
$T_{LLN_{CMD}}$	left lift nozzle thrust command, lb
T_{RLN}	right lift nozzle thrust, lb
$T_{RLN_{CMD}}$	right lift nozzle thrust command, lb
T_T	core engine total thrust, lb
$T_{T_{CMD}}$	core engine total thrust command, lb
U_B	aircraft velocity along x body axis, ft/sec
V	airspeed, ft/sec
V_{af}	filtered airspeed, ft/sec
V_B, V_y	aircraft velocity along y body axis, ft/sec
V_T	true airspeed, ft/sec
V_x, V_j	ground speed along x axis, ft/sec
W	aircraft weight, lb
W_B	aircraft velocity along z body axis, ft/sec
x_{CN}	longitudinal distance from cruise nozzle to aircraft center of gravity, ft
x_{LF}	longitudinal distance from lift fan nozzle to aircraft center of gravity, ft
x_{LN}	longitudinal distance from lift nozzle to aircraft center of gravity, ft
y_{LN}	lateral distance from lift nozzle to aircraft center of gravity, ft
z_{CN}	vertical distance from cruise nozzle to aircraft center of gravity, ft
z_{LF}	vertical distance from lift fan nozzle to aircraft center of gravity, ft
z_{LN}	vertical distance from lift nozzle to aircraft center of gravity, ft
α	angle of attack, rad
α_c	commanded angle of attack, rad
β_L	limited angle of sideslip, rad
γ_{CMD}	commanded flightpath angle, rad
γ_o	flightpath angle at engagement of flightpath command, rad
γ_q	quickened flightpath angle, deg
ΔL_{LF}	jet-induced rolling moment increment due to lift fan thrust
ΔL_{LN}	jet-induced rolling moment increment due to lift nozzle thrust
ΔX	x body axis force commands, lb
ΔZ	z body axis force commands, lb
δ_A	aileron deflection, deg
δ_C	canard deflection, deg
δ_F	flap deflection, deg
δ_{CN}	cruise nozzle deflection, deg
δ_{LF}	lift fan nozzle longitudinal deflection, deg
δ_{LN}	lift nozzle longitudinal deflection, deg
δ_{LN_y}	lift nozzle lateral deflection, deg
δ_{LLN}	left lift nozzle deflection, deg
δ_{long}	longitudinal stick deflection, in.
δ_{PRCS}	pitch reaction control system thrust, lb
δ_R	rudder deflection, deg
δ_{RLN}	right lift nozzle deflection, deg
δ_{RRCS}	roll reaction control system thrust, lb

δ_T	throttle position, percent of maximum
δ_{TDB}	throttle position deadband for flightpath command, percent of maximum
δ_{To}	throttle position at engagement of flightpath command, percent of maximum
δ_{Tp}	past value of throttle position, percent of maximum
$\delta_{T_{\gamma=0}}$	throttle position for level flight command, percent of maximum
δ_{YRCS}	yaw reaction control system thrust, lb
η_{CN}	cruise nozzle efficiency factor
η_{LF}	lift fan nozzle efficiency factor
η_{LN}	lift nozzle efficiency factor
θ	pitch attitude, rad
θ_s, θ_c	commanded pitch attitude, rad
θ_N, θ_j	resultant thrust vector angle, deg
τ	time constant, sec
ϕ	bank angle, rad
ψ	heading angle, rad
ω	core (lift-cruise) engine natural frequency, rad/sec

Acronyms

APP	approach control mode
ASTOVL	advanced short takeoff and vertical landing
CTO	cruise/takeoff control mode
HUD	head-up display
IGV	inlet guide vane
MTV	manual thrust vector control mode
RCS	reaction control system
STOVL	short takeoff and vertical landing
TRC	translational rate command control mode
VMS	Vertical Motion Simulator
VSRA	V/STOL Systems Research Aircraft
V/STOL	vertical or short takeoff and landing
wow	weight on wheels

Revised Simulation Model of the Control System, Displays, and Propulsion System for an ASTOVL Lift Fan Aircraft

JAMES A. FRANKLIN

Ames Research Center

Summary

This report describes revisions to a simulation model that was developed for use in piloted evaluations of takeoff, transition, hover, and landing characteristics of an advanced short takeoff and vertical landing lift fan fighter aircraft. These revisions have been made to the flight/propulsion control system, head-up display, and propulsion system to reflect recent flight and simulation experience with short takeoff and vertical landing operations. They include nonlinear inverse control laws in all axes (eliminating earlier versions with state rate feedback), throttle scaling laws for flightpath and thrust command, control selector commands apportioned based on relative effectiveness of the individual controls, lateral guidance algorithms that provide more flexibility for terminal area operations, and a simpler representation of the propulsion system.

The model includes modes tailored to the phases of the aircraft's operation, with several response types which are coupled to the aircraft's aerodynamic and propulsion system effectors through a control selector tailored to the propulsion system. Head-up display modes for approach and hover are integrated with the corresponding control modes. Propulsion system components modeled include a remote lift fan and a lift-cruise engine. Their static performance and dynamic responses are represented by the model. A separate report describes the subsonic, power-off aerodynamics and jet induced aerodynamics in hover and forward flight, including ground effects.

Introduction

The development of a mathematical model for simulation of a representative advanced short takeoff and vertical landing (ASTOVL) aircraft concept is reported in references 1 and 2. Those reports include descriptions of the aircraft's aerodynamic characteristics, flight/propulsion control system, head-up display (HUD), and the propulsion system performance and dynamic response. This simulation model was used in an experiment on Ames Research Center's Vertical Motion Simulator (VMS) to gain initial experience with control system behavior and flying qualities for this aircraft concept.

Based on the results of that simulation, as well as experience gained in flight experiments on NASA's vertical or short takeoff and landing (V/STOL) Systems Research Aircraft (VSRA), reported in reference 3, modifications have been made to the control system, HUD, and propulsion system. This report describes these modifications in detail. In particular, the control system was altered to incorporate nonlinear inverse control laws in all axes. In the model of reference 1, the nonlinear inversion appeared in the augmented control on longitudinal and vertical velocity and for yaw control in forward flight. The inverse scheme is now employed in the pitch and roll axes as well. State rate feedback control has been eliminated in the control system, with the exception of the vertical axis, based on concerns of the practical utility of angular accelerometers for pitch, roll, and yaw control, and of the need to use linear accelerometers to achieve acceptable control response and disturbance suppression for control of longitudinal and lateral velocity in hover. Additionally, new schemes for scaling the throttle inceptor for use as a thrust or vertical velocity controller have been added to the model. The control selector has been revised to apportion commands to the individual control effectors based on their force or moment producing capability depending on the aircraft configuration and flight condition. Display modifications have been incorporated to include lateral guidance for the approach from the two-circle guidance concept of reference 4. Additional symbology changes have been included in the HUD to bring the format into conformance with an operational display. Finally, the propulsion system model has been revised to include a simple calculation of transient response for the core engine and for thrust transfer between the lift fan and lift and lift/cruise nozzles.

This report presents a description of the entire control system, HUD, and propulsion system, including the modifications incorporated, to provide continuity with the description of these systems in reference 1.

Basic Lift Fan STOVL Aircraft

The lift fan STOVL aircraft is a single-place, single-engine fighter/attack aircraft, shown in figure 1, featuring a wing-canard arrangement with twin vertical tails. Geometric characteristics of the configuration are summarized in table 1; mass properties are specified in table 2.

The propulsion system concept is presented in figure 2. It consists of a remote lift fan coupled to a lift-cruise turbofan engine to permit continuous transfer of energy from the lift-cruise engine to the lift fan. Further, the lift-cruise engine exhaust is either ducted aft to a thrust deflecting cruise nozzle in conventional flight or diverted to two deflecting lift nozzles in vertical flight. Throughout transition, flow can be continuously transferred between the cruise and lift nozzles. Lift fan and lift nozzle thrust can be deflected downward from 45 to 100 deg relative to the aircraft waterline, and lift nozzle thrust can be deflected ±10 deg laterally as well. The cruise nozzle can be deflected ±20 deg relative to the aircraft waterline in the vertical plane.

The basic flight control system consists of the canard, ailerons, and twin rudders for aerodynamic effectors during forward flight. For powered-lift operation, control is provided by differential thrust transfer between the lift fan and lift nozzles, deflection of lift fan and lift nozzle thrust, and deflection of cruise nozzle thrust. Pitch control is achieved by a combination of canard deflection, thrust transfer between the lift fan and lift nozzles, and deflection of the cruise nozzle. Roll control is produced by the ailerons and differential thrust transfer between the lift nozzles. Yaw control is derived from the combination of rudder deflection and lateral deflection of lift nozzle thrust. As an option, reaction control, powered by engine compressor bleed air, can provide additional control moments through nozzles located in the wing extremities and in the tail. Longitudinal acceleration is achieved through thrust transfer between the lift fan, lift nozzles, and cruise nozzles and by deflection of the lift fan and lift nozzle thrust.

The control loop structure with its significant elements is shown in figure 3. It includes task commands to the guidance module, display of guidance and situation information to the pilot, commands to the mode selector and associated control response types through the inceptors, the nonlinear inversion using the nonlinear aerodynamic/propulsion model, and the control selector for the aerodynamic and propulsion control effectors. Each element of this structure will be described in the following sections.

Guidance

For precision tasks such as the approach and vertical landing, the system described in reference 4 has been incorporated to provide lateral and vertical guidance from the point of guidance selection to hover at the intended landing site. The reference flightpath, shown in figure 4, is constructed on a horizontal profile based on two circles connected by tangent lines that represent the aircraft's initial path, a segment connecting the two circles, and a final approach segment. Experience to date has shown that reasonable settings for the parameters of the horizontal path called for in reference 4 are as follows:

Acquiring segment length	5,000 ft
Final segment length	10,000 ft
Acquiring circle minimum radius	8,000 ft
Approach circle minimum radius	6,000 ft

The length of the acquiring segment allows sufficient time after guidance selection to prepare for the turn onto the acquiring circle. Length of the final segment permits the aircraft to be set up on the final approach in preparation for the increased flightpath control workload associated with the transition from wing-borne to jet-borne flight. Minimum radii of the respective circles ensure that bank angles are acceptable for operation under instrument meteorological conditions.

Vertical guidance provides altitude hold commands from the point of guidance selection until acquisition of the glideslope. The glideslope is specified along the horizontal path derived above. The vertical path levels at the intended hover height at a distance from the hover point sufficient to allow for the final stages of deceleration in level flight.

Mode Selection

Four control modes, shown in table 3, have been provided for operation of the aircraft in wing-borne and jet-borne flight. They enable operation in all regimes of conventional wing-borne flight and jet-borne operation with manual thrust management consistent with current Harrier operations. In addition, they include control augmentation that provides for precise, low-workload control of the aircraft in jet-borne flight that permits operation in adverse weather conditions that is not achievable with the current Harrier fleet.

In the cruise/takeoff (CTO) mode, the aircraft can be flown conventionally for wing-borne takeoff, cruise, and landing. The pilot has direct control of lift-cruise engine thrust; however, the propulsive lift system is not in use, and the pilot has no direct control of thrust vector angle. Rate damping augmentation and angle-of-attack stability are provided for pitch control, rate damping augmentation is provided for roll control, and sideslip rate damping and directional stability are included for yaw control.

The manual thrust vector (MTV) mode provides for operation in jet-borne flight including vertical and short takeoff, transition, hover, and vertical and slow landing. In this mode, the pilot has manual control of the magnitude of the propulsion system thrust (lift fan plus lift-cruise engine thrust) and the deflection of the resultant thrust vector, thus allowing the aircraft to be configured and controlled for the phases of operation noted above. No feedback control loops are used for either speed or flightpath control. Pitch and roll are controlled through rate command/attitude hold augmentation in transition, blending to attitude command/attitude hold at low speed. Yaw control is the same as for CTO at higher airspeeds during transition, and then blends to yaw rate command at low speed.

The approach (APP) mode is designed to reduce workload and improve precision of control of the longitudinal and vertical response during the decelerating transition to hover or for slow landings. It provides the pilot with independent control of the longitudinal and vertical axes. In so doing, it activates a longitudinal acceleration command/velocity hold system, with thrust vector angle as the speed control effector. As the aircraft decelerates from wing-borne to jet-borne flight, a flightpath command augmentation system is activated when the propulsion system is configured to provide effective control of the vertical axis. This mode is engaged when the resultant thrust vector angle exceeds 70 deg and the commanded core engine thrust exceeds 60 percent of its maximum value. This system remains engaged until the net thrust vector angle decreases below 47 deg or the throttle angle is reduced below 20 percent of full throw. Until the flightpath command augmentation is engaged, the pilot still has direct control of lift-cruise engine thrust. When the throttle is advanced beyond 95 percent of full throw, direct command of thrust is once again available. The flightpath command system will then reengage once the throttle is reduced below 90 percent of full throw. Pitch, roll, and yaw control are identical to that for MTV.

The translational rate command (TRC) mode is available for precision control of hover positioning and vertical landing. In this mode, decoupled command of longitudinal, lateral, and vertical velocity is provided. Longitudinal velocity control is achieved through deflection of the thrust vector at constant pitch attitude. Lateral velocity command is realized through roll control. The yaw axis control remains the same as that for MTV.

Control mode availability is subject to the restrictions shown in figure 5. The lift fan has a 250 knot airspeed operational limit; thus CTO is the only mode available for this and higher airspeeds. The pilot engages the lift fan by selecting MTV or APP when the airspeed is between 250 and 150 knots; if the lift fan is not engaged and the airspeed decreases below 150 knots, then flight must be continued in CTO mode. TRC cannot be selected until ground speed relative to the intended landing position has dropped below 20 ft/sec. Upon landing in jet-borne flight, the flight control mode reverts to MTV and direct control of thrust. MTV mode is used for vertical and short takeoff with the pilot in direct control of the thrust vector. The CTO mode can also be selected while the aircraft is on the ground for a conventional takeoff. The lift fan will be shut down automatically in flight if the airspeed exceeds 250 knots; the pilot can manually disengage the lift fan by selecting CTO mode, but this option is available only if the net thrust vector angle is directed fully aft. The MTV mode can be selected any time the lift fan is engaged by depressing a button on the nozzle lever. This button disengages the clutch that backdrives the thrust vector handle and allows the pilot to manually direct the thrust vector, providing a rapid acceleration or wave-off capability.

Displays

The HUD, described in detail in reference 5, provides the primary flight display for all phases of operation. A baseline set of symbology is presented for all flight regimes and is augmented by command and situation information for precision approach and hover. The baseline display includes aircraft attitude, speed, angle-of-attack reference, altitude, engine rpm, thrust vector angle, flap angle, longitudinal acceleration, heading, and distance to the hover point, as shown in figure 6.

Symbology added to the display for precision guided approach to hover are also shown in figure 6. This information appears upon guidance selection in either the MTV or APP mode. The guidance display is a flightpath centered, pursuit presentation that enhances the external visual cues, centers them on the aircraft's flightpath, and presents the pilot with a pursuit tracking task for following the intended transition and approach guidance to a final hover point. Course and glideslope guidance are provided in the form of a leader (ghost) aircraft that follows the desired flight profile. The pilot's task is to

track the ghost aircraft with the flightpath symbol. As indicated in reference 5, the flightpath symbol is quickened to compensate for lags in the airframe and propulsion system response. This quickening is employed only when guidance is selected. Otherwise, the symbol presents the aircraft's actual flightpath. For control modes where thrust is controlled manually using the throttle (CTO and MTV), the flightpath compensation includes lagged pitch rate and washed-out throttle commands in combination with the true flightpath in accord with the following equations:

$$\gamma_q = \frac{K_q \dot{\theta}}{s+\sigma_w} + \tan^{-1}\left(\frac{K_{\delta_T}\delta_T}{V_T}\right)\left(\frac{s}{s+\sigma_w}\right) + \tan^{-1}\left(\frac{\dot{h}}{V_T}\right) \tag{1}$$

and

$$\sigma_w = Z_{w_{hover}} + V_{af} Z'_w \qquad Z_{w_{hover}} = g(\dot{m}_e / W)$$
$$Z'_w = 1.58\rho g S / W \qquad K_{\delta_T} = A_{\delta_T} \sin\theta_j / \sigma_w \tag{2}$$

The pitch rate term is blended out for speeds below 70 knots, and true airspeed is frozen at 100 ft/sec for speeds less than 100 ft/sec. Gains and washout frequencies are $K_q = 1$, $A_{\delta_T} = 0.3$ ft/ sec^2/pct. When flightpath command augmentation is engaged and flightpath is commanded directly by the throttle in APP mode, the flightpath symbol drive is complemented with its commanded value in the short term according to

$$\gamma_q = \tan^{-1}\frac{\dot{h}_c}{V_T}\left(\frac{s}{s+\omega_\gamma}\right) + \tan^{-1}\left(\frac{\dot{h}}{V_T}\right) \tag{3}$$

The washout frequency ω_γ is 0.7 rad/sec. Lateral flightpath, scaled to avoid symbol limiting in the presence of winds, is represented by the flightpath symbol. For the APP mode, deceleration guidance is presented by an acceleration error ribbon on the left side of the flightpath symbol which the pilot nulls to follow the deceleration schedule. When guidance is not selected, the guidance related symbols (ghost aircraft, acceleration error ribbon, longitudinal acceleration scale, landing deck, and glideslope reference line) are removed from the display. In this case, the longitudinal acceleration caret is scaled in degrees to be read in reference to the pitch ladder and represents potential flightpath, that is, the flightpath which can be achieved in unaccelerated flight.

During the latter stages of deceleration as the aircraft approaches the intended point of hover, selective changes are made to the approach display to provide guidance for the hover point capture. Specifically, the longitudinal velocity vector, predicted longitudinal velocity, and station-keeping cross appear referenced to the vertical velocity diamond symbol as shown in figure 7. The longitudinal velocity symbol is driven by the velocity commanded by the control system. The pilot controls the velocity predictor toward the station-keeping cross position and adjusts velocity to bring the cross to rest at the reference hover point, indicated by the cross being adjacent to the vertical velocity diamond. This added symbol group is removed from the display while on the ground.

When the translational rate command (TRC) mode is selected for precision hover and vertical landing, the HUD format superimposes vertical and plan views and provides command and situation information in a pursuit tracking presentation (fig. 8). In the horizontal situation, the aircraft velocity vector is represented by a line emanating from the aircraft symbol. A pad symbol represents the landing area. Horizontal and vertical velocity predictor symbols, whose displacement and orientation from the aircraft symbol indicate magnitude and direction, provide the pilot lead information for hover maneuvering. Horizontal velocities commanded by the control system are displayed directly by the predictor ball. The vertical situation is displayed by a diamond referenced to the right leg of the aircraft symbol whose displacement, t_{w_c}, is proportional to complemented vertical speed. Vertical velocity is complemented with the washed-out vertical velocity command to provide the command

$$t_{w_c} = K_w\left[\dot{h} + \dot{h}_c\left(\frac{s}{s+\omega_\gamma}\right)\right] \tag{4}$$

where $\omega_\gamma = 0.7$ The diamond symbol is displayed against a vertical bar whose length represents the operational vertical velocity limits for the landing gear. The length of the bar is based on the vertical velocity relative to the landing pad. For shipboard operation, when vertical deck motion can be uplinked to the aircraft, relative closure rate to the deck is presented on this symbol. This bar provides the pilot with an indication of sink rate margin for the vertical landing. A horizontal bar indicates the altitude remaining to touchdown.

A panel mounted head-down display of simple format presents a compass rose and a plan view of the reference flightpath following guidance select. Digital display of ground speed along track is also provided.

Inceptors

Inceptors available in the cockpit and their relation to response types for the various control modes are shown in figure 9. Individual inceptors are the center stick and trim switch, pedals, throttle lever, nozzle lever, throttle

thumbwheel, and flap switch. The relationship of each inceptor to response type can be interpreted using the key for the individual control modes shown in the upper left corner of the figure.

The center stick commands pitch and roll rate in CTO, pitch and roll rate command/attitude hold in MTV and APP at higher speeds, blending to attitude command/attitude hold at lower speeds, and longitudinal and lateral inertial velocity in TRC. The blending range in MTV and APP for pitch control is between 60 and 70 knots; for roll control the range is 40 to 60 knots. Mechanical characteristics of the stick, presented by a McFadden control loader, include control throws of ±5.65 in. for pitch and ±4.25 in. for roll. Force characteristics include a pitch gradient of 1 lb/in., breakout force of 1 lb, and hysteresis band of 0.5 lb. Comparable characteristics for roll are a gradient of 0.7 lb/in., breakout of 0.5 lb, and hysteresis of 0.2 lb. These characteristics are fixed and do not vary with flight condition. The trim switch on the stick provides pitch and roll rate trim in CTO, and in MTV and APP in conjunction with the rate command/attitude hold response type. At low speed when the attitude command response type is functional, the trim switch provides attitude trim. In TRC, the trim switch adjusts the commanded longitudinal and lateral inertial velocities.

In CTO, pedals function as sideslip command, while in MTV and APP they provide sideslip command at high speed, blending to yaw rate command at low speed. The blend occurs from 40 to 60 knots. Pedals provide yaw rate command in TRC. Mechanical characteristics consist of a full throw of ±2.1 in., force gradient of 15 lb/in., breakout of 5 lb, and hysteresis of 2 lb.

The throttle controller commands total thrust magnitude in CTO and MTV modes, and in APP mode when flightpath command augmentation is not engaged. When flightpath command is engaged in APP mode, the throttle commands flightpath angle when ground speed is greater than 60 knots and vertical velocity when speed is less than 60 knots. In TRC, the throttle controls vertical velocity.

To eliminate any transient response during the throttle control's reconfiguration, the throttle control command is scaled to match the new control command state at the mode switch. Figure 10 provides an illustration of this scaling; table 4 presents the associated logic flow diagrams. When the flightpath command mode engages, the current flightpath angle and throttle position are used to establish a point on the flightpath-throttle curve in figure 10(a). A second point is defined by maximum commanded flightpath angle and maximum throttle position to ensure capability to achieve the maximum commanded climb capability. These two points define the upper slope for throttle scaling. The upper slope is extended down to a point associated with a defined throttle position or to the minimum flightpath. The lower slope extends from that defined throttle position and its associated flightpath angle down to the minimum flightpath and throttle position. The new control sensitivity of the throttle is bounded by upper and lower scaling slopes in figure 10(a) to prevent any unreasonable control sensitivity change due to the mode switch. If flightpath command engages outside these boundaries, the maximum or minimum slope is used, and is anchored on the point for maximum flightpath and throttle position. The commanded flightpath is adjusted to match the current throttle position on that limiting slope. For flightpath control, the throttle is scaled typically from 20 to 95 percent, and the maximum and minimum commands and the slopes are listed in table 5. Flightpath command is disengaged for throttle positions outside this range and the throttle reverts to thrust command. The maximum and minimum slopes are selected to provide reasonable control sensitivities and to allow only reasonable mode switching transients should they occur.

When the throttle reverts from flightpath to thrust command, the throttle position and total thrust existing at that instant are used, along with the maximum throttle position and thrust, to define an upper slope for the thrust-throttle curve shown in figure 10(b). A lower slope, defined for lower throttle positions, connects the point for throttle and thrust at the mode switch to the point for idle thrust and throttle. Since the upper and lower slopes can differ from the baseline (and desired) linear slope defined by minimum and maximum thrust and throttle, these two slopes are adjusted after the mode switch to restore the linear relationship. This adjustment is accomplished by modifying the upper and lower slopes as the throttle is moved to connect the maximum and minimum thrust and throttle points to the new thrust and throttle position. An example of two cycles of this adjustment (fig. 10(b)) shows an initial throttle increase with commanded thrust advancing along the original upper slope. The lower slope is then adjusted to the new throttle position. Subsequently, the throttle is retarded, producing a thrust command defined by the new lower slope, and the upper slope is readjusted to this throttle position and thrust. These adjustments proceed with succeeding throttle movements until the upper and lower slopes are restored, within tolerances, to establish the original linear relationship between throttle and thrust. These tolerances are such as to bring the slopes between 0.99 and 1.01.

The nozzle lever has the sole function of command of the resultant thrust vector angle in MTV. Otherwise, it is backdriven to a position consistent with the thrust vector angle being commanded for CTO, APP, or TRC mode, so as to be in the correct position when a switch occurs from

any of these modes to MTV. Activation of the wave-off switch on the top of the nozzle lever will initiate a switch from any of these modes to MTV so long as the nozzle lever is in a position consistent with the current thrust vector angle. If the nozzle lever is not properly positioned within a specified threshold, the mode switch to MTV will not occur.

The throttle thumbwheel serves the function of command of longitudinal acceleration/velocity hold in APP mode. It is a proportional control with center detent and adjustable friction. When in the detent, the thumbwheel commands the system to hold the existing inertial velocity. The APP mode cannot be engaged if the thumbwheel is out of detent position. If the thumbwheel is moved from the detent in TRC mode, the mode control logic will interpret this input as an acceleration command and will switch the system to APP mode.

A two-position flap switch is located on the left side console in front of the throttle quadrant. The switch commands the flaps to either the up on down position.

Response Types

The response types are subdivided corresponding to pitch, roll, and yaw attitude control and vertical, longitudinal, and lateral velocity control. They consist of feed-forward command shaping, conventional state feedbacks, and proportional-plus-integral control in the forward path where appropriate. The discussion to follow covers the control law structures for each axis and the accommodation of the response types associated with the individual control modes.

Pitch Control

A block diagram of the overall pitch control structure is shown in figure 11. The pilot's inputs are introduced through the control stick and trim switch. Rate command, rate command/attitude hold, or attitude command/attitude hold response types can be implemented, depending on whether the gain K_{qCAH} is zero or not, and whether flaps are up or down. Rate-command/attitude hold is blended to and from attitude-command/attitude hold between 70 and 60 knots through the blending gain K_{BQ}. The rate command integrator is initialized to the current value of $K_{\theta}\theta$ if flaps are up or the aircraft has weight on wheels (wow). If the authority of the pitch control effectors is exceeded and the pilot's command would drive the controls further into saturation, the output of the integrator is held at its past value. Gain K_{THECAH} establishes control sensitivity for attitude command; K_{qCAH} serves the same purpose for the rate command while K_{THEH} is used to adjust overshoot in pitch response for that response type. Control sensitivity in CTO mode is set by K_{qC}. Pitch trim is introduced as a bias to the commands initiating from the stick. Trim inputs originate from the trim switch and from a preset input for short takeoffs, should the latter be selected.

Gain K_{FB} blends feedback variables between body angular rate and angle of attack and Euler axis sensors depending on flap position (K_{FB} = 0 flaps up; 1 flaps down). Angle-of-attack feedback is referenced to the angle of attack that exists at CTO mode engage. Proportional-plus-integral control in the forward path is obtained from the positive feedback of the pitch command through the first-order lag defined by τ_{pitch} and is used for both the rate command/attitude hold and attitude command response types. When on the ground, the input to the first-order lag is set to zero. Rate and position limits on the combined command and feedback variables, prior to input to the lag filter, provide protection against integrator windup. This output is then multiplied by the aircraft's pitch moment of inertia and differenced with the nonlinear model to obtain the pitching moment command to the control selector.

Gains and time constants for the pitch control laws are given in table 6. System response characteristics for the pitch rate command/attitude hold system at 200 knots are portrayed in figure 12. Representative time history data are shown in figure 12(a) and frequency responses are presented in figure 12(b). Overshoot in attitude response is desirable to quicken flightpath response. Bandwidth for attitude control is 3.8 rad/sec. Similar data are shown in figure 13 for the attitude command system in hover. Here the response is deadbeat as desired. In this case, the bandwidth is 6.7 rad/sec.

Roll and Lateral Velocity Control

Roll control modes are presented in figure 14. Rate command, rate command/attitude hold, or attitude command/attitude hold modes are produced with the same form of control laws as for pitch. The control stick and trim switch provide the pilot's inputs, and the control gains and limiting logic are completely analogous to those for pitch. As was the case for pitch control, rate command/attitude hold is blended to and from attitude command/attitude hold through the gain K_{BP} between 60 and 40 knots. The rate command integrator is limited in a similar fashion to the pitch rate command. Gain K_{PHICAH} establishes control sensitivity for attitude command; K_{pCAH} serves this purpose for the rate command mode while K_{PHIH} is used to adjust overshoot in roll response. Gain K_{PC} establishes control sensitivity in CTO mode. Roll trim is introduced as a bias to the roll

command. Again, K_{FB} blends body angular rate and Euler axis feedbacks, depending on flap position.

When operating in conventional flight, the command and feedback loops are referenced to stability rather than body axes. Therefore, the roll and yaw commands are transformed into body axes in this mode (when flaps are up) before being sent to the control selector. Rate and position limits on the combined command and feedback variables, prior to input to the lag filter, provide protection against integrator windup.

Lateral velocity control is accomplished by introducing bank angle commands to the roll attitude command/attitude hold control laws. The switch in figure 14 selects the lateral velocity command path from the stick for TRC mode. Gain K_{Vyc} sets velocity command control sensitivity and K_{Vy} provides the desired control bandwidth. The pilot's commands with the stick input neutral are referenced to the speed of the intended landing spot, whether shipboard or land based. Proportional-plus-integral control through the lagged feedback is also employed for the TRC mode.

The output of the roll command and feedback control is multiplied by the aircraft's roll moment of inertia and differenced with the nonlinear model to obtain the rolling moment command to the control selector.

Gains and time constants for the roll and lateral velocity control laws are given in table 6. Time histories and frequency response data for the roll rate command/attitude hold system at 200 knots are shown in figure 15. Bandwidth for attitude control is 3.3 rad/sec. Similar data are shown in figure 16 for the attitude command system in hover. Here the bandwidth is 7.1 rad/sec. Data for lateral velocity response in TRC mode are shown in figure 17. In this case, the bandwidth for lateral position control is 0.6 rad/sec.

Yaw Control

Yaw control modes, shown in figure 18, provide sideslip command during wing-borne and semi-jet-borne flight and blend to yaw rate command at low speed and in hover. The gain K_B provides a linear blend between the two modes over the speed range from 60 to 40 knots. At higher speeds, control sensitivity is adjusted with $K_{\delta p}$ and sideslip command is produced by a second-order Dutch roll model derived from measured sideslip and sideslip rate, where K_β is chosen to set Dutch roll frequency and the sideslip rate gain $K_{\dot{\beta}}$ establishes Dutch roll damping. During low speed and hover, $K_{\delta pH}$ sets control sensitivity and yaw rate command is based on the feedback of heading rate. When operating in conventional flight, the command and feedback loops are referenced to stability rather than body axes. Therefore, the roll and yaw commands are transformed into body axes in this mode (when flaps are up) before being sent to the control selector. The output of the yaw command and feedback control is multiplied by the aircraft's yaw moment of inertia and differenced with the nonlinear model to obtain the yawing moment command to the control selector.

Gains and time constants for the sideslip and yaw rate command control laws are given in table 6. Representative time and frequency response characteristics for the sideslip command system at 200 knots and the yaw rate command system in hover are shown in figure 19. Bandwidth for heading control in hover is 3.1 rad/sec.

Longitudinal Velocity Control

Longitudinal velocity control laws provide an acceleration command/velocity hold response type for APP mode and velocity command in TRC mode. The system block diagram is shown in figure 20. During transition between forward flight and hover, the pilot commands longitudinal acceleration using the throttle thumbwheel. Control sensitivity is established by the combination of the gain $K_{\dot{V}_X}$ and shaping on the thumbwheel input. If the longitudinal control effectors are limited, the thumbwheel input to the velocity command integrator is replaced by sensed longitudinal acceleration to update the velocity command at the rate sustainable by the control effectors. For TRC, the thumbwheel is switched out and the control stick provides longitudinal velocity commands. Control sensitivity is now set by K_{VXc}. In this mode, the stick is disconnected from the pitch attitude command system and hover maneuvering is performed at a constant pitch attitude. The pilot's commands with the stick input neutral are referenced to the speed of the intended landing spot, shipboard or land based. Velocity control bandwidth is based on K_{VX}.

Proportional-plus-integral control in the forward path is based on the first-order lag feedback defined by τ_{long}. When on the ground or with the system not engaged, the output of the first-order lag is set to zero. Rate and position limits on the combined command and feedback variables, prior to input to the lag filter, provide protection against integrator windup. This output is then multiplied by the aircraft's mass, resolved into body axes, and differenced with the nonlinear model to obtain the longitudinal force command to the control selector.

Gains and time constants for the longitudinal velocity command are given in table 6. Time histories and frequency responses for longitudinal velocity in TRC mode are shown in figure 21. Bandwidth for longitudinal position control is 0.8 rad/sec.

Vertical Velocity Control

When APP or TRC mode is engaged and thrust vector angle and throttle position satisfy the engage criteria, the vertical velocity command control laws, shown in figure 22, are activated. The throttle lever introduces a flightpath command input through command scaling discussed previously. The combination of this command and the flightpath command from pitch attitude changes forms the total flightpath command which is then converted to vertical velocity command. Since flightpath command from pitch attitude is not appropriate at jet-borne speeds, it is blended out between 90 and 70 knots. The velocity V_X is ground speed along track and is used to convert the pilot's flightpath angle command to an equivalent vertical velocity command. For ground speeds below 100 ft/sec, this velocity is frozen at that value to convert the pilot's command from flightpath angle to a scaled vertical velocity command appropriate for hover and low speed flight. Control bandwidth is established by the gains K_{V_Z} and $K_{\dot{V}_Z}$ on vertical velocity and acceleration feedback, where $K_{\dot{V}_Z}$ is normally unity.

Proportional-plus-integral control in the forward path is based on the first-order lag feedback defined by τ_{vert}. When on the ground or with the system not engaged, the output of the first-order lag is set to zero. Rate and position limits on the combined command and feedback variables, prior to input to the lag filter, provide protection against integrator windup. This output is then multiplied by the aircraft's mass, resolved into body axes, and differenced with the nonlinear model to obtain the vertical force command to the control selector.

Gains and time constants for the vertical velocity command control laws are given in table 6. Time histories and frequency response data for vertical velocity in TRC mode are shown in figure 23. Bandwidth for height control is 0.75 rad/sec.

Nonlinear Inverse Control Scheme

The principle of nonlinear inverse control as applied here follows the concept of the author's colleague, G. Meyer, reported in reference 6, and as subsequently applied by the author to several V/STOL aircraft concepts and summarized in reference 7. The inversion of the aircraft dynamics is achieved by determining the forces and moments currently developed by the aircraft (derived from a nonlinear aerodynamic and propulsion model and measurements of the aircraft's current states) and differencing them with the forces and moments commanded by the pilot through the response types. These incremental forces and moments then become the commands to the force and moment control effectors required to achieve the desired response.

In the control law descriptions for the pitch, roll, yaw, longitudinal, and vertical axes in figures 11, 14, 18, 20, and 22, the nonlinear model elements are shown at the lower right of each figure. These elements include contributions from the aircraft's nonlinear aerodynamics for pitch, roll, and yaw moments, lift and drag, flow momentum forces from the lift fan and lift-cruise engine inlets, gravitational forces, and moments arising from inertial coupling. Elements of the computation of these forces and moments may derive from multidimensional tabular data of aerodynamic coefficients, aircraft state measurements, aircraft configuration geometry, weight, and inertias. Each of the figures mentioned above should be consulted for specific contributions to the forces and moments for each control axis.

Control Selector

The control selector receives force and moment commands as derived above and generates the appropriate control surface, cruise nozzle deflection, propulsion system nozzle thrusts and deflections, and reaction control system commands. The following two subsections describe the attitude control moment generators and control of the propulsion system components' thrust and thrust deflection.

Attitude Control

As noted in the description of the basic aircraft, a number of control effectors are required to provide moment control over the aircraft's flight envelope. As the aircraft transitions from wing-borne to jet-borne flight, a redundancy exists between purely aerodynamic and propulsion generated controls. The design approach to resolve this redundancy is to utilize each effector in accord with its control effectiveness depending on flight condition and aircraft configuration. Thus, moment commands, produced by the pitch, roll, and yaw control response types and by the nonlinear model, are apportioned to the individual control effectors in proportion to the moment generating capacity of each effector for the existing aircraft configuration and flight condition. This distribution of control can be represented generally by

$$\text{Moment Command}_i = \left(\text{Max Moment}_i/\text{Max Moment}\right) \times \text{Total Moment Command} \tag{5}$$

$$\text{Max Moment} = \Sigma_i \text{ Max Moment}_i \tag{6}$$

where the subscript i refers to the individual moment effectors. Specific implementation of the pitch, roll, and yaw controls follows.

Pitch control– The block diagram of figure 24 sets forth the control selector for pitch control. Command paths for the individual controls (canard, cruise nozzle, thrust split between the lift fan and lift nozzles, and reaction control) are indicated. Since, in general, pitching moment authorities for the individual controls are not symmetric about neutral, the control path distinguishes between positive and negative pitch commands, and maximum and minimum values must be established in each case. Individual pitching moment authorities are as follows, first for the canard.

$$PMCANMX = (CMCANMX - CMADCA0)\bar{q}Sc \quad (7)$$

$$PMCANMN = (CMCANMN - CMADCA0)\bar{q}Sc \quad (8)$$

where CMCANMX and CMCANMN are presented in figures 25 and 26 and represent the limiting values of pitching moment coefficient that can be achieved at a given angle of attack. These limits do not necessarily correspond to the physical limits of the canard deflection since canard stall is encountered in some instances before reaching maximum deflection. Cruse nozzle authorities are symmetric and are related to the maximum nozzle deflection by

$$PMCNMX = -T_{CN} * x_{CN} * \sin(DPCNMX) \quad (9)$$

$$PMCNMN = -PMCNMX \quad (10)$$

and are based on the cruise nozzle deflection limit DPCNMX of 20 deg. Authorities for thrust split between the lift fan and lift nozzles depend on whether either thrust is approaching its limit. The maximum lift fan thrust TLFMAX is 20,000 lb and maximum lift nozzle thrust TLNMAX is 24,000 lb. Depending on whether the lift fan is operating near its maximum or minimum thrust, two limits must be observed. They are

$$PMTHRMX1 = (TLFMAX - T_{LF})(L_{LF} - L_{LN}) \quad (11)$$

$$PMTHRMX2 = T_{LN}(L_{LF} - L_{LN}) \quad (12)$$

where T_{LF} and T_{LN} are the respective lift fan and lift nozzle thrusts excluding pitch control inputs. PMTHRMX then is the lesser of PMTHRMX1 or PMTHRMX2. The minimum (or nose down) authority is defined similarly by

$$PMTHRMN1 = -(TLNMAX - T_{LN})(L_{LF} - L_{LN}) \quad (13)$$

$$PMTHRMN2 = -T_{LF}(L_{LF} - L_{LN}) \quad (14)$$

and PMTHRMN is the greater of PMTHRMN1 and PMTRHMN2. Reaction control, when selected, has a symmetrical authority defined by

$$PMRCSMX = -DPRCSMX * x_{RCS} \quad (15)$$

$$PMRCSMN = -PMRCSMX \quad (16)$$

where the maximum pitch reaction control thrust DPRCSMX is 1250 lb. Finally, the total pitch control authorities for nose up and nose down control are

$$PMMAX = PMCANMX + PMCNMX + PMTHRMX + PMRCSMX \quad (17)$$

$$PMMIN = PMCANMN + PMCNMN + PMTHRMN + PMRCSMN \quad (18)$$

With these definitions of the individual and total control authorities, the individual control commands can now be determined. For the canard, the command is

$$PMCAN = (PMCANMX / PMMAX)PITCH_{CMD} \quad \text{or} \quad (PMCANMN / PMMIN)PITCH_{CMD} \quad (19)$$

depending on whether the total pitch command is positive or negative. This command is then nondimensionalized and used as the pitching moment coefficient input to the inverse table shown graphically in figure 27 to obtain the required canard deflection. The output of the table is limited to ±30 deg, while the table contains internal limits to avoid regions of canard stall. This value becomes the canard servo command. Cruise nozzle pitch commands are derived similarly, based on cruise nozzle pitch effectiveness. This command is converted to a nondimensional argument as a function of nozzle thrust, and cruise nozzle deflection is derived from the arcsin of that argument. Pitching moment commands for lift fan–lift nozzle thrust split are sent to the thrust management system to arrive at the individual nozzle thrusts. Reaction control thrust, when selected, is simply the ratio of the moment command and the reaction control system (RCS) nozzle moment arm to the center of gravity.

Roll control– The control selector for roll control appears in figure 28. Command paths are shown for the individual controls (ailerons, thrust split between the right and left lift nozzles, and reaction control). Rolling moment authorities for the individual controls are symmetric about neutral, thus only the maximum authority need be defined. Individual rolling moment authorities, starting with the aileron, are as follows:

$$RMAILMX = CLAILMX * \bar{q}Sb \quad (20)$$

where CLAILMX, presented in figure 29, represents the limiting value of rolling moment coefficient that can be achieved at a given angle of attack. Authorities for thrust split between the right and left lift nozzles depend on the level of lift nozzle thrust. The individual nozzles are oversized for roll control and the maximum individual lift nozzle thrust available exceeds the baseline limit for that nozzle by 30 percent. Thus for TLNMAX = 24,000 lb, TLLNMAX = 1.3*(24000/2) = 15,600 lb. The maximum roll control authority, based on the level of lift nozzle thrust, is

$$RMLNMX = 1.3 * T_{LN} * y_{LN} * \cos\delta_{LN} \quad (21)$$

Reaction control, when selected, has an authority defined by

$$RMRCSMX = DRRCSMX * y_{RCS} \quad (22)$$

where the maximum roll reaction control thrust DRRCSMX is 1250 lb. Taking the three controls into account, the total roll control authority is

$$RMMAX = RMAILMX + RMLNMX + RMRCSMX \quad (23)$$

Individual roll control commands can now be determined, as indicated in figure 28. For the aileron, the command is nondimensionalized and combined with the nondimensional yaw command, CNRUD, to produce decoupled rolling and yawing moments from the ailerons and rudder. In this case, where aileron and rudder effectiveness are linear, the decoupling is accomplished by solving the linear equations for aerodynamic moments from the ailerons and rudder for aileron and rudder position. The two equations are

$$CLDA * DAIL + CLDR * DRUD = CLAIL \quad (24)$$

$$CNDA * DAIL + CNDR * DRUD = CNRUD \quad (25)$$

The four control effectiveness derivatives (CLDA, CLDR, CNDA, and CNDR) in body axes are presented as functions of angle of attack in figures 30–33. If control effectiveness were nonlinear, rolling and yawing moment coefficients from the aileron and rudder could be combined in a two-dimensional table with inputs of CLAIL and CNRUD and outputs of DAIL and DRUD. Rolling moment commands for lift nozzle thrust split are resolved into the vertical axis through the cosine of lift nozzle deflection and divided by the lift nozzle moment arm to arrive at the differential nozzle thrust command. The differential commands are summed with the lift nozzle thrust determined by the thrust management system to produce the right and left lift nozzle thrust commands. Reaction control thrust, as for the case of pitch, is the ratio of the moment command and the RCS nozzle moment arm to the center of gravity.

Yaw control– Figure 34 presents the control selector for yaw control. Command paths for the individual controls (rudder, lateral deflection of lift nozzle thrust, and reaction control) are shown in the figure. Yawing moment authorities for the individual controls are symmetric about neutral, and only the maximum authority is defined. Individual yawing moment authorities, first for the rudder, are as follows:

$$YMRUDMX = -CNDR * RUDMAX * \bar{q}Sb \quad (26)$$

where RUDMAX is 30 deg. Authority for lift nozzle thrust deflection is determined by

$$YMLNMX = -T_{LN} * x_{LN} * DYLNMX \quad (27)$$

where the limit of lateral thrust deflection of the lift nozzles is 10 deg. Reaction control, when selected, has an authority defined by

$$YMRCSMX = -DYRCSMX * x_{RCS} \quad (28)$$

where the maximum roll reaction control thrust DYRCSMX is 1250 lb. The total yaw control authority is

$$YMMAX = YMRUDMX + YMLNMX + YMRCSMX \quad (29)$$

Commands for each control are shown in figure 34. The rudder command is nondimensionalized and combined with the nondimensional roll command, CLAIL, to produce decoupled rolling and yawing moments as described in the roll control discussion. Yawing moment commands for lift nozzle thrust deflection are converted to a nondimensional argument as a function of nozzle thrust, and lift nozzle deflection is derived from the arcsin of that argument. When the lift nozzle deflection angle does not coincide with the vertical axis of the aircraft, differential lift nozzle thrust for roll control produces uncommanded yawing moments. To cancel these moments, an interconnect between differential lift nozzle thrust and lateral lift nozzle deflection is introduced as a function of the sine of lift nozzle longitudinal deflection δ_{LN}. Reaction control thrust again is the ratio of the moment command and the RCS nozzle moment arm to the center of gravity.

Thrust Management

The purpose of the thrust management system is to convert commands from the longitudinal and vertical velocity control response types via the control selector and from the pilot's throttle and nozzle levers to the appropriate lift fan, lift nozzle, and cruise nozzle thrusts

and lift fan and lift nozzle deflections. This process is governed by the mode selected for the phase of operation. In CTO and MTV modes, the throttle directly controls the core engine's total thrust magnitude. In CTO mode, thrust is not deflected, thrust vector angle is zero, and the nozzle lever is positioned against its forward stop. In MTV mode, the nozzle lever commands thrust vector angle. The total thrust command and the thrust vector angle command are sent to the thrust management system to calculate each nozzle thrust command and deflection. In APP mode when flightpath command is not engaged, the pilot also has direct control of the core engine thrust while longitudinal velocity control laws command thrust deflection. When flightpath command is engaged in either APP or TRC mode, the longitudinal and vertical velocity control laws and nonlinear inverse drive the individual thrust and thrust deflection commands. Allocation of thrust to the cruise nozzle, lift nozzles, and lift fan, as well as their deflections, is determined by four situations: the three methods used for the CTO mode, MTV mode, and the APP mode (without flightpath command engaged) are presented first, followed by the fourth method used in conjunction with the flightpath command portion of the APP mode and vertical velocity command for the TRC mode.

The first propulsion system solution applies to CTO or MTV mode when the lift fan is inoperative or when the commanded net thrust vector angle is less than or equal to 0 deg. Lift fan and lift nozzle thrusts are set equal to zero, and the longitudinal deflection angles of the lift fan and lift nozzles are fully aft at 45 deg. Core engine thrust, commanded by the throttle lever, is directed to the cruise nozzle. The basic thrust equation for the aircraft, regardless of control mode, is

$$\frac{T_{LF}}{K_{AUG}\eta_{LF}} + \frac{T_{LN}}{\eta_{LN}} + \frac{T_{CN}}{\eta_{CN}} = T_{T_{CMD}} \tag{30}$$

where $\eta_{LF} = 0.98$, $\eta_{LN} = 0.98$, and $\eta_{CN} = 0.99$ and are the efficiency factors of the lift fan, the lift nozzles, and the cruise nozzle, respectively. The lift fan augmentation ratio $K_{AUG} = 2.07$. For the case in which the pilot has manual control of the core engine thrust, the net cruise nozzle thrust T_{CN} is simply the product of $T_{T_{CMD}}$ and η_{CN}.

The second case is applicable for MTV and APP modes without flightpath command, where the commanded net thrust vector angle is less than 45 deg. The lift fan and lift nozzle deflections are fully aft at 45 deg. In MTV, the thrust vector angle is commanded by the nozzle lever. In APP, the command is derived from the longitudinal velocity control law by

$$\theta_N = \tan^{-1}(\Delta X / F_{TOT}) \tag{31}$$

where the total resultant thrust is made up of the axial and normal force components:

$$F_{TOT} = \sqrt{F_x^2 + F_z^2} \tag{32}$$

$$F_x = T_{LF}\sin\delta_{LF} + T_{LN}\sin\delta_{LN} + T_{CN} \tag{33}$$

$$F_z = T_{LF}(\cos\delta_{LF} + DLJEI) + T_{LN}(\cos\delta_{LF} + DLJEI) \tag{34}$$

and DLJEI is the contribution to normal force of the jet-induced aerodynamic lift from lift fan and lift nozzle thrust taken from reference 2. The relevant equations to satisfy in determining lift fan, lift nozzle, and cruise nozzle thrust are those for total thrust, resultant thrust vector angle, and pitching moment commanded by the control system. The total thrust relationship appears in equation 30. The resultant thrust vector angle can be expressed in terms of the axial and normal components of the individual nozzle thrusts necessary to meet the commanded value of θ_N:

$$\frac{\left[T_{LF}(\cos\delta_{LF} + DLJEI) + T_{LN}(\cos\delta_{LN} + DLJEI)\right]}{T_{LF}\sin\delta_{LF} + T_{LN}\sin\delta_{LN} + T_{CN}} = \tan\theta_N \tag{35}$$

Equation 35 can be rewritten in terms of the individual nozzle thrusts as

$$T_{LF}[\sin\delta_{LF}\tan\theta_N - \cos\delta_{LF} - DLJEI] + T_{LN}[\sin\delta_{LN}\tan\theta_N - \cos\delta_{LN} - DLJEI] + T_{CN}[\tan\theta_N] = 0 \tag{36}$$

The pitching moment contributions of each nozzle in response to the commanded pitching moment $PITCH_{CMD}$ are

$$T_{LF}(L_{LF} + DPMJEI) + T_{LN}(L_{LN} + DPMJEI) = PITCH_{CMD} \tag{37}$$

where the lift fan pitch moment arm and the lift nozzle moment arm are calculated from the respective nozzle deflections (fully aft in this case) and the distances of these nozzles from the center of gravity of the aircraft:

$$L_{LF} = x_{LF}\cos\delta_{LF} + z_{LF}\sin\delta_{LF} \tag{38}$$

$$L_{LN} = x_{LN}\cos\delta_{LN} + z_{LN}\sin\delta_{LN} \tag{39}$$

The term DPMJEI is the sum of the jet-induced pitching moments generated by lift fan and lift nozzle thrust (ref. 2). Equations 30, 36, and 37 are solved for lift fan, lift nozzle, and cruise nozzle thrust. If the lift nozzle or lift fan thrusts are negative or if they exceed their maximum allowable values, then the equations for $T_{T_{CMD}}$ and pitching moment are solved again, with the lift fan or lift nozzle thrust set to the appropriate limit.

If the cruise nozzle thrust calculated above is less than zero, or if the commanded net thrust deflection angle is greater than or equal to 45 deg, then the cruise nozzle thrust is set to zero. This is the third propulsion control case for manual thrust control. The total thrust equation is essentially the same as above, with T_{CN} set to zero:

$$\frac{T_{LF}}{K_{AUG}\eta_{LF}} + \frac{T_{LN}}{\eta_{LN}} = T_{T_{CMD}} \tag{40}$$

The lift fan and lift nozzle deflection angles are both commanded to a common angle, δ_N, which is determined by the commanded thrust vector angle, θ_N according to the following relationship:

$$\delta_N = 90 - \cos^{-1}\left(\cos\theta_N\sqrt{1+2\cos\delta_N\,DLJEI+DLJEI^2}\right) \tag{41}$$

Jet-induced lift accounts for shift of the resultant vector angle θ_N away from the physical angle of the lift fan and lift nozzles, δ_N. Moment arms are calculated for the lift fan and lift nozzle from equations 38 and 39. The relationship between the lift fan and lift nozzle thrust to satisfy the pitching moment command is the same as for equation 37, that is

$$T_{LF}(L_{LF}+DPMJEI)+T_{LN}(L_{LN}+DPMJEI) = PITCH_{CMD} \tag{42}$$

Equations 40 and 42 are solved simultaneously to find the lift fan and lift nozzle thrusts. If either of the calculated thrusts exceeds its limits, that thrust is limited accordingly, and then the pitching moment equation is solved again, with the lift fan or lift nozzle thrust set to the appropriate limit. Total thrust is then recalculated based on the two nozzle thrusts according to equation 40. This means that the total thrust command from the control system is overridden so as to satisfy the demands for pitch control.

A different propulsion system control scheme is used for the APP mode with flightpath command engaged and for the TRC mode. In these cases, the longitudinal and vertical velocity control and pitching moment laws determine the axial and normal forces (ΔX and ΔZ) and the pitching moment ($PITCH_{CMD}$) that the propulsion system must provide. This scheme comprises the fourth method for determination of lift fan and lift nozzle thrust and thrust deflection. When these modes are engaged, lift fan and lift nozzles are free to deflect as needed to meet the thrust vector angle command. Thrust is allocated between these nozzles to satisfy axial and normal force and pitching moment requirements in conjunction with the system's commanded nozzle deflection angles. In this case, the lift fan and lift nozzle deflection is defined by

$$\delta_N = 90 - \cos^{-1}\left(\frac{\Delta X\sqrt{1+2\cos\delta_N\,DLJEI+DLJEI^2}}{\sqrt{\Delta X^2+\Delta Z^2}}\right) \tag{43}$$

The equation for total resultant force replaces the total thrust equation:

$$(T_{LF}+T_{LN})\sqrt{1+2\cos\delta_N DLJEI+DLJEI^2} = \sqrt{\Delta X^2+\Delta Z^2} \tag{44}$$

and the pitching moment relationship remains the same as in equation 42. Lift fan and lift nozzle thrust is obtained from the simultaneous solution of equations 42 and 44, with the nozzle moment arms based on the nozzle deflection angle δ_N. If nozzle deflection limits and nozzle thrust limits are reached, control over the longitudinal axis is relinquished first, followed by control over the vertical axis. If either of the calculated thrusts exceeds its limits, that thrust is limited accordingly, and then the pitching moment equation is solved again, with the lift fan or lift nozzle thrust set to the appropriate limit. Total thrust is then determined based on the two nozzle thrusts according to equation 40.

Propulsion System

The propulsion system model developed for this experiment is a representation of a lift fan coupled to a lift-cruise engine as shown in figure 2. The nozzle of the lift-cruise engine provides axial thrust in cruise as well as thrust vectoring for pitch control. Thrust can be transferred from the cruise nozzle to the lift nozzles and the lift fan to produce longitudinal and vertical thrust during transition and hover.

The lift-cruise engine responds to total thrust command, $T_{T_{CMD}}$, which is calculated as a sum of the individual nozzle thrust commands that are generated from the control selector as given by equation 30 or 40. The closed loop core thrust dynamic response is modeled by a second-order transfer function with a damping ratio ζ and natural frequency ω_{core}:

$$T_T = \left(\frac{\omega_{core}^2}{s^2 + 2\zeta\omega_{core}\, s + \omega_{core}^2} \right) T_{T_{CMD}} \qquad (45)$$

A rate limit, $\dot{T}_{T_{max}}$, and lift-cruise engine thrust magnitude limit, $T_{T_{max}}$, are included in the second-order transfer function model to represent physical thermal limits of the propulsion system. Nominal values for these dynamic properties are

$$\zeta = 0.707 \quad \omega_{core} = 10 \text{ rad/sec} \quad \dot{T}_{T_{max}} = 8000 \text{ lb/sec}$$

The proportion of total thrust distributed to each component is determined by the ratio of each nozzle thrust command to the total thrust command:

$$T_i = \frac{T_{i_{CMD}}}{T_{T_{CMD}}} T_T \eta_i \qquad (46)$$

where i represents the individual components (CN, LF, LLN, and RLN). The thrust transfer rate for each nozzle, $\dot{T}_{i_{TF}}$, is limited to $\dot{T}_{TF_{max}}$, nominally 30,000 lb/sec. The factor η_i is the efficiency factor for each nozzle.

For this experiment, a generic energy transfer between the lift-cruise engine and the lift fan is assumed. Dynamically, the lift fan thrust at the lift fan nozzle exit, T_{LF} from equation 46, is dependent on lift fan rotational speed and inlet guide vane setting. The dynamic response is modeled by a first-order transfer function with a time constant of ω_{LF}, plus a first-order washout transfer function, as shown in figure 2. A rate limit, $\dot{T}_{LF\,max}$, and a maximum lift fan thrust limit, T_{LFmax}, are included to represent physical constraints of the lift fan dynamics. The upper and lower inlet guide vane (IGV) authorities are defined as shown in equation 47, in which K_{IGV_U} and K_{IGV_L} are in percent of total lift fan thrust:

$$TIGV_U = K_{IGV_U}\, T_{LF_S}, \quad TIGV_L = K_{IGV_L}\, T_{LF_S} \qquad (47)$$

The total lift fan thrust, T_{LF}, is in part due to rotational speed and in part to IGV thrust, where η_{LF} is the lift fan efficiency constant:

$$T_{LF} = \left(T_{LF_S} + T_{LF_F} \right) \times \eta_{LF} \qquad (48)$$

The mass flow rates of the primary and auxiliary inlets are functions of the maximum lift-cruise engine thrust and the respective maximum mass flow rates from the individual inlets as shown in equations 49 and 50. A maximum mass flow rate of 11.2 slug/sec was used in each case. Primary inlets are opened in CTO and APP, and are closed in TRC. Auxiliary inlets are only opened in TRC to reduce hot gas reingestion. The mass flow rate of the lift fan inlet is modeled as a function of lift fan thrust, maximum lift fan thrust, and the maximum lift fan mass flow rate (eq. 51) which was set to 14.0 slug/sec:

$$\dot{m}_{PI} = \left(\frac{T_T}{T_{TMAX}} \right) \dot{m}_{PImax} \qquad (49)$$

$$\dot{m}_{AI} = \left(\frac{T_T}{T_{TMAX}} \right) \dot{m}_{AImax} \qquad (50)$$

$$\dot{m}_{LFI} = \left(\frac{T_{LF}}{T_{LFMAX}} \right) \dot{m}_{LFImax} \qquad (51)$$

Aggregate propulsion forces and moments from each component are resolved into the aircraft body axes and appear in the following equations:

Axial force

$$F_{EX} = F_{CN_x} + F_{LLN_x} + F_{RLN_x} + F_{LF_x} + F_{PI_x} + F_{AI_x} + F_{LFI_x} \qquad (52)$$

where

$$F_{CN_x} = T_{CN} \cos\delta_{CN}$$

$$F_{LLN_x} = T_{LLN} \sin\delta_{LN} \cos\delta_{LNy}$$

$$F_{RLN_x} = T_{RLN} \sin\delta_{LN} \cos\delta_{LNy}$$

$$F_{LF_x} = T_{LF} \sin\delta_{LF}$$

$$F_{PI_x} = \dot{m}_{PI}\left(-U_B - Q_B z_{PI}\right)$$

$$F_{AI_x} = \dot{m}_{AI}\left(-U_B - Q_B z_{AI}\right)$$

$$F_{LFI_x} = \dot{m}_{LFI}\left(-U_B - Q_B z_{LFI}\right)$$

Side force

$$F_{EY} = F_{LNy} + F_{PI_y} + F_{AI_y} + F_{LFI_y} + F_{RCS_y} \qquad (53)$$

where

$$F_{LNy} = T_{LN} \sin\delta_{LNy}$$

$$F_{RCSy} = -\delta_{YRCS}$$

$$F_{PIy} = \dot{m}_{PI}\left(-V_B + P_B z_{PI} - R_B x_{PI}\right)$$

$$F_{AIy} = \dot{m}_{AI}\left(-V_B + P_B z_{AI} - R_B x_{AI}\right)$$

$$F_{LFIy} = \dot{m}_{LFI}\left(-V_B + P_B z_{LFI} - R_B x_{LFI}\right)$$

Normal force

$$F_{EZ} = F_{CN_z} + F_{LLN_z} + F_{RLN_z} + F_{LF_z} + F_{PI_z} + F_{AI_z} + F_{LFI_z} + F_{RCSz} \qquad (54)$$

where

$$F_{CN_z} = -T_{CN} \sin \delta_{CN}$$

$$F_{LLN_z} = -T_{LLN} \cos \delta_{LN} \cos \delta_{LNy}$$

$$F_{RLN_z} = -T_{RLN} \cos \delta_{LN} \cos \delta_{LNy}$$

$$F_{LF_z} = -T_{LF} \cos \delta_{LF}$$

$$F_{RCSz} = \delta_{PRCS}$$

$$F_{PI_z} = \dot{m}_{PI}(-W_B + Q_B x_{PI})$$

$$F_{AI_z} = \dot{m}_{AI}(-W_B + Q_B x_{AI})$$

$$F_{LFI_z} = \dot{m}_{LFI}(-W_B + Q_B x_{LFI})$$

Rolling moment

$$T_{EL} = -F_{LLN_z} y_{LLN} + F_{RLN_z} y_{RLN} + \delta_{RRCS} y_{RCS} - F_{PI_y} z_{PI} - F_{AI_y} z_{AI} - F_{LFI_y} z_{LFI} \quad (55)$$

Pitching moment

$$T_{EM} = -F_{CN_z} x_{CN} - F_{LLN_z} x_{LLN} - F_{RLN_z} x_{RLN} - F_{LF_z} x_{LF} + F_{CN_x} z_{CN} + F_{LLN_x} z_{LLN} + F_{RLN_x} z_{RLN} + F_{LF_x} z_{LF} - F_{RCSz} x_{RCS} - F_{PI_z} x_{PI} - F_{AI_z} x_{AI} - F_{LFI_z} x_{LFI} + F_{PI_x} z_{PI} + F_{AI_x} z_{AI} + F_{LFI_x} z_{LFI} \quad (56)$$

Yawing moment

$$T_{EN} = F_{LNy} x_{LN} + F_{LLN_x} y_{LLN} - F_{RLN_x} y_{RLN} + F_{RCSy} x_{RCS} + F_{PI_y} x_{PI} + F_{AI_y} x_{AI} + F_{LFI_y} x_{LFI} \quad (57)$$

Concluding Remarks

The models of the integrated flight/propulsion control system, propulsion system, and head-up display, used in the simulation of an advanced short takeoff and vertical landing lift fan fighter aircraft, have been modified to reflect recent experience from flight and simulation experiments with STOVL operations. These revisions have been made based on evaluations during earlier simulations of this lift fan STOVL configuration, as well as from the V/STOL Systems Research Aircraft. They include nonlinear inverse control laws in all axes (eliminating earlier versions with state rate feedback), throttle scaling laws for flightpath and thrust command, control selector commands apportioned based on relative effectiveness of the individual controls, lateral guidance algorithms that provide more flexibility for terminal area operations, and a simpler representation of the propulsion system. A separate report describes the aircraft's aerodynamics in wing-borne and jet-borne flight.

References

1. Chung, W. W. Y.; Borchers, P. F.; and Franklin, J. A.: Simulation Model of the Integrated Flight/Propulsion Control System, Displays, and Propulsion System for an ASTOVL Lift Fan Aircraft. NASA TM-108866, April 1995.

2. Birckelbaw, L. G.; McNeill, W. E.; and Wardwell, D. A.: Aerodynamics Model for Generic Lift-Fan Aircraft. NASA TM-110347, April 1995.

3. Franklin, J. A.; Stortz, M. W.; Borchers, P. F.; and Moralez, E.: Flight Evaluation of Advanced Controls and Displays for Transition and Landing on the NASA V/STOL Systems Research Aircraft. NASA TP-3607, April 1996.

4. Merrick, V. K.; and Jeske, J. A.: Flightpath Synthesis and HUD Scaling for V/STOL Terminal Area Operations. NASA TM-110348, April 1995.

5. Merrick, V. K.; Farris, G. G.; and Vanags, A. A.: A Head Up Display for Application to V/STOL Aircraft Approach and Landing. NASA TM-102216, January 1990.

6. Meyer, G.; and Cicolani, L: Application of Nonlinear Inverses to Automatic Flight Control Design – System Concepts and Flight Evaluations. AGARDograph No. 251, 1981.

7. Franklin, J. A.: Application of Nonlinear Inverse Methods to the Control of Powered-Lift Aircraft Over the Low-Speed Flight Envelope. International Journal of Control, vol. 59, no. 1, January 1994.

Table 1. Aircraft geometry

	Overall length	55.4 ft
	Overall height	14.16 ft
Wing	Area	523.3 ft^2
	Span	36.17 ft
	Mean aerodynamic chord	18.42 ft
	Aspect ratio	2.50
	Leading edge sweep	40.0 deg
	Trailing edge sweep	30.0 deg
	Airfoil	NACA 64A005
Canard	Area	243.1 ft^2
	Span	24.65 ft
	Mean aerodynamic chord	12.55 ft
	Aspect ratio	2.50
	Leading edge sweep	40.0 deg
	Trailing edge sweep	30.0 deg
	Airfoil	NACA 64A004.5
Vertical tail (each)	Area	39.0 ft^2
	Span	6.98 ft
	Mean aerodynamic chord	7.11 ft
	Aspect ratio	1.25
	Leading edge sweep	40.0 deg
	Trailing edge sweep	30.0 deg
	Airfoil	NACA 64A004.5

Table 2. Mass properties

Weight	30,000 lb
x cg location	373.3 in.
y cg location	0.0 in.
z cg location	96.0 in.
Pitch moment of inertia	91,200 slug-ft^2
Roll moment of inertia	14,300 slug-ft^2
Yaw moment of inertia	101,000 slug-ft^2
Product of inertia	0 slug-ft^2

Table 3. Flight control modes

Control axis	Control mode designations (applicable flight phases)			
	CTO (wing-borne flight)	MTV (transition, hover) APP (transition)	APP (transition, hover)	TRC (hover)
Pitch/roll	Rate command	Rate command – attitude hold, blend to attitude command	Rate command – attitude hold, blend to attitude command	
Yaw	Sideslip command	Sideslip command, blend to yaw rate command	Sideslip command, blend to yaw rate command	Yaw rate command
Vertical	Aerodynamic lift	Thrust magnitude	Flightpath command, blend to velocity command	Velocity command
Longitudinal	Thrust magnitude	Thrust vector angle (MTV), acceleration command – velocity hold (APP)	Acceleration command – velocity hold	Velocity command
Lateral				Velocity command

Table 4. Throttle scaling logic flow

(a) Flightpath command

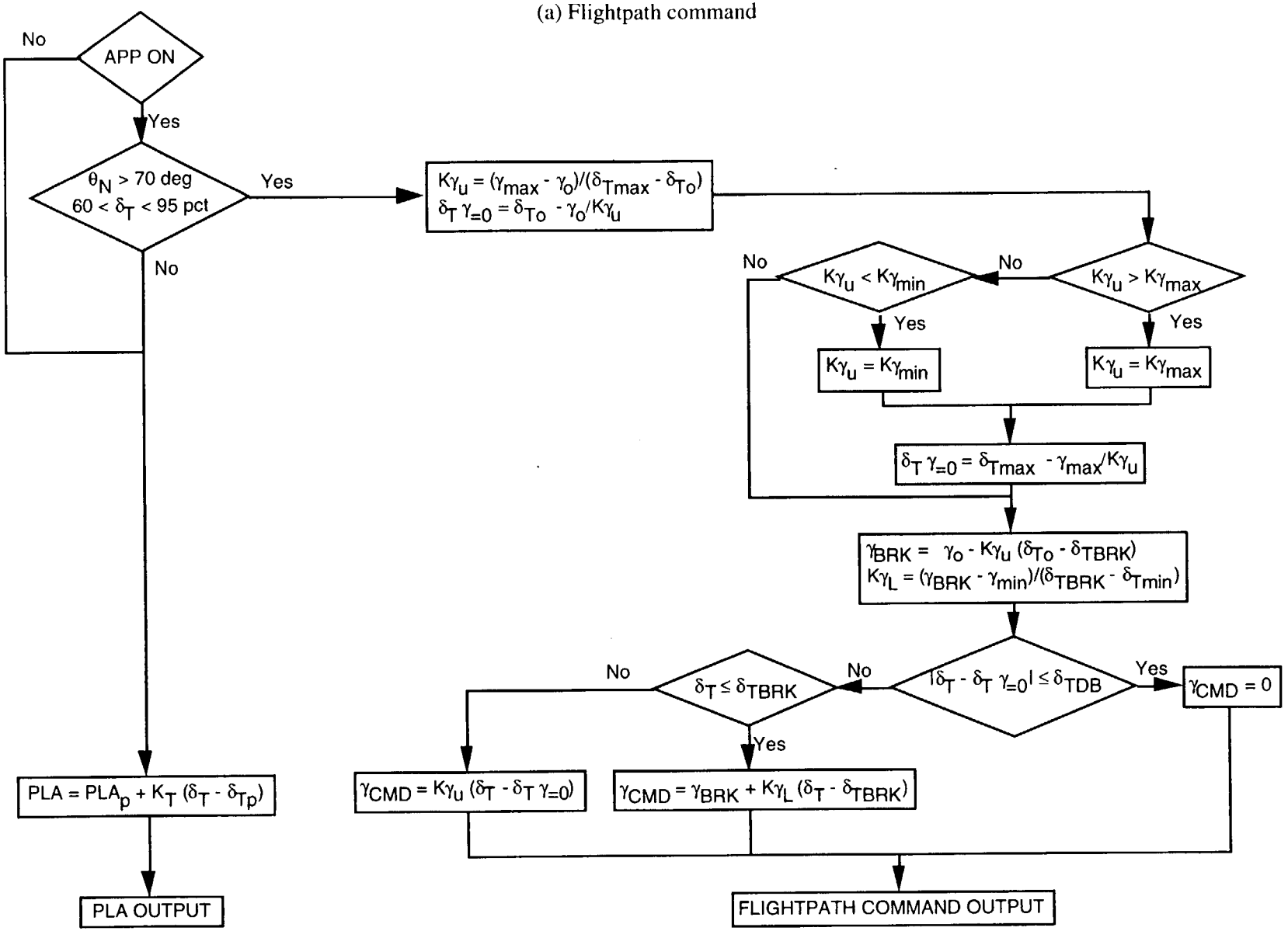

Table 4. Concluded

(b) Thrust command

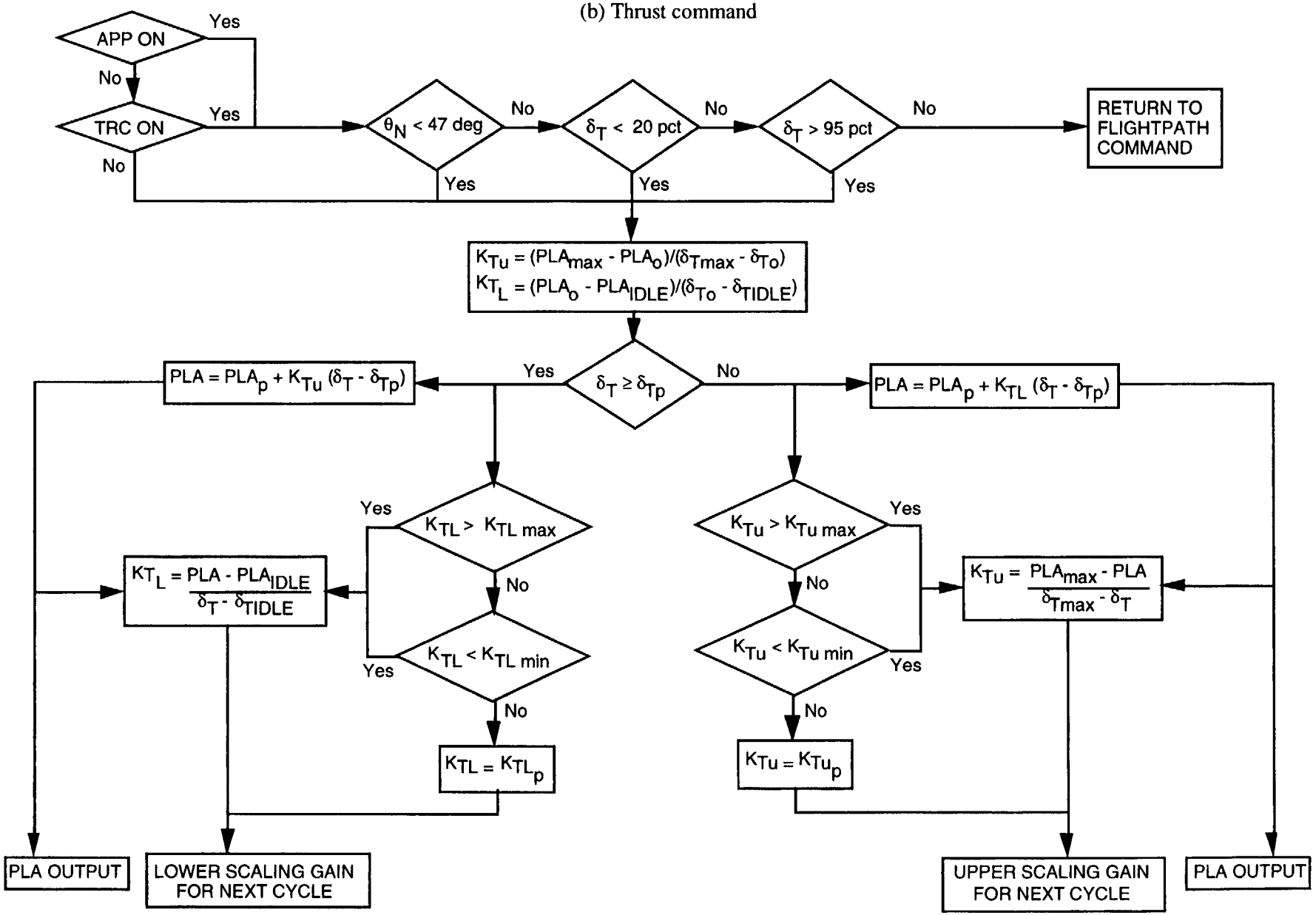

Table 5. Maximum and minimum throttle control commands and control sensitivity slopes

δ_{cmd}	Maximum	Minimum	Max slope	Min slope
Thrust magnitude, %	100	3	1.01	0.99
Flightpath angle, γ, deg	10	−10	0.43 deg/%	0.23 deg/%
Vertical velocity, $\dot{h}$, ft/sec	17.5	−17.5	0.75 ft/sec/%	0.4 ft/sec/%

Table 6. Control mode gains

Attitude control	
Pitch	Roll
Control limits = ±5.65 in.	Control limits = ±4.2 in.
Force gradient = 1 lb/in.	Force gradient = 0.7 lb/in.
Breakout = 0.15 in.	Breakout = 0.05 in.
K_{qCAH} = 0.6 rad/sec^3/in.	K_{pCAH} = 2 rad/sec^3/in.
K_{THEH} = 0.2 rad/sec^2/in.	K_{PHIH} = 0.7 rad/sec^2/in.
K_{THECAH} = 0.6 rad/sec^2/in.	K_{PHICAH} = 1.5 rad/sec^2/in.
K_{θ} = 9 sec^{-2}	K_{ϕ} = 9 sec^{-2}
$K_{\dot{\theta}}$ = 6 sec^{-1}	$K_{\dot{\phi}}$ = 6 sec^{-1}
K_{qC} = 0.66 rad/sec^2/in.	K_{pC} = 3 rad/sec^2/in.
K_{α} = 4 sec^{-2}	K_{ps} = 6 sec^{-1}
K_q = 6 sec^{-1}	
τ_{pitch} = 1 sec	
Yaw – transition	Yaw – hover
Control limits = ±2.12 in.	Same
Force gradient = 15 lb/in.	Same
Breakout = 0.1 in.	Same
$K_{\delta p}$ = 0.5 rad/sec^2/in.	$K_{\delta pH}$ = 1.4
$K_{\dot{\beta}}$ = 2.8 sec^{-1}	$K_{\dot{\psi}}$ = 4 sec^{-1}
K_{β} = 4 sec^{-2}	K_B = 0 (V ≤ 40 knots); 1.0 (V ≥ 60 knots)
τ_{BETA} =0.25 sec	
Velocity control	
Longitudinal velocity	Vertical velocity
Control limits	$K_{\gamma\theta}$ = 1 rad/rad
Stick = ±2.25 in.	K_{Vz} = 0.8 sec^{-1}
Thumbwheel = ±100 deg	K_{AZ} = 1
Breakout	τ_{vert} = 0.1 sec
Stick = 0.225 in.	
Thumbwheel = 5.5 deg	Lateral velocity
$K_{\dot{V}_X}$ = 0.1 ft/sec^2/deg	K_{Vyc} = 5 ft/sec/in.
τ_{long} = 2 sec	K_{Vy} = 0.25 rad/sec^2/ft/sec
K_{Vxc} = 8 ft/sec/in.	τ_{lat} = 5 sec
K_{Vx} = 1 sec^{-1}	Rate limit = 5 ft/sec^2/in.
τ_{Vc} = 2 sec	

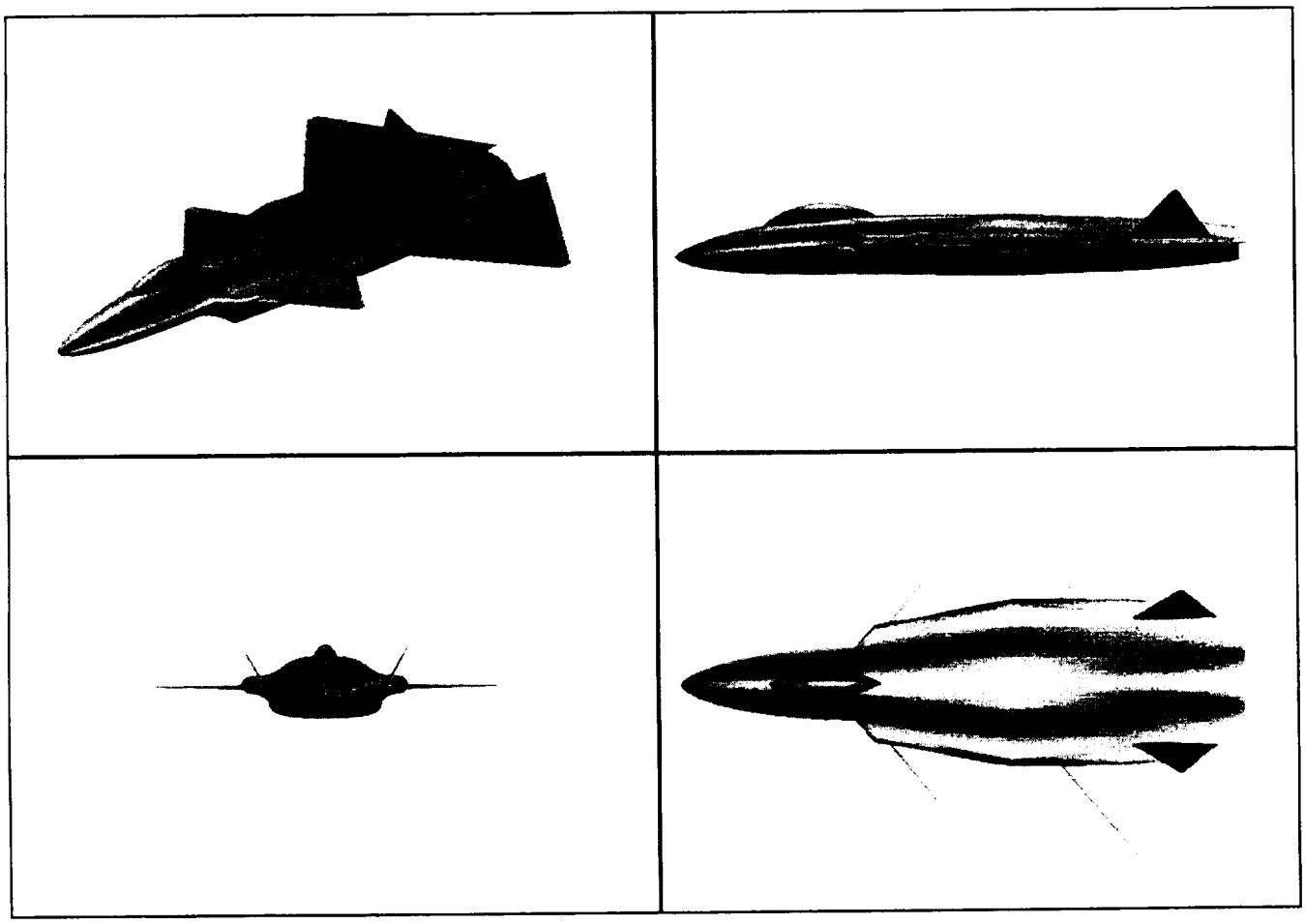

Figure 1. Views of the ASTOVL lift-fan aircraft.

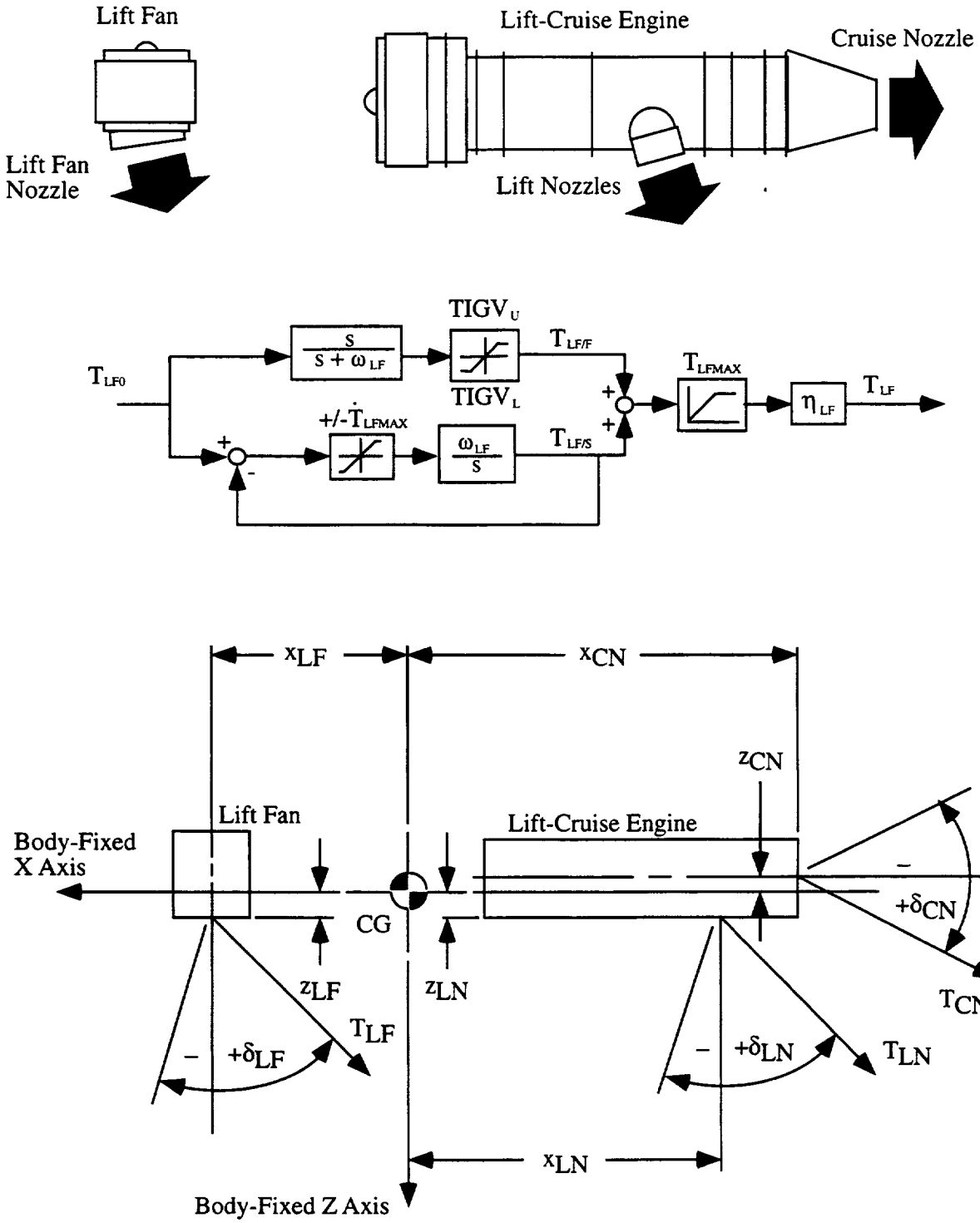

Note: Distances measured forward of the center of gravity are considered positive. Distances measured below the center of gravity are considered positive.

x_{CN} = -19.72 ft	z_{CN} = 0 ft	δ_{CN} range = +20°, -20°
x_{LF} = 11.70 ft	z_{LF} = 1.93 ft	δ_{LF} range = +45°, -10°
x_{LN} = - 8.93 ft	z_{LN} = 0 ft	δ_{LN} range = +45°, -10°
y_{LN} = 4.04 ft		δ_{LNy} range = +10°, -10°

Figure 2. Propulsion system configuration.

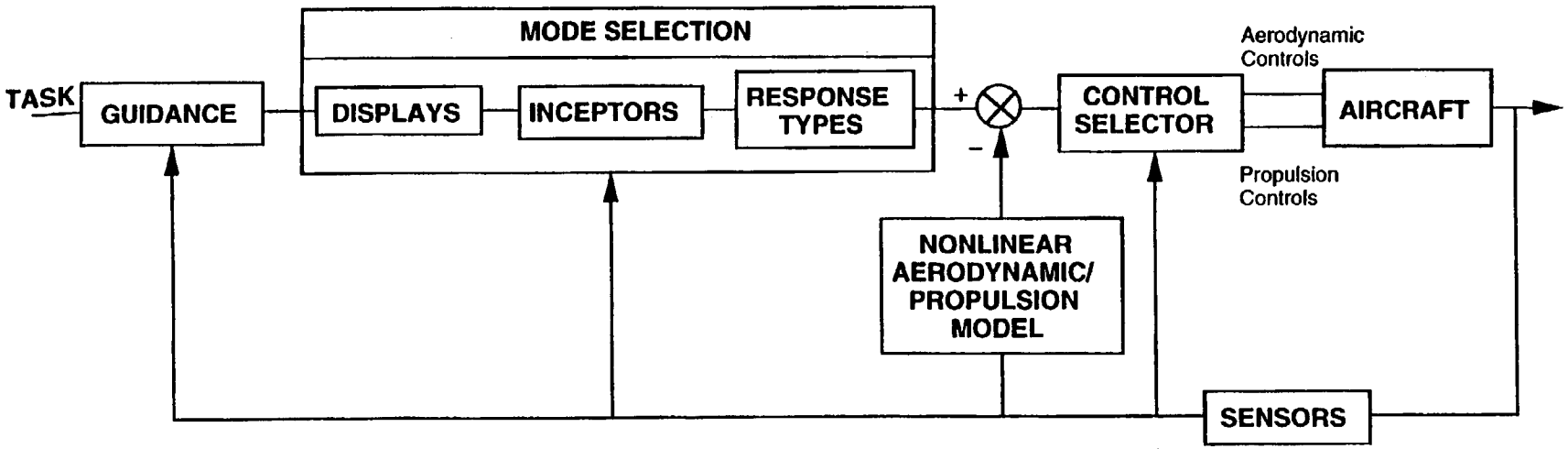

Figure 3. Control Loop structure.

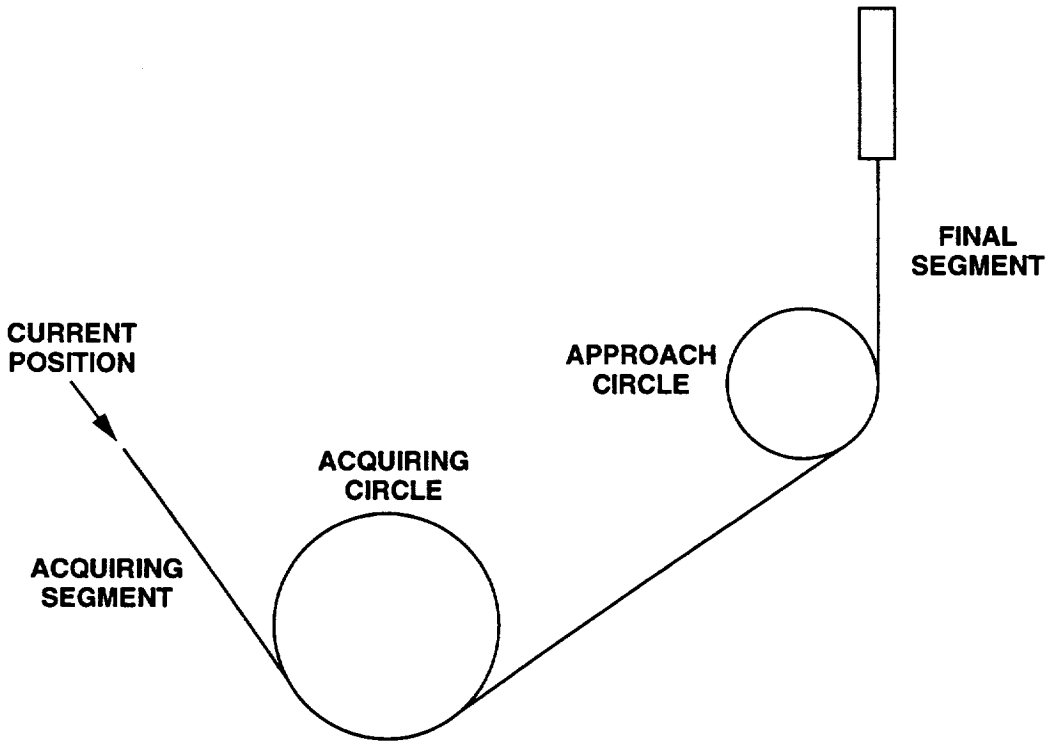

Figure 4. Horizontal guidance.

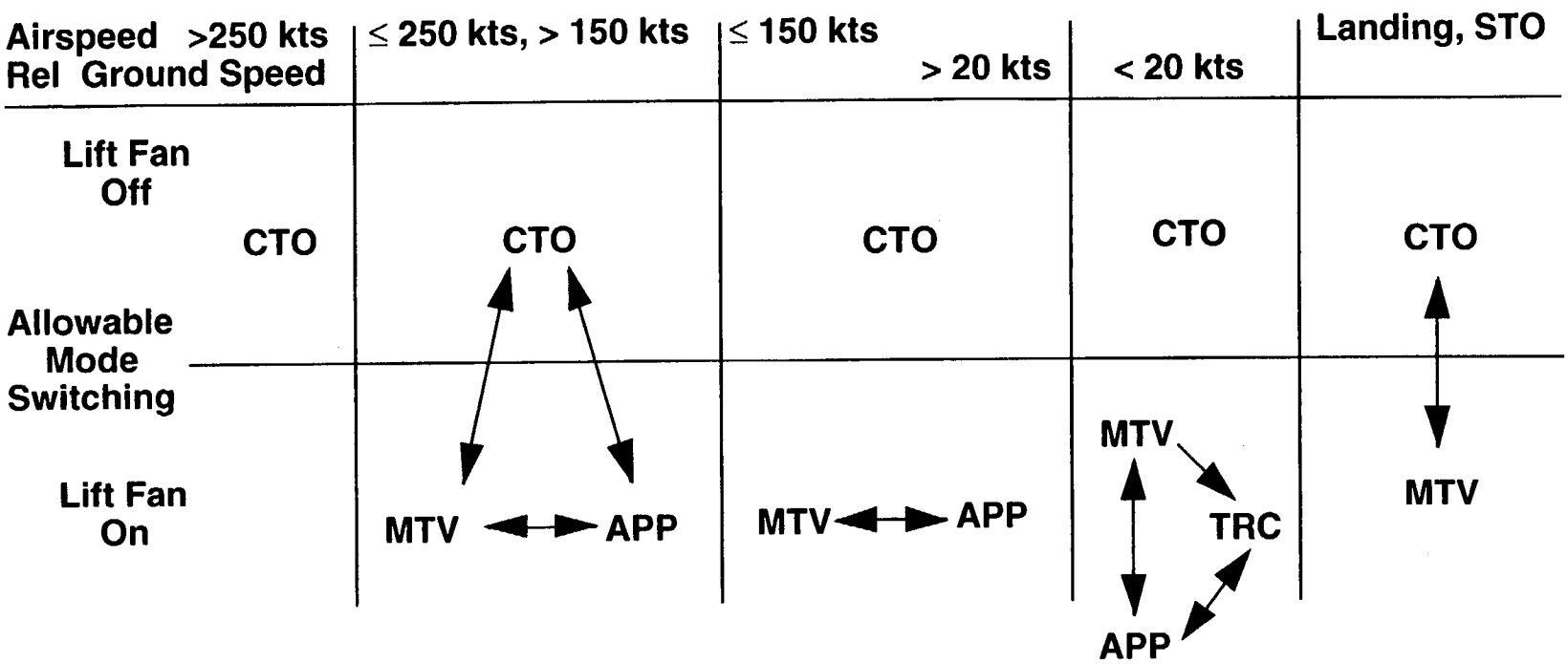

- When airborne, the pilot cannot manually disengage the lift fan until the thrust vector deflection angle reaches its minimum
- Disengagement of nozzle lever clutch in APP or TRC mode causes reversion to MTV mode

Figure 5. Control mode selection logic.

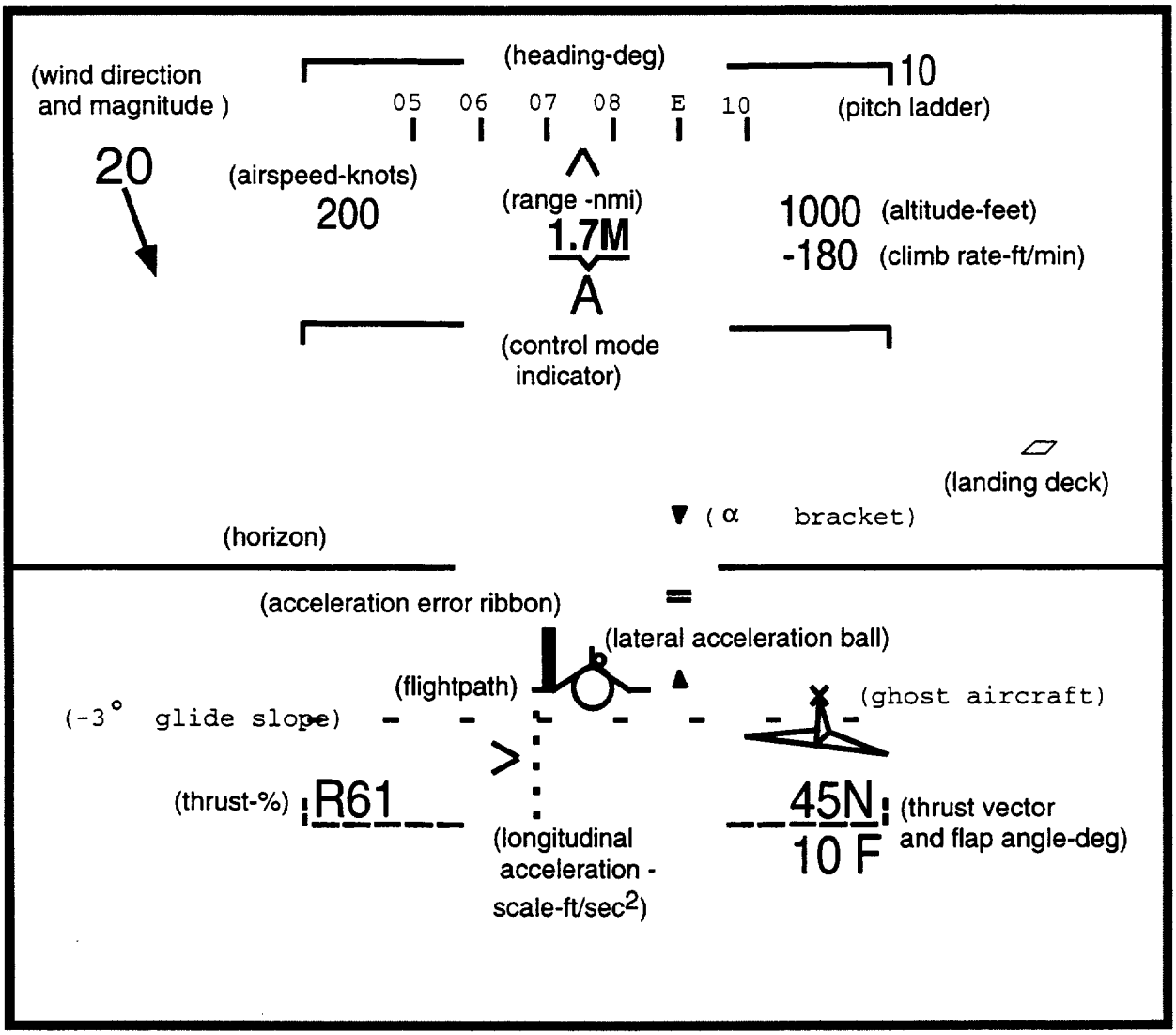

Figure 6. Approach display.

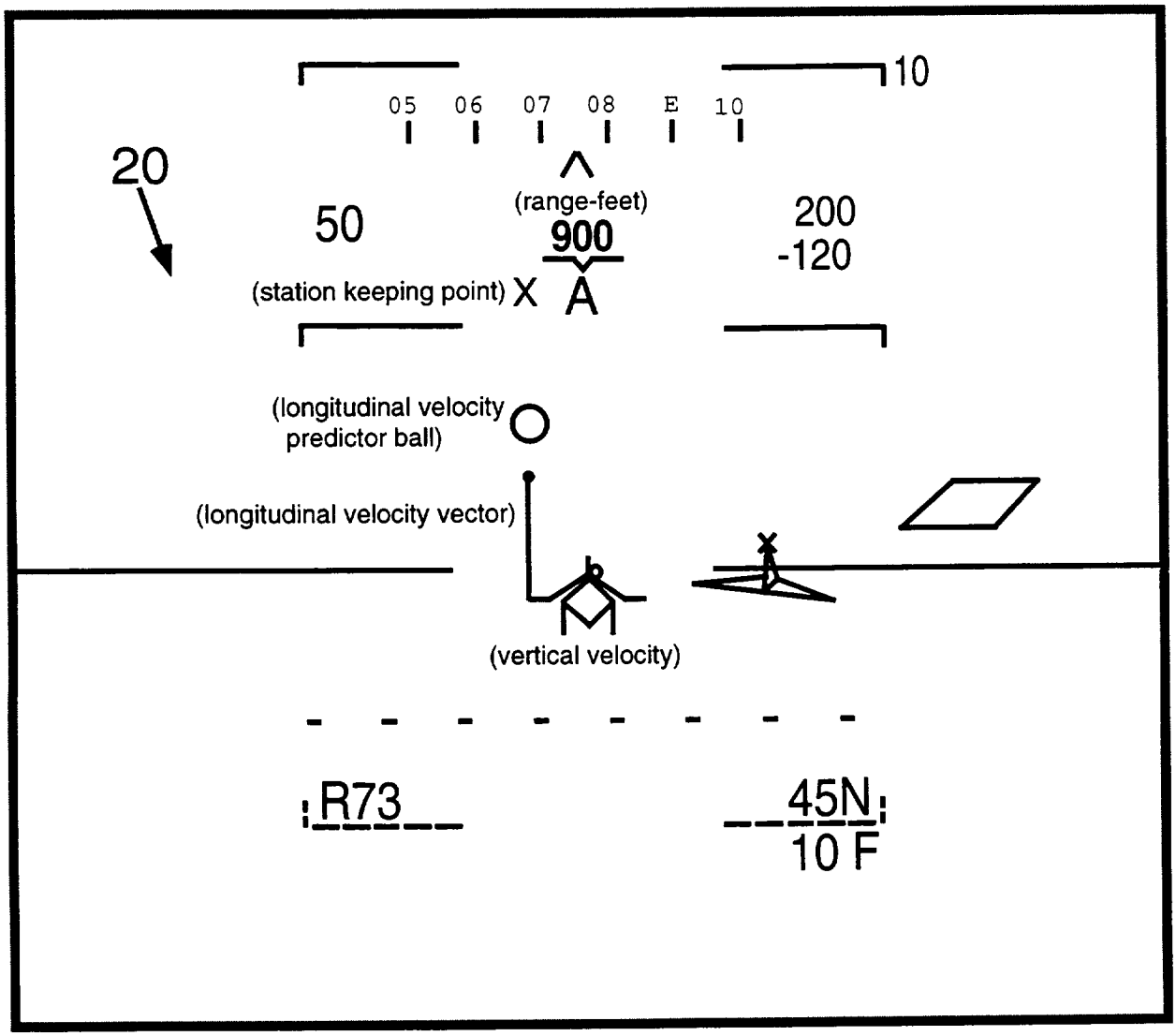

Figure 7. Symbology for station keeping point capture.

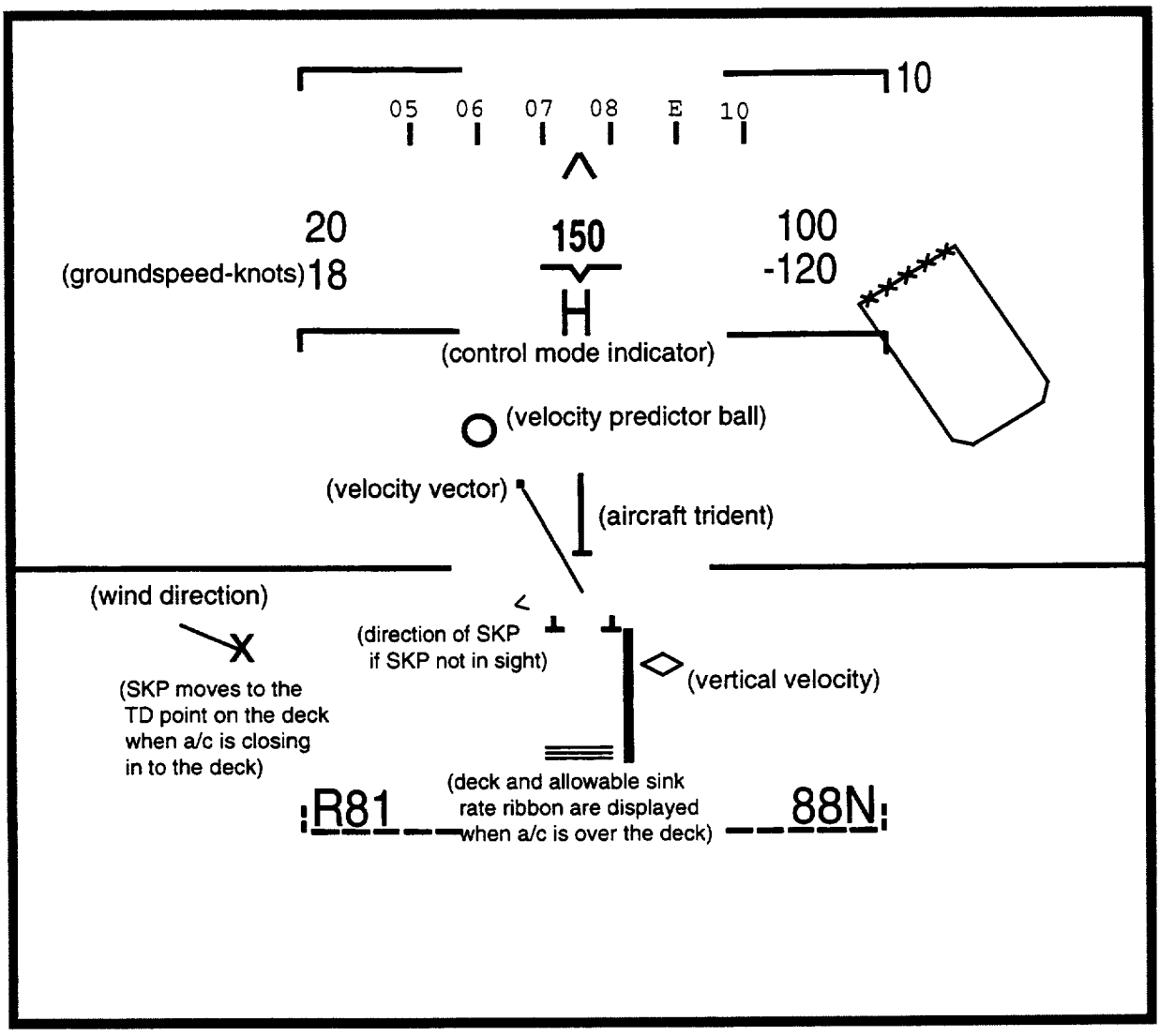

Figure 8. Hover display.

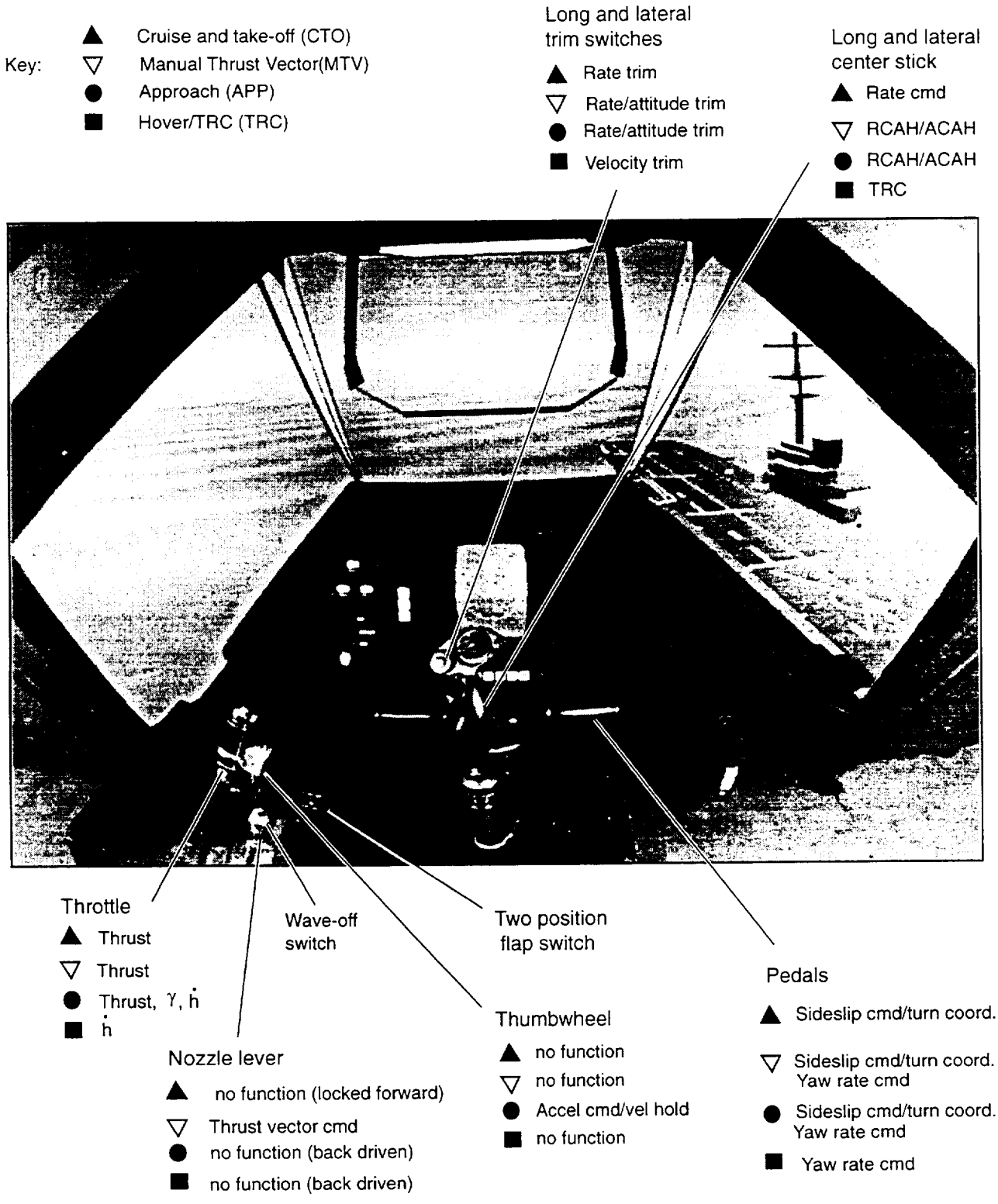

Figure 9. Inceptor functions.

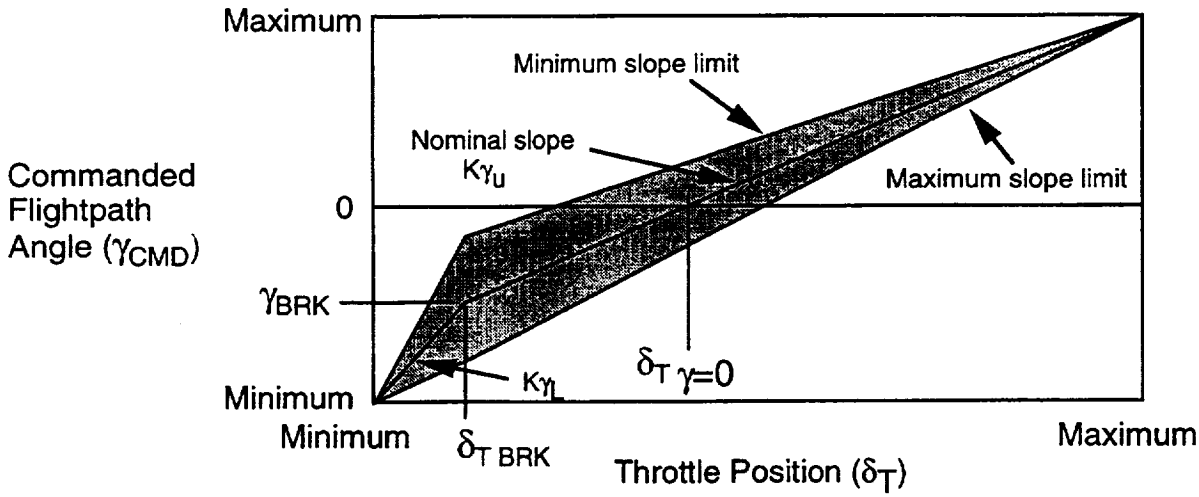

10a. Flightpath command

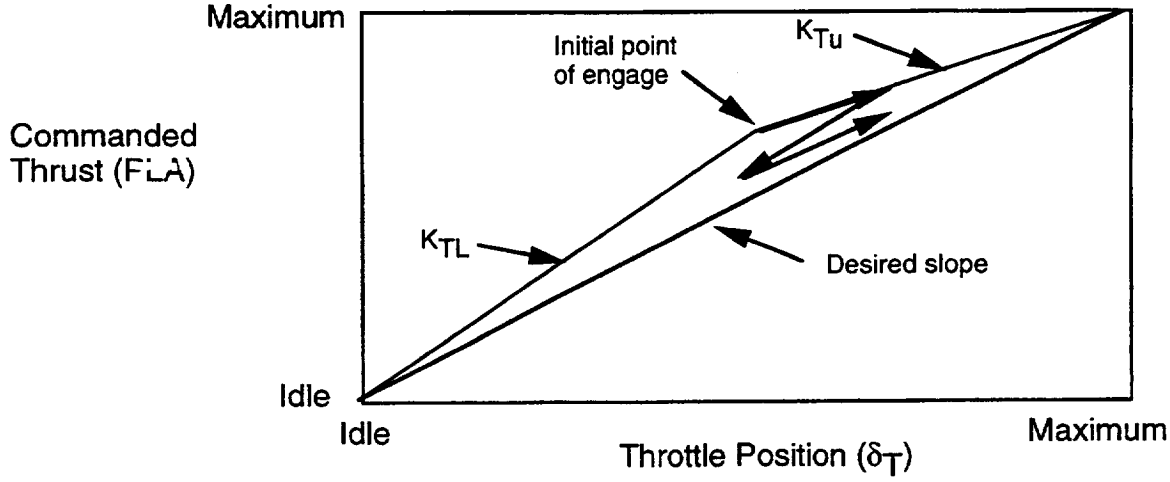

10b. Thrust command

Figure 10. Throttle command relationships.

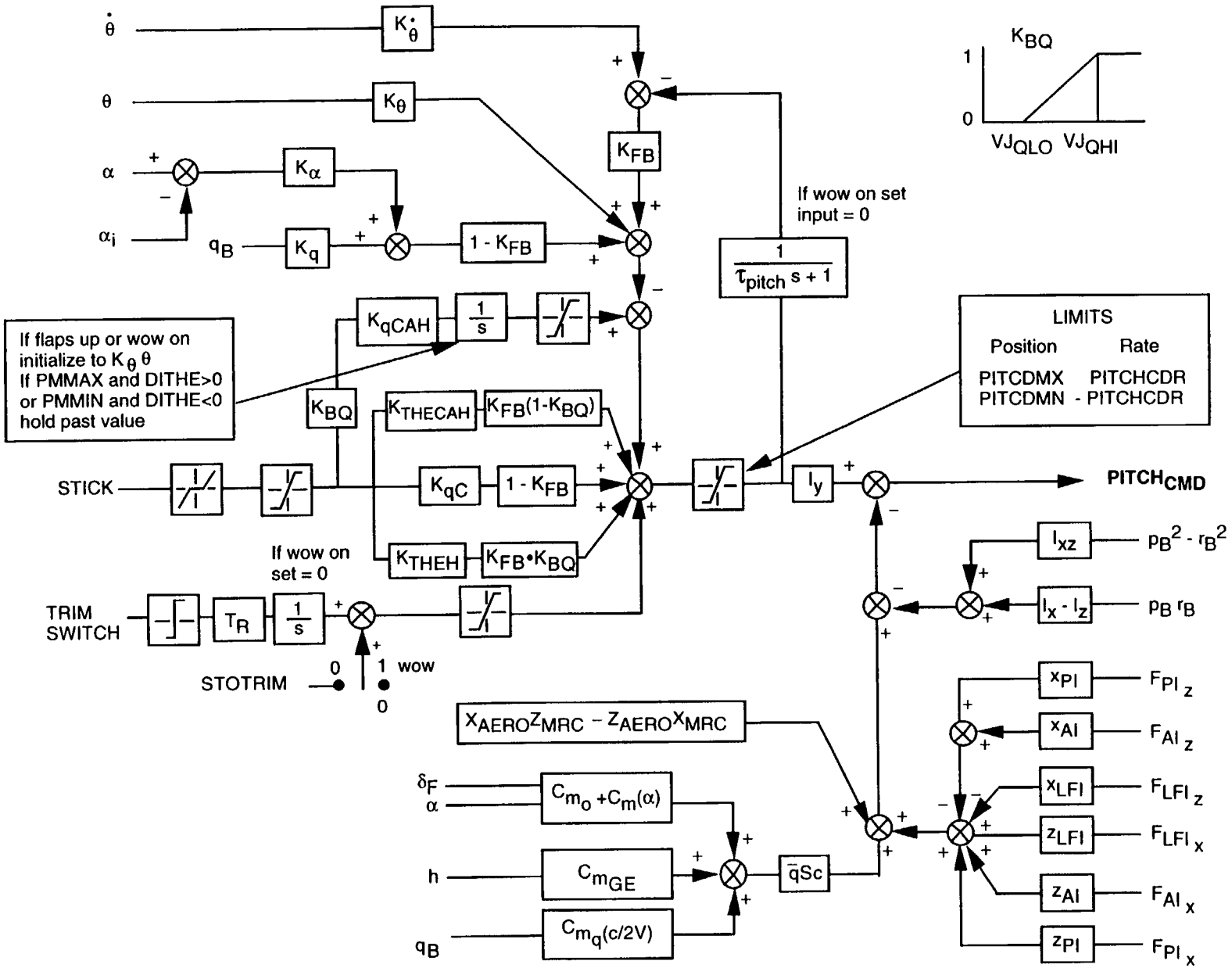

Figure 11. Pitch stabilization and command augmentation.

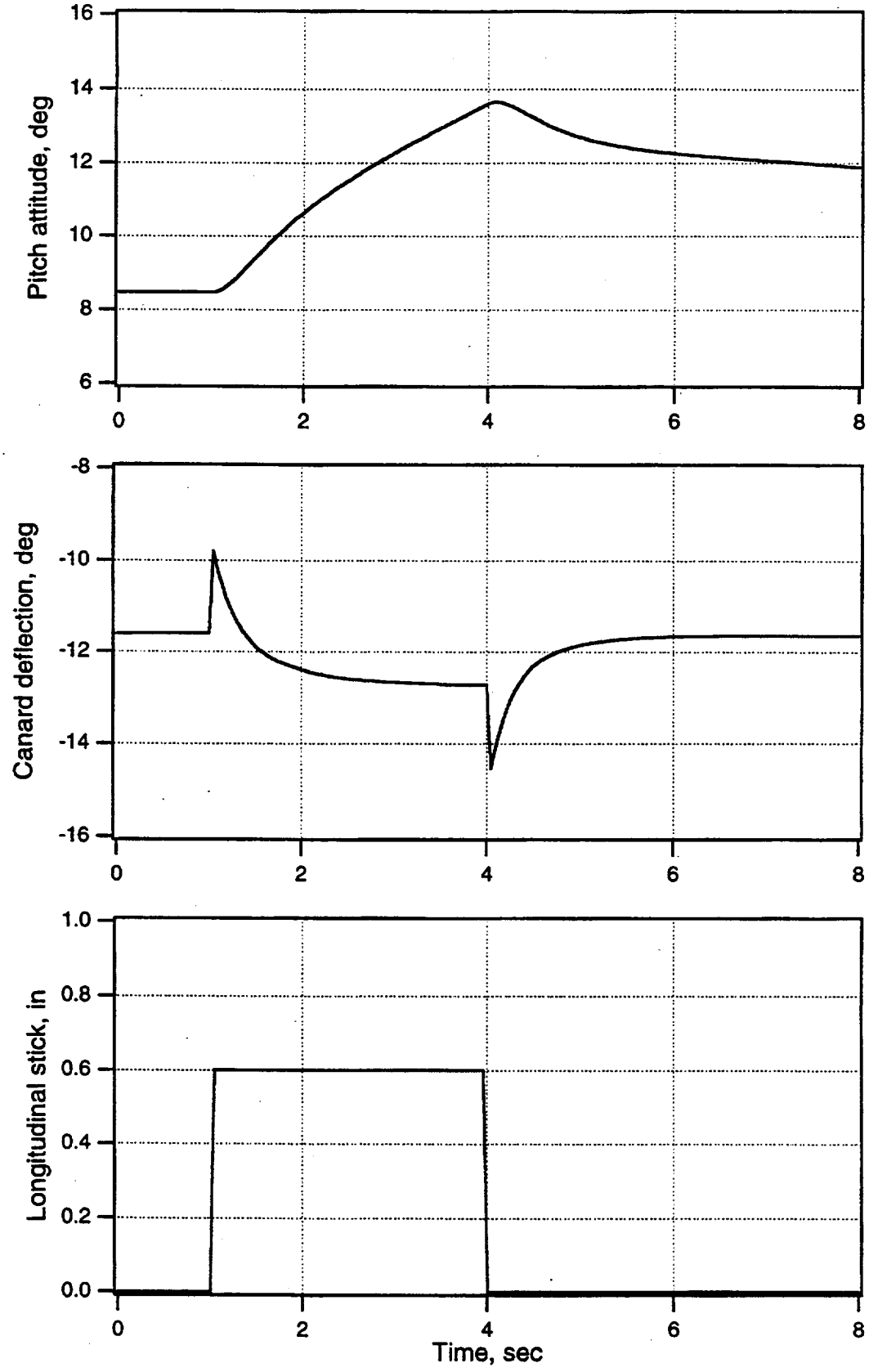

Figure 12a. Pitch response to pitch rate command at 200 knots.

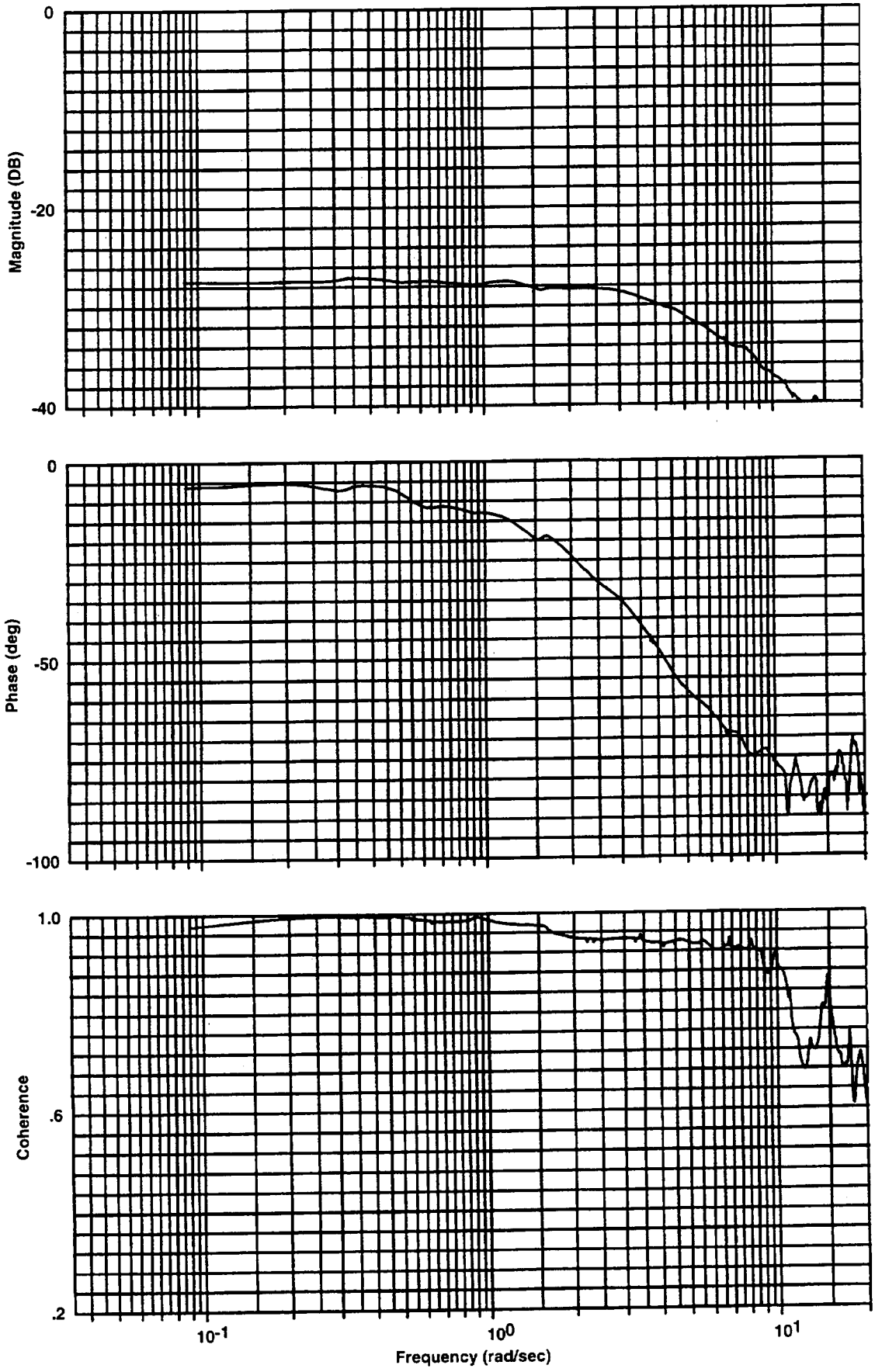

Figure 12b. Closed loop frequency response of pitch rate to pitch rate command for pitch rate command/attitude hold system at 200 knots.

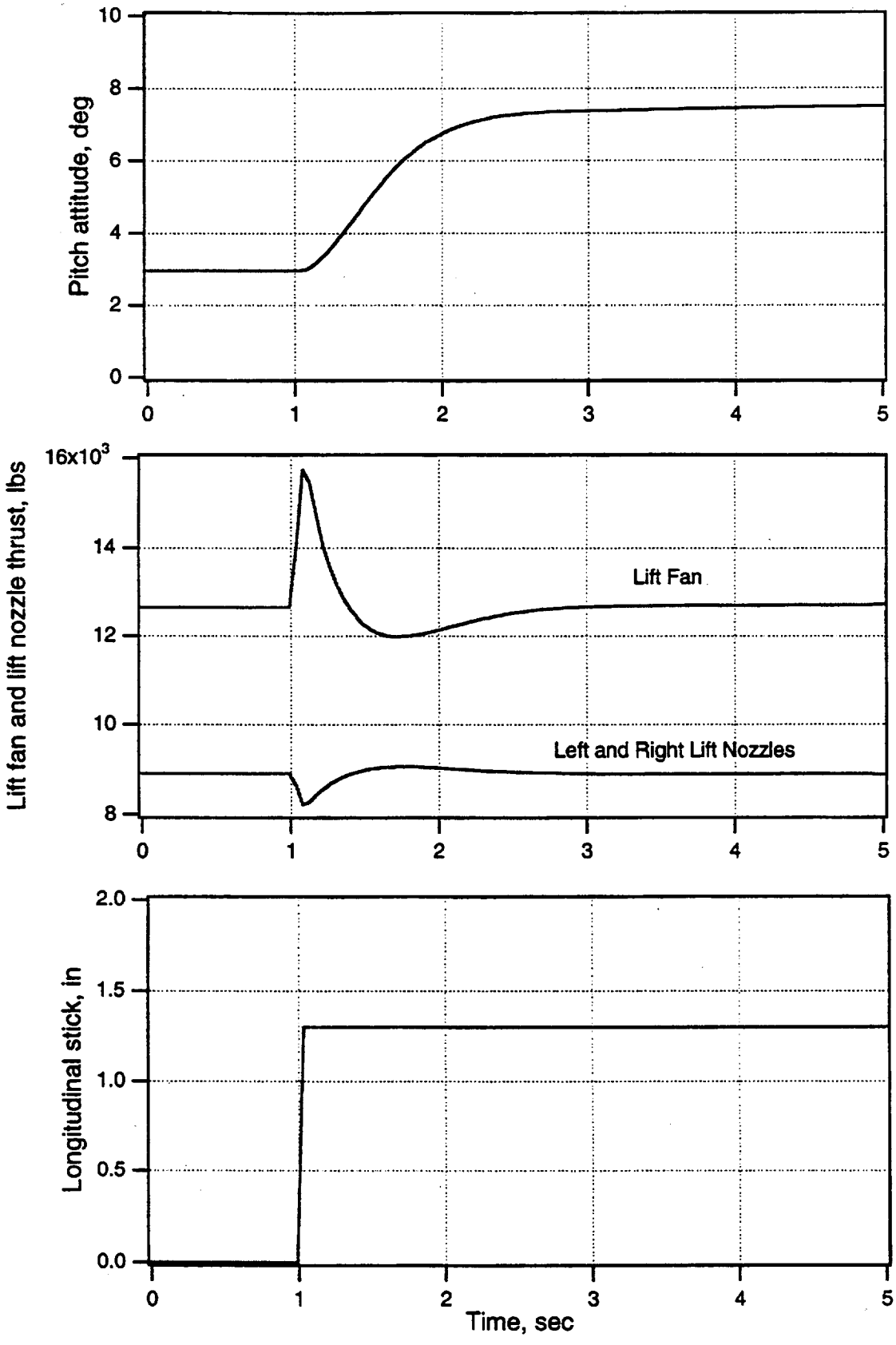

Figure 13a. Pitch response to pitch attitude command in hover.

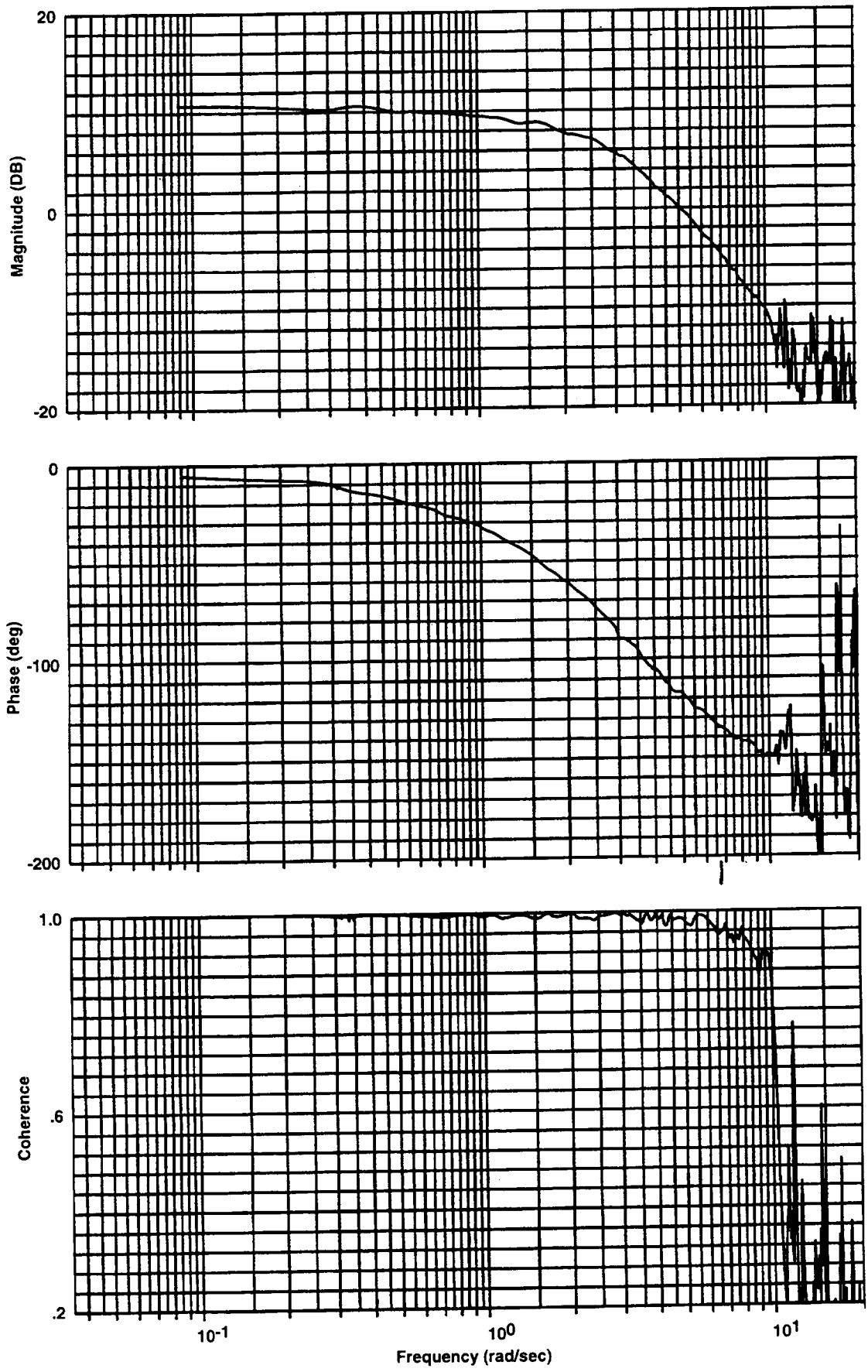

Figure 13b. Closed loop frequency response of pitch attitude to pitch attitude command for pitch attitude command/attitude hold system in hover.

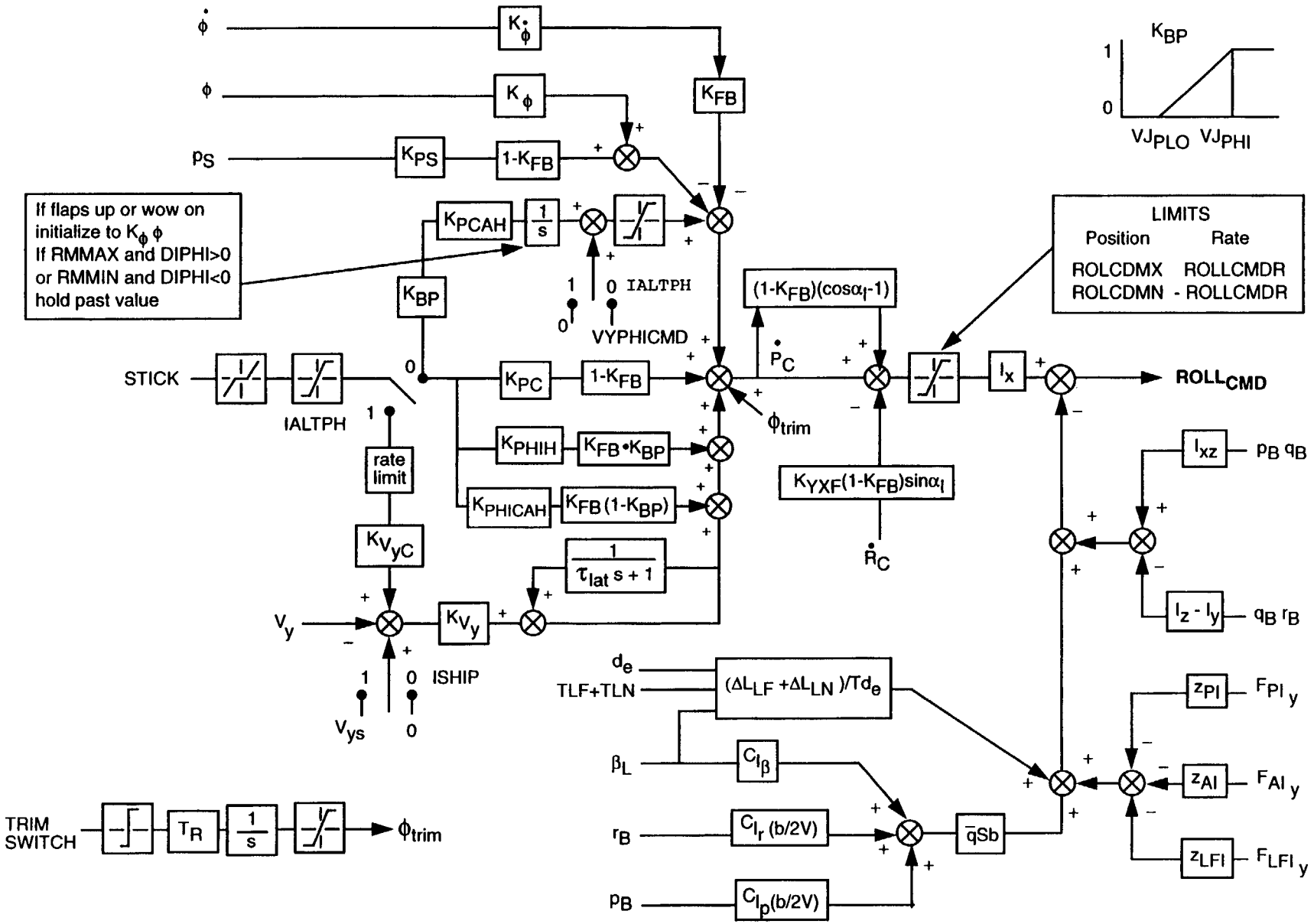

Figure 14. Roll stabilization and command augmentation.

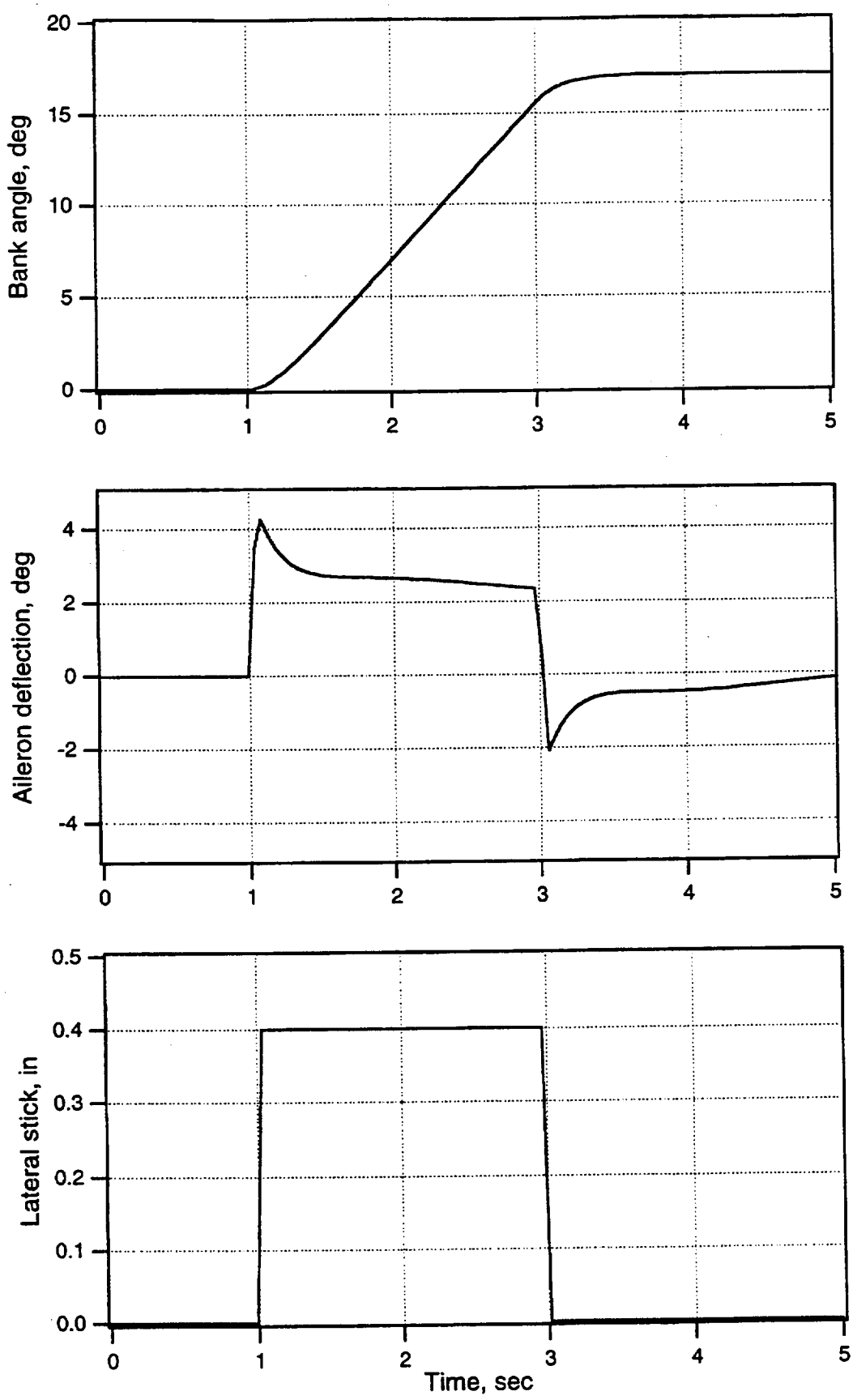

Figure 15a. Roll response to roll rate command at 200 knots.

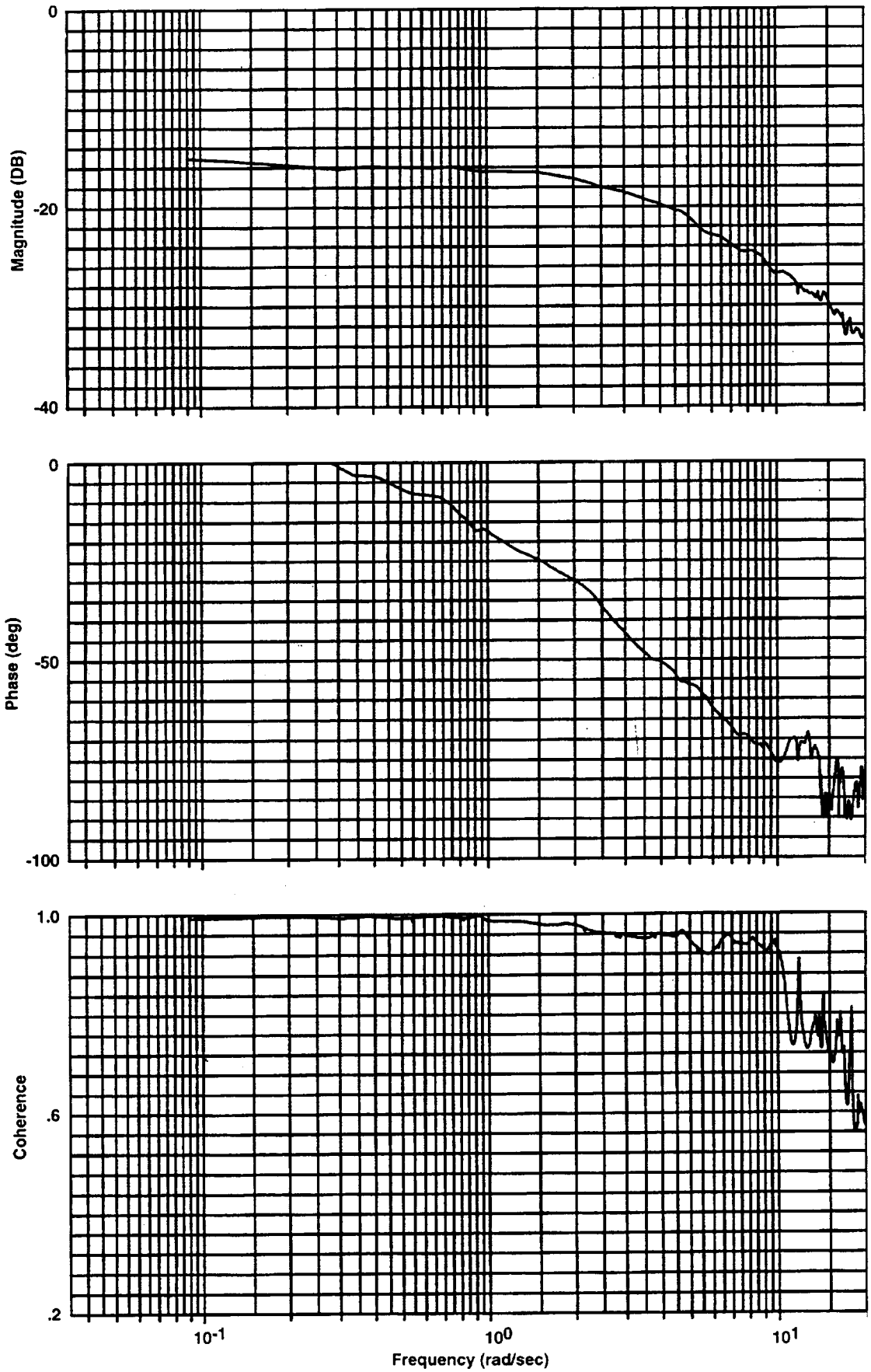

Figure 15b. Closed loop frequency response of roll rate to roll rate command for roll rate command/attitude hold system at 200 knots.

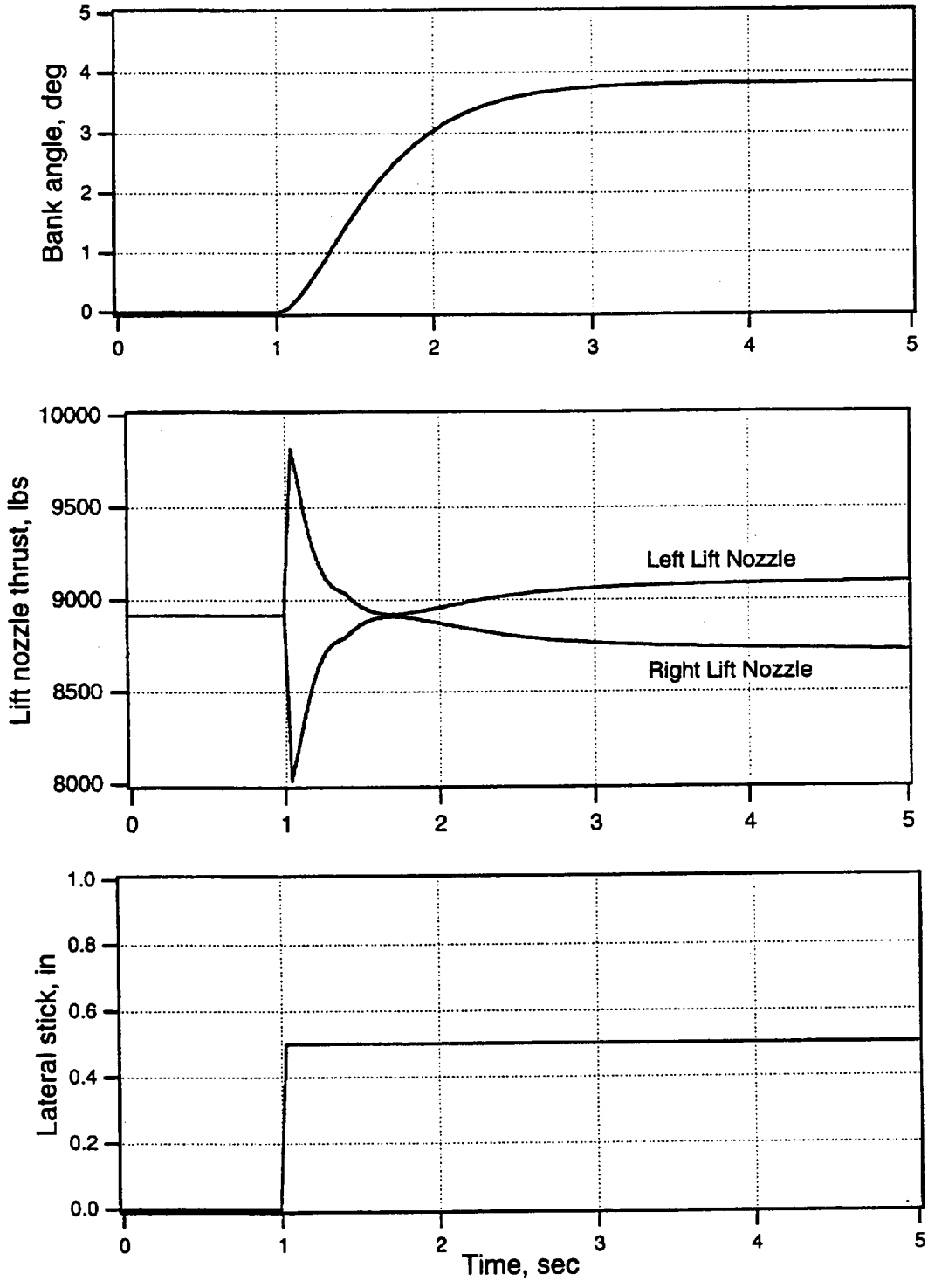

Figure 16a. Roll response to roll attitude command in hover.

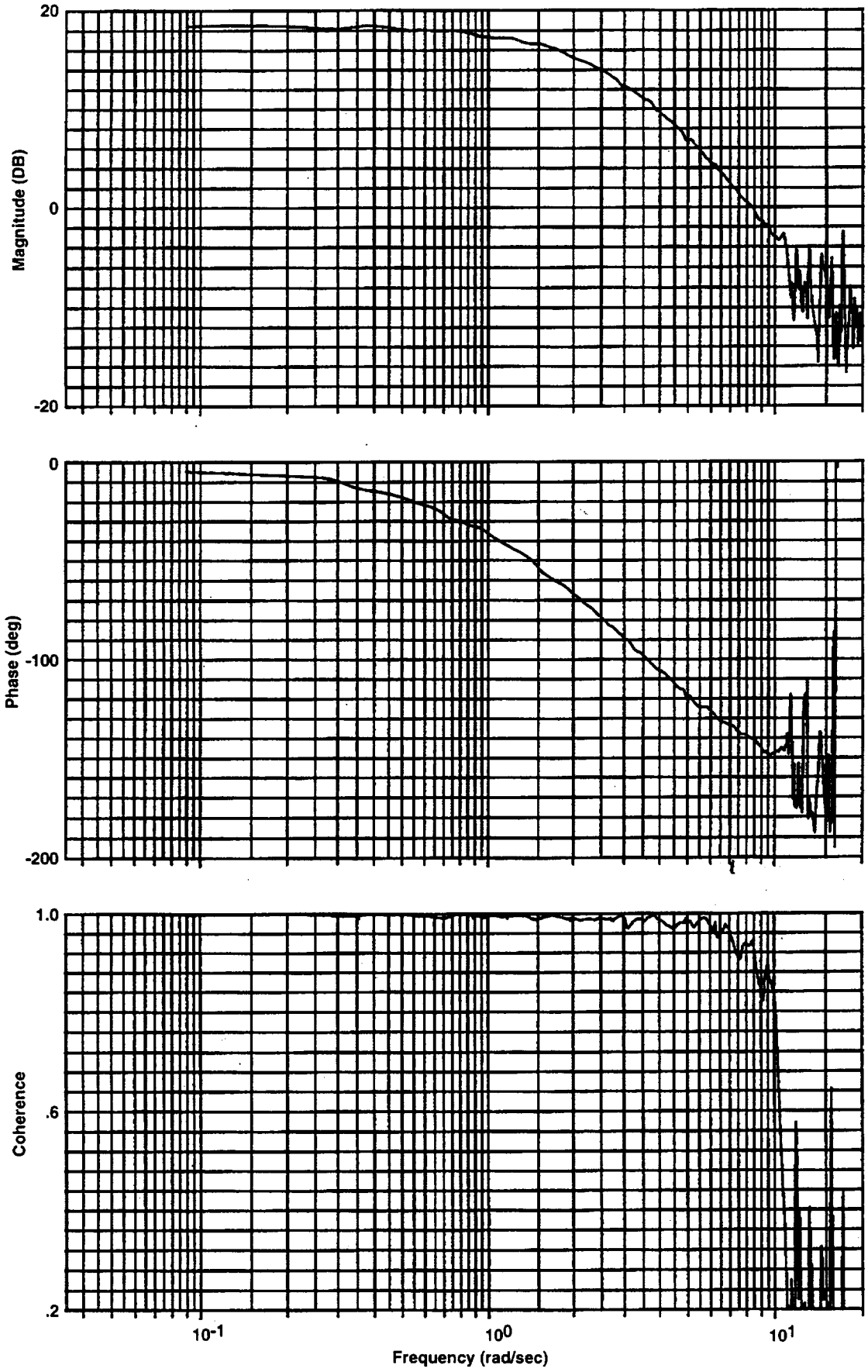

Figure 16b. Closed loop frequency response of roll attitude to roll attitude command for roll attitude command/attitude hold system in hover.

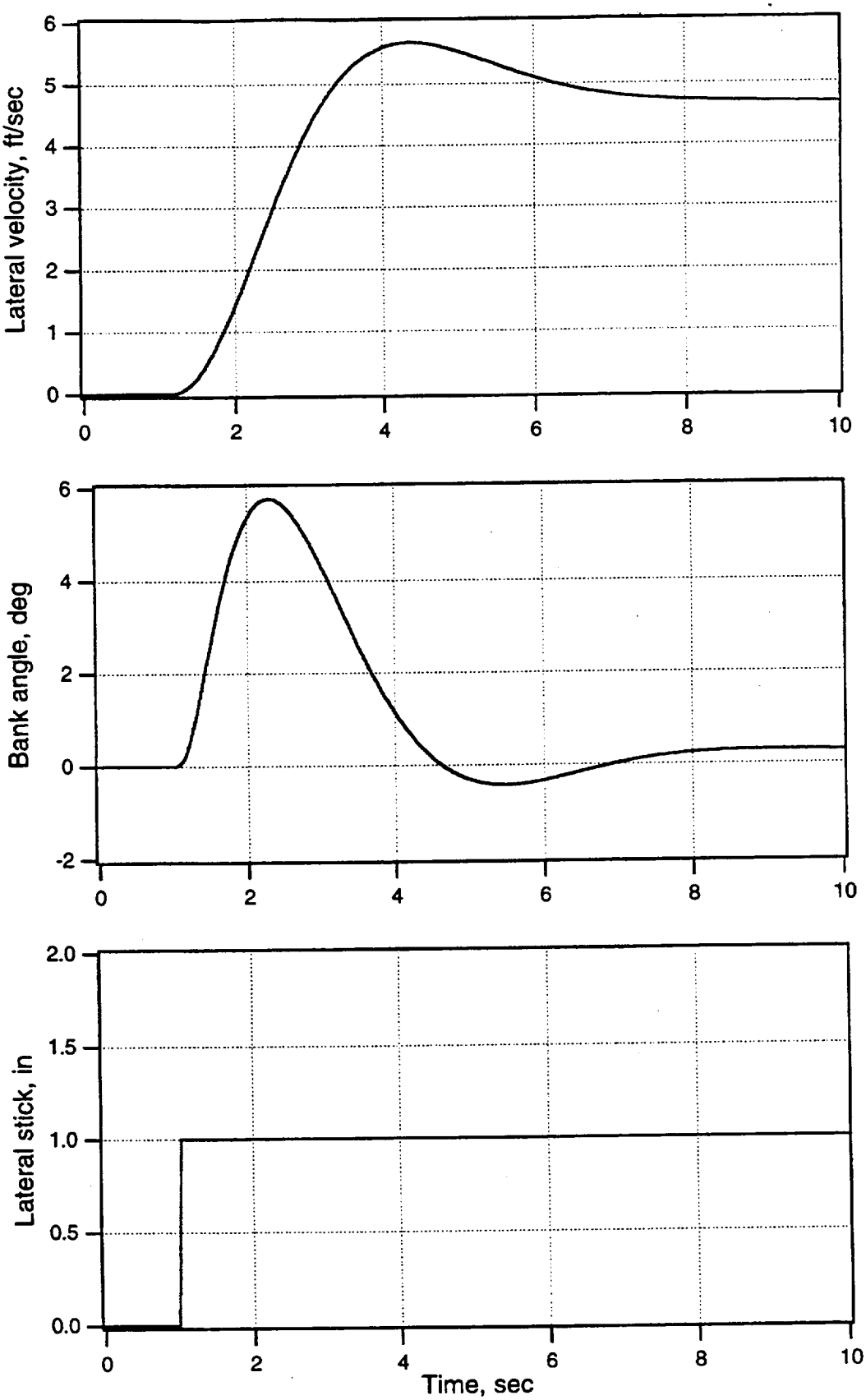

Figure 17a. Lateral velocity response to lateral velocity command in hover.

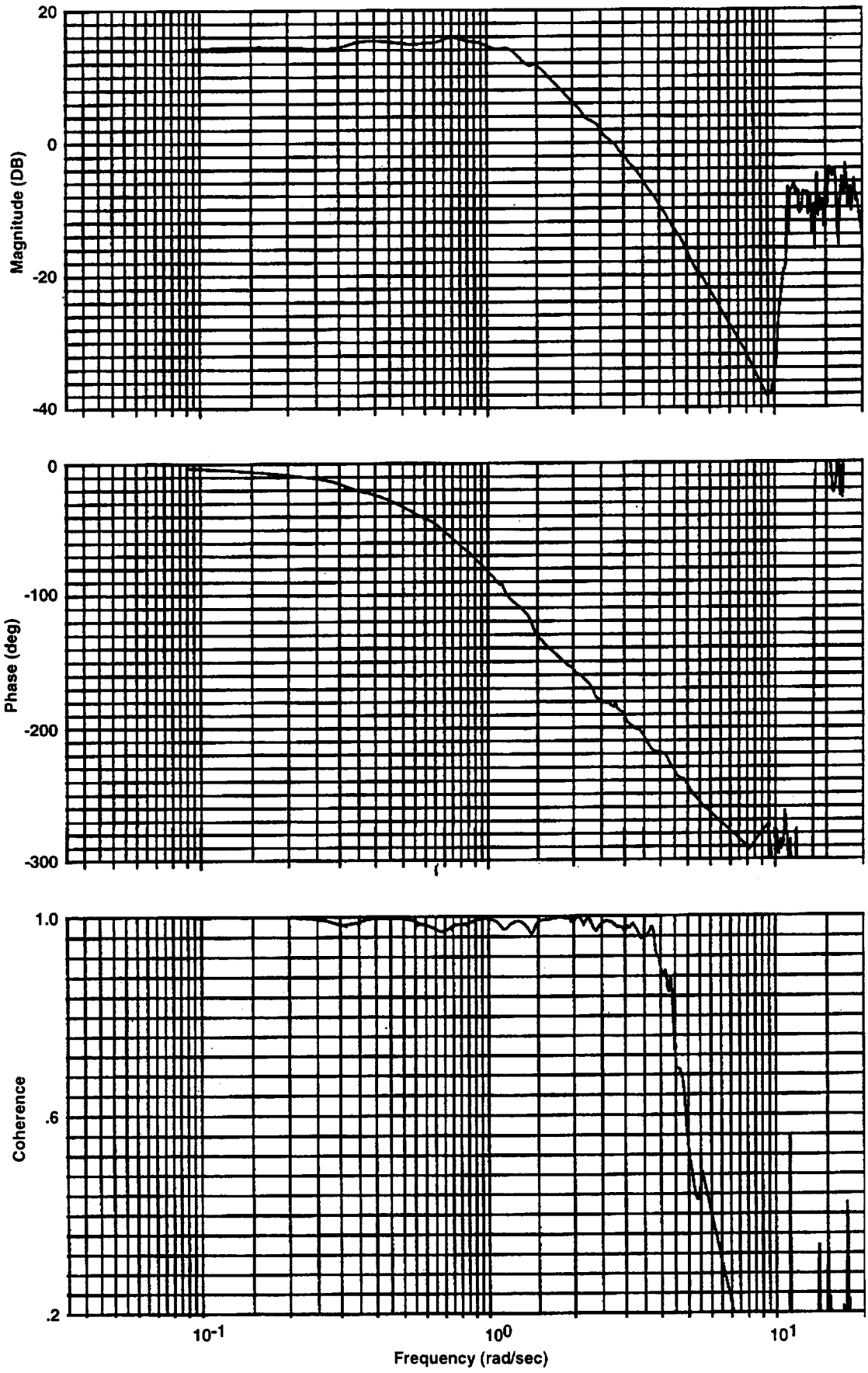

Figure 17b. Closed loop frequency response of lateral velocity to lateral velocity command for translational rate command system in hover.

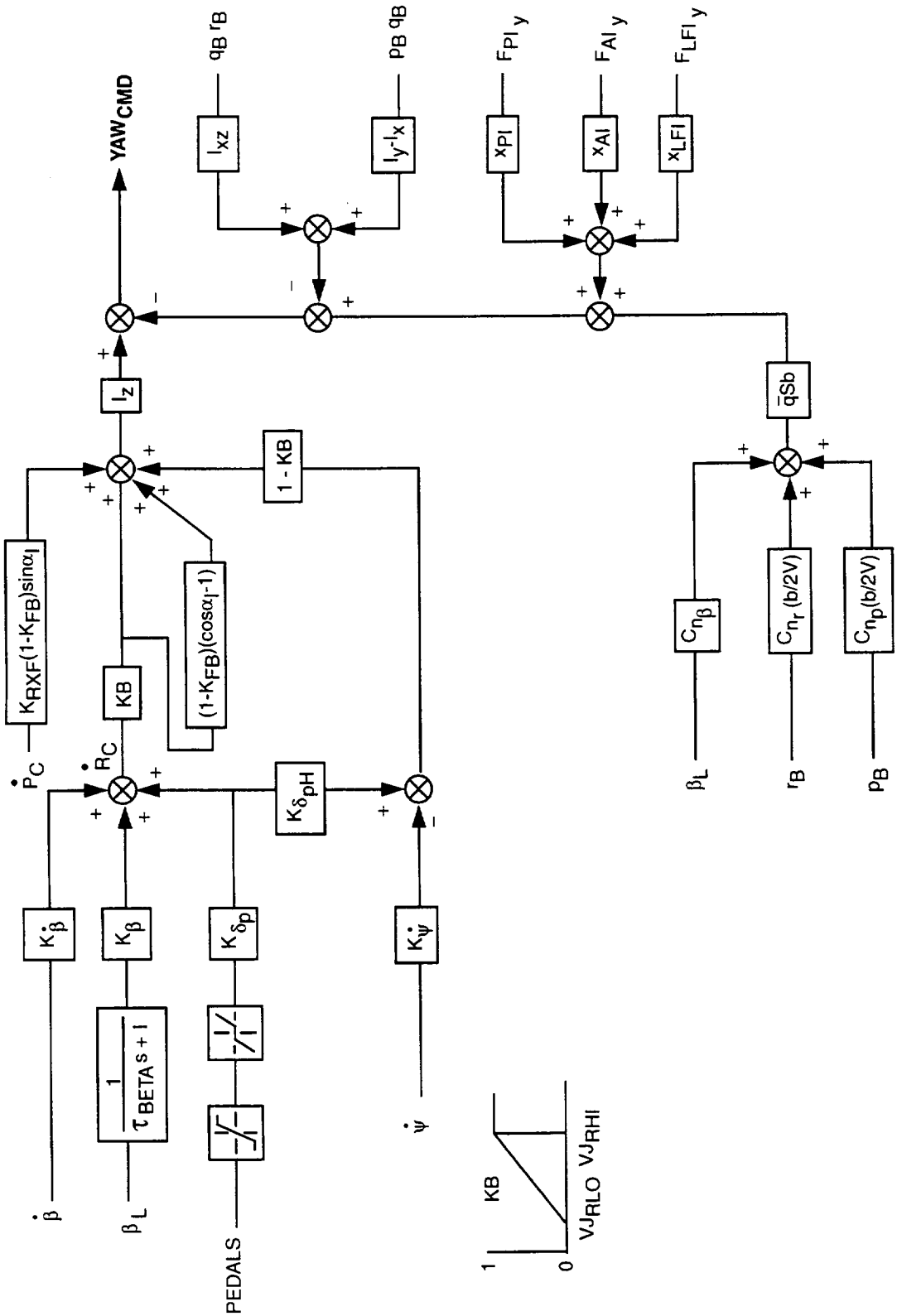

Figure 18. Yaw stabilization and command augmentation.

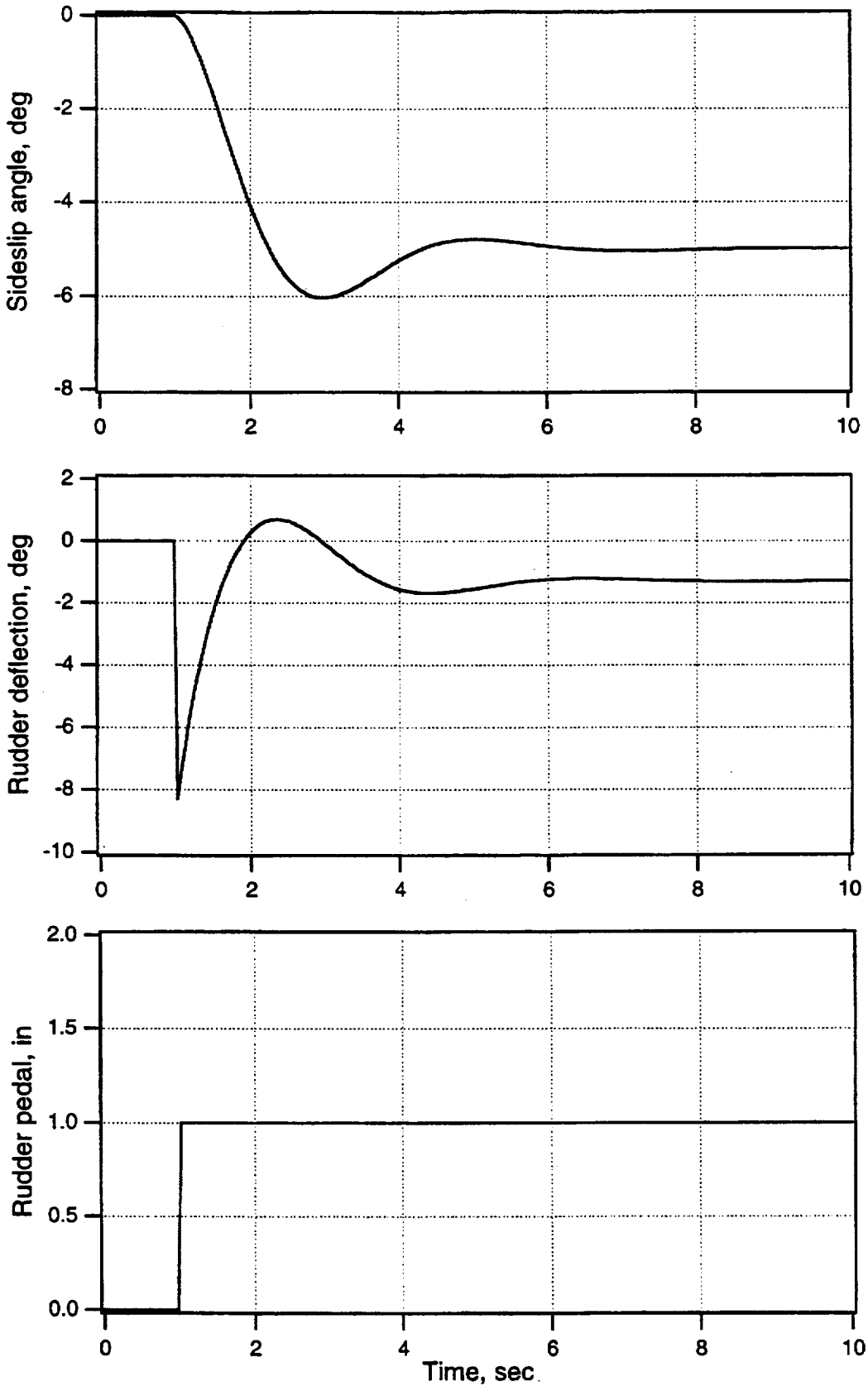

Figure 19a. Sideslip response to sideslip command at 200 knots.

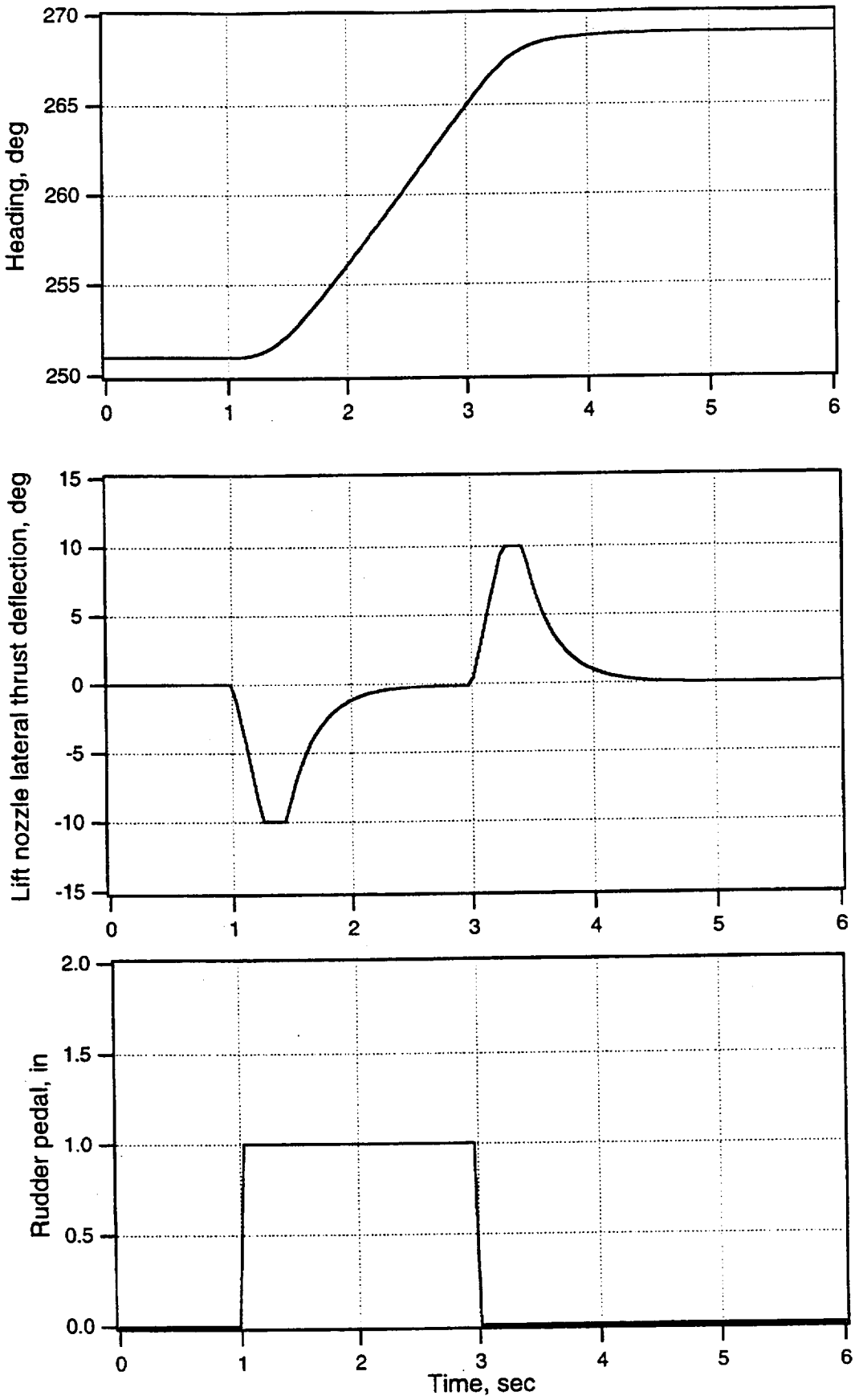

Figure 19b. Yaw response to yaw rate command in hover.

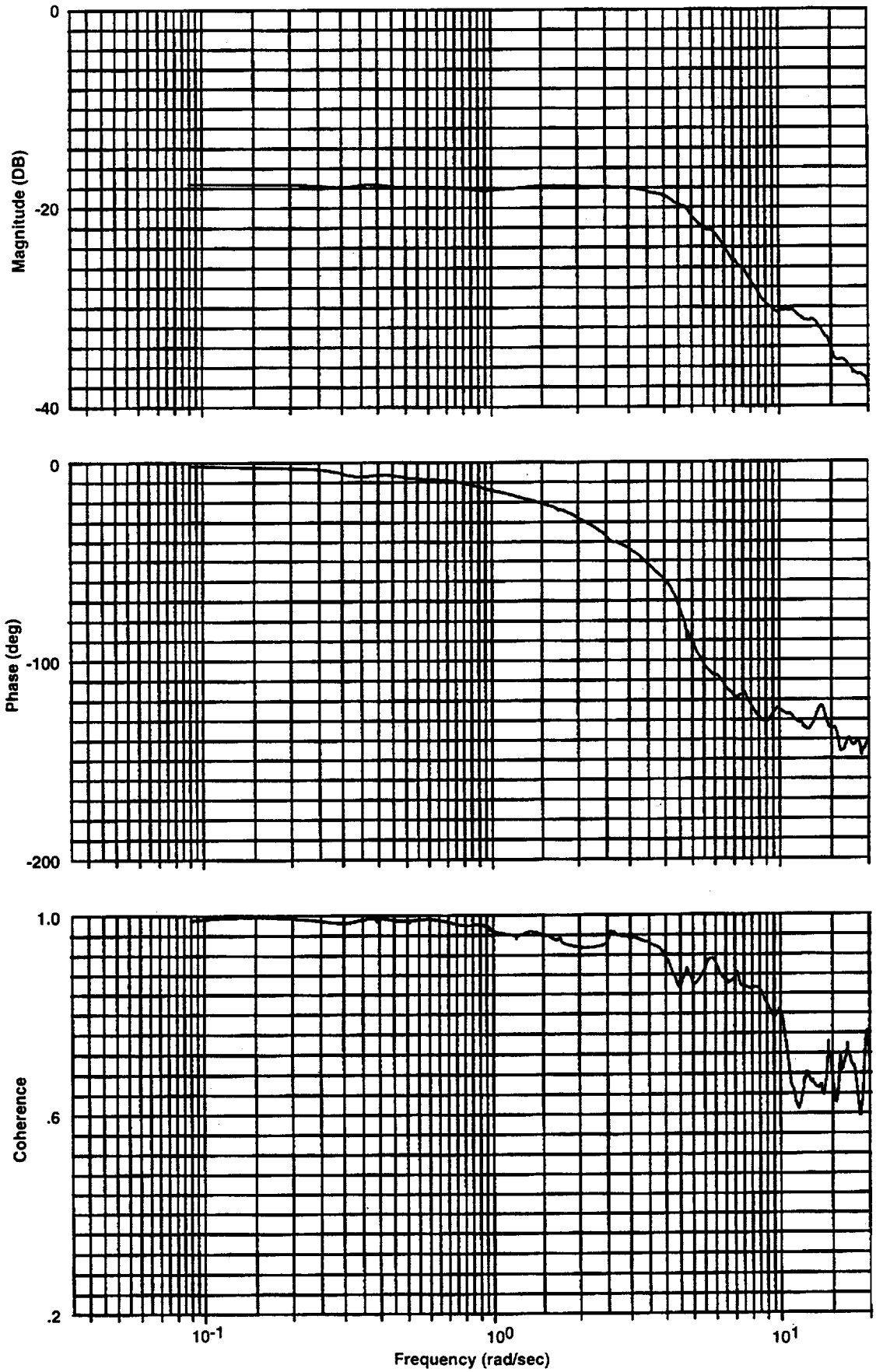

Figure 19c. Closed loop frequency response of heading rate to heading rate command for heading rate command system in hover.

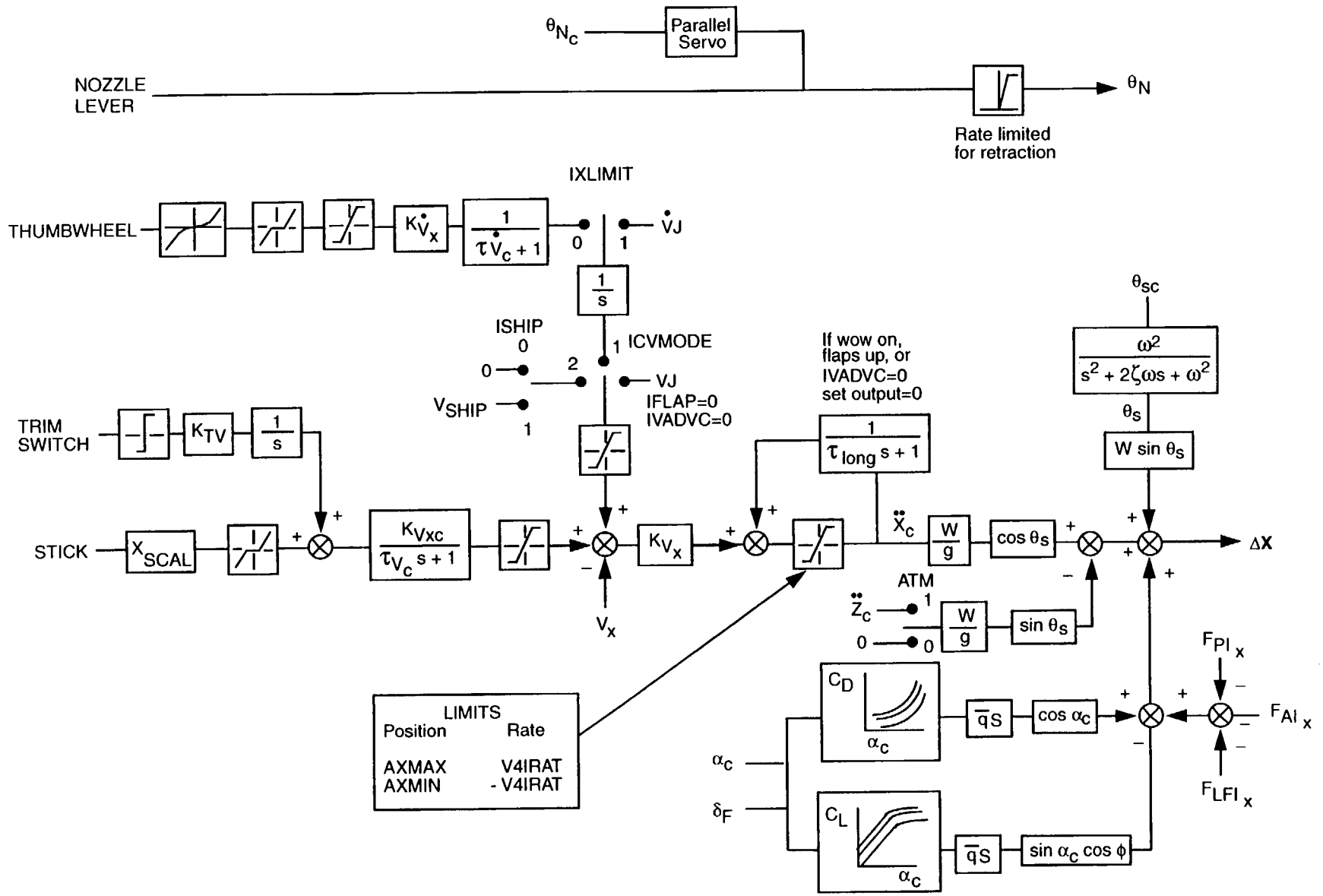

Figure 20. Longitudinal velocity stabilization and command augmentation.

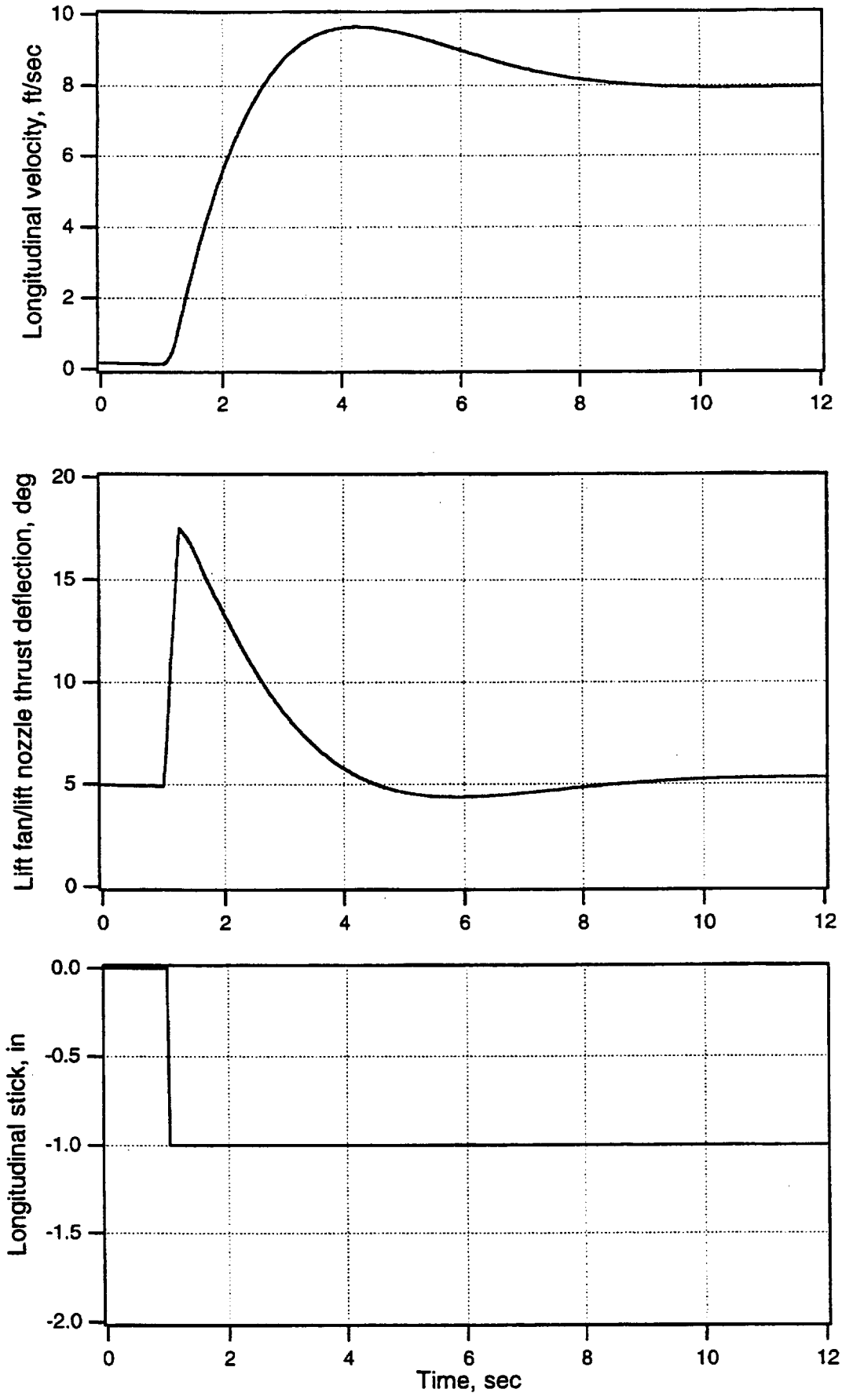

Figure 21a. Longitudinal velocity response to longitudinal velocity command in hover.

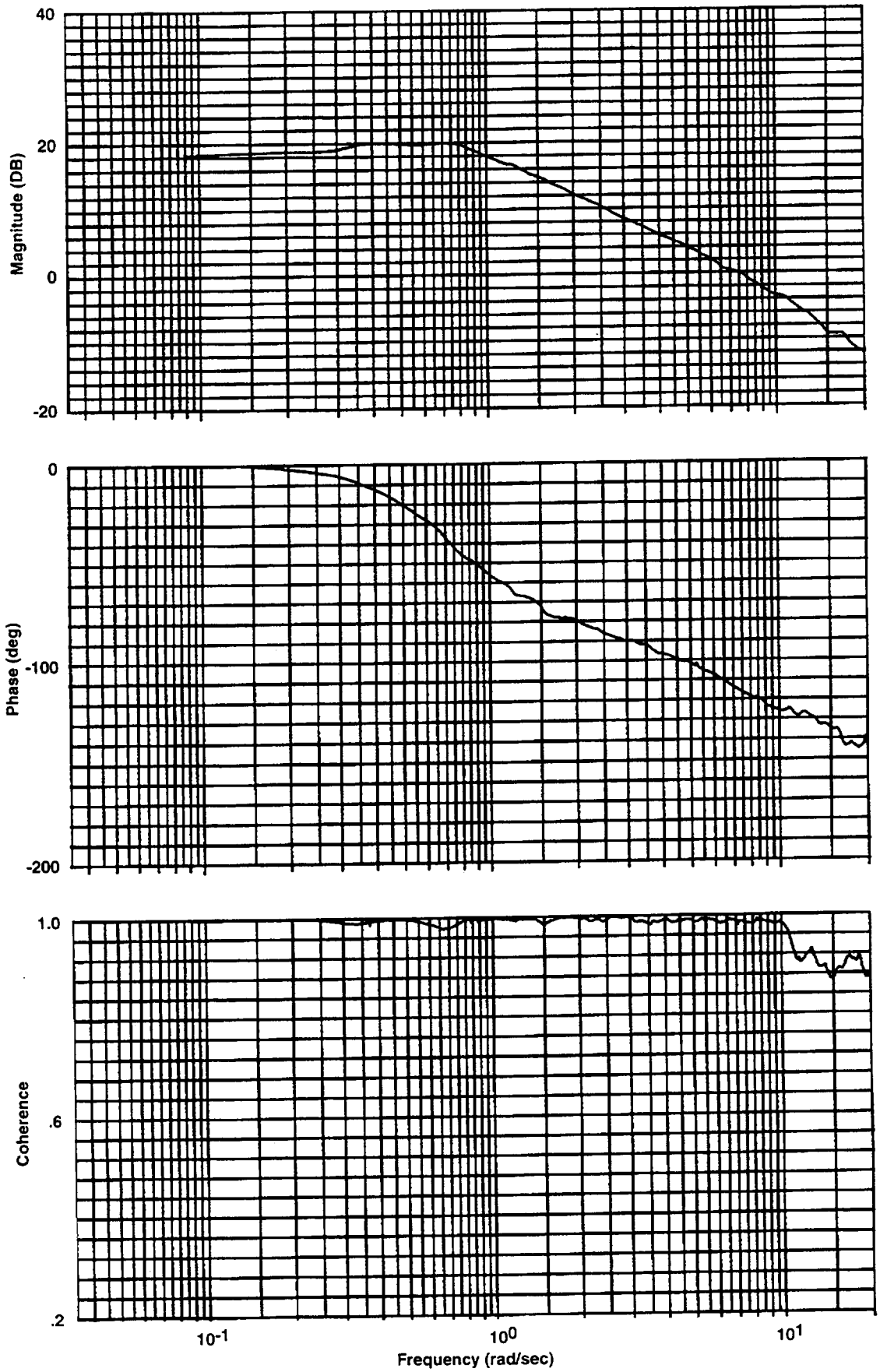

Figure 21b. Closed loop frequency response of longitudinal velocity to longitudinal velocity command for translational rate command system in hover.

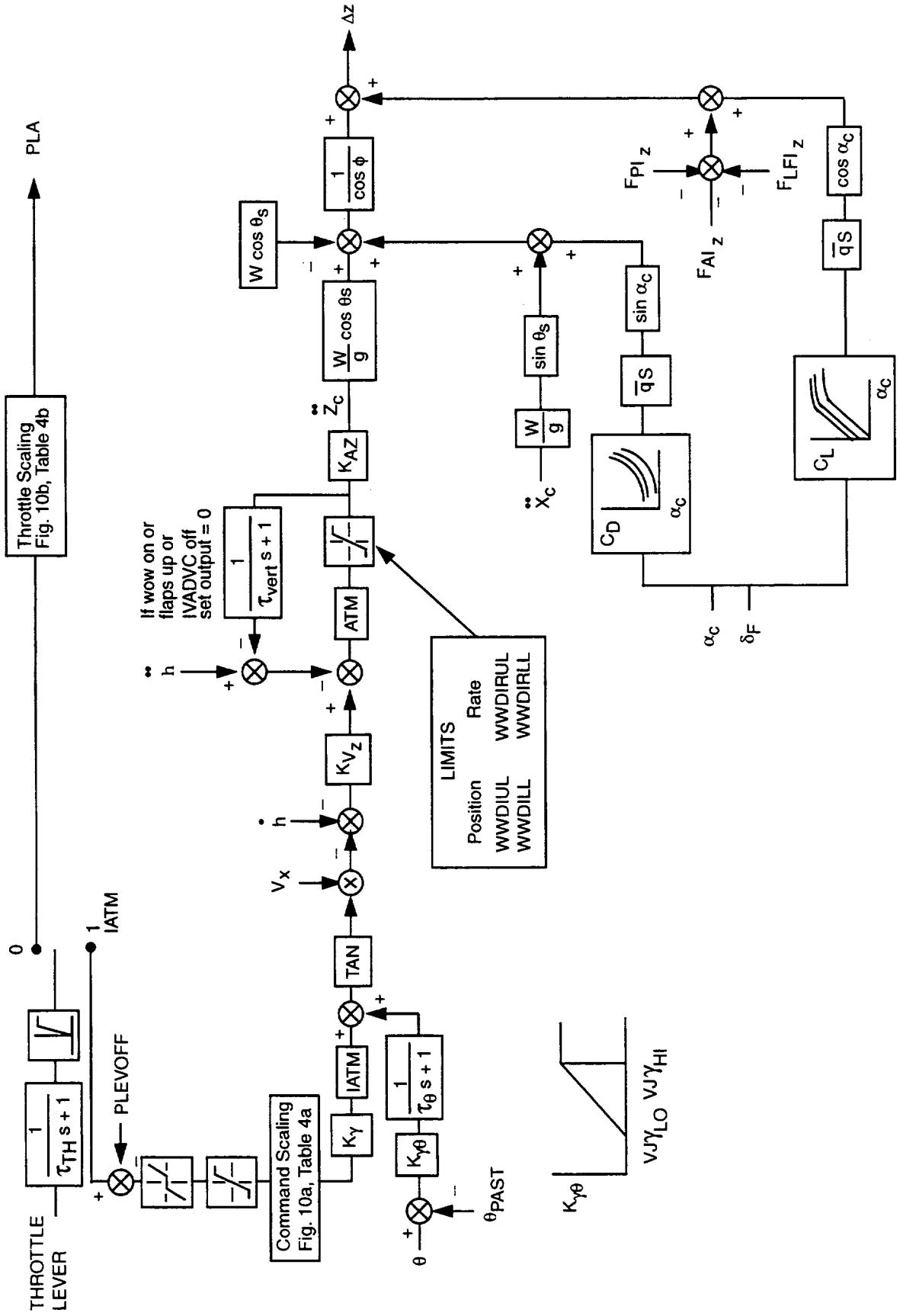

Figure 22. Vertical velocity stabilization and command augmentation.

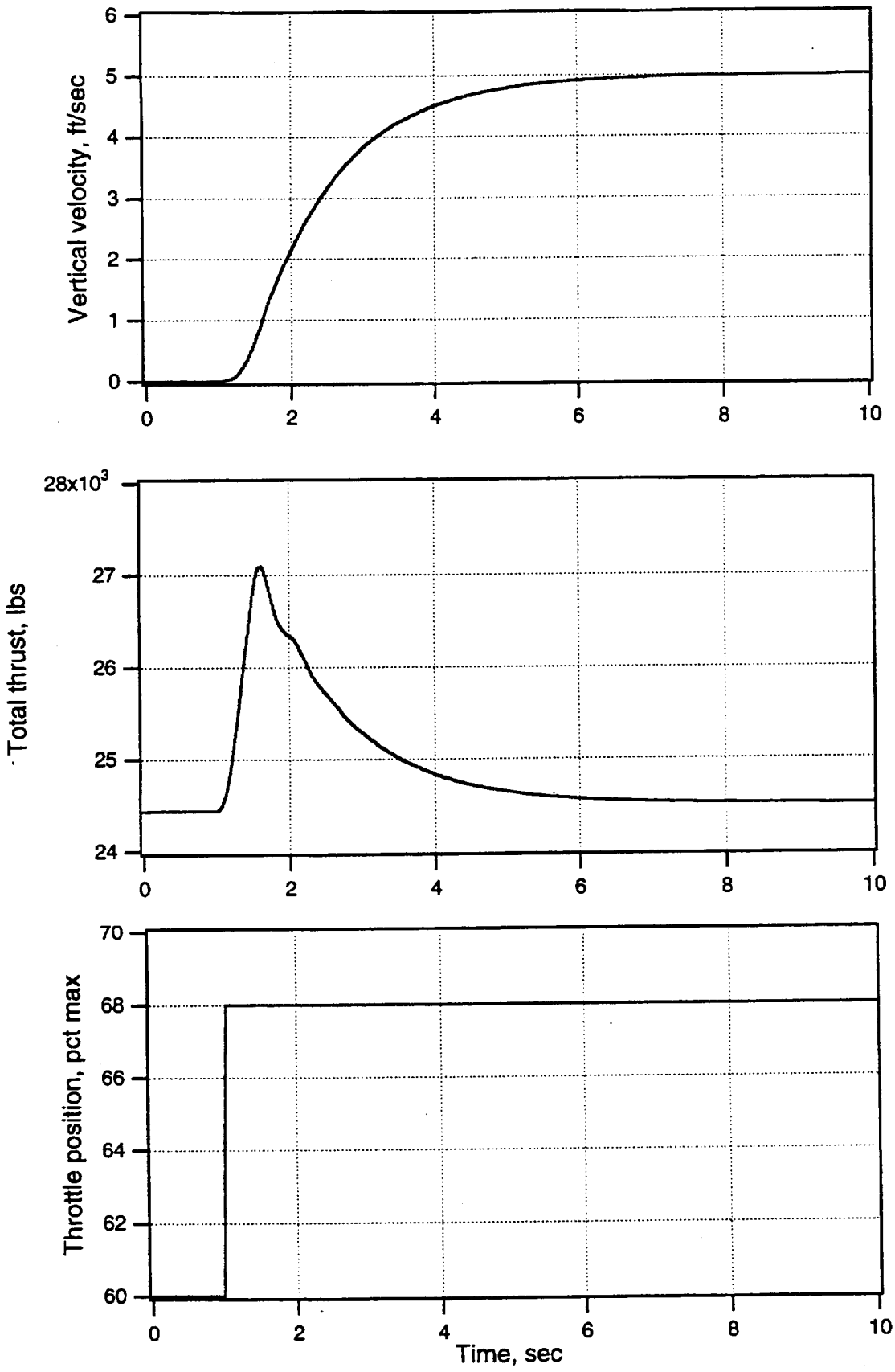

Figure 23a. Vertical velocity response to vertical velocity command in hover.

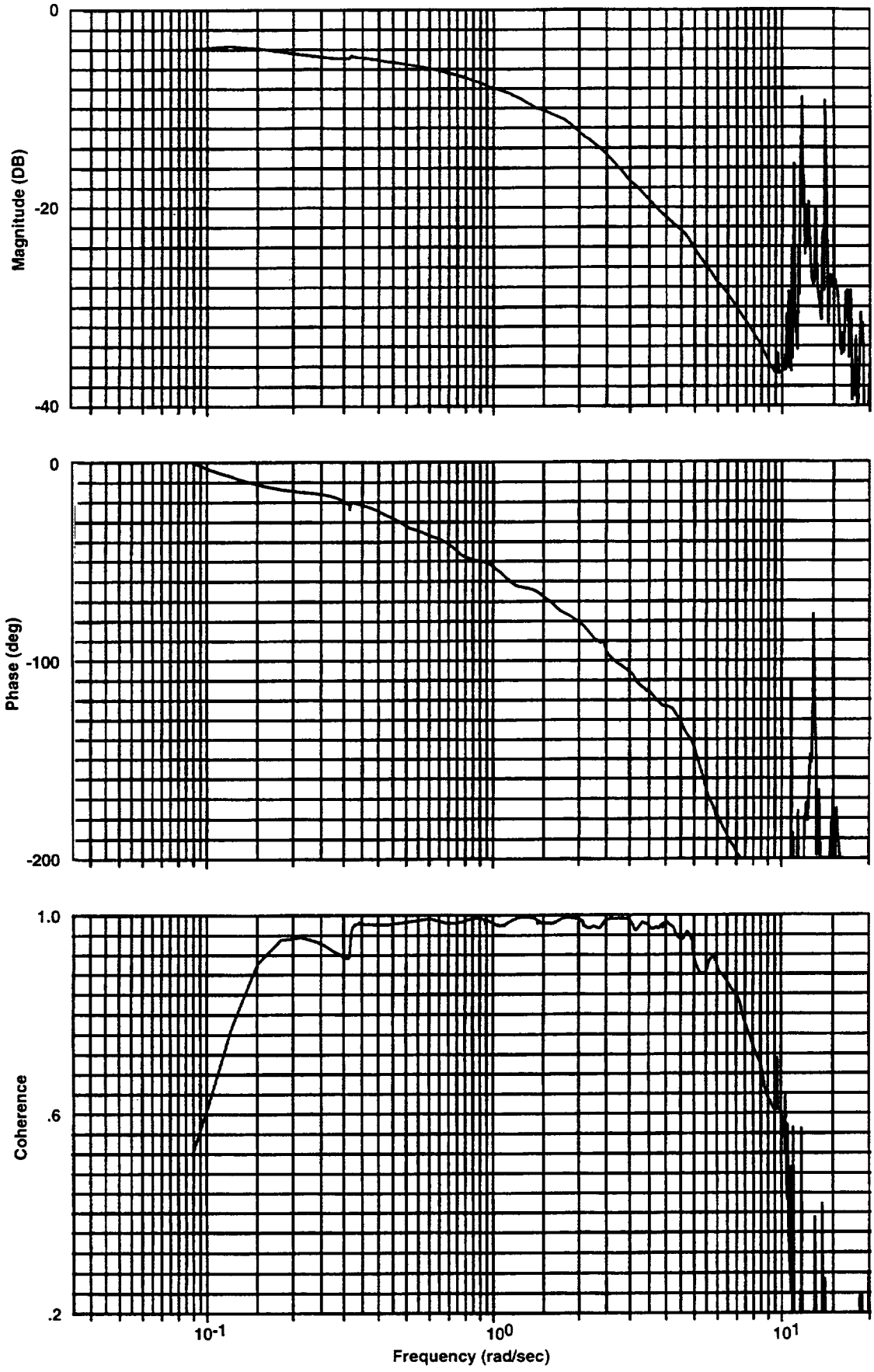

Figure 23b. Closed loop frequency response of vertical velocity to vertical velocity command for vertical velocity command system in hover.

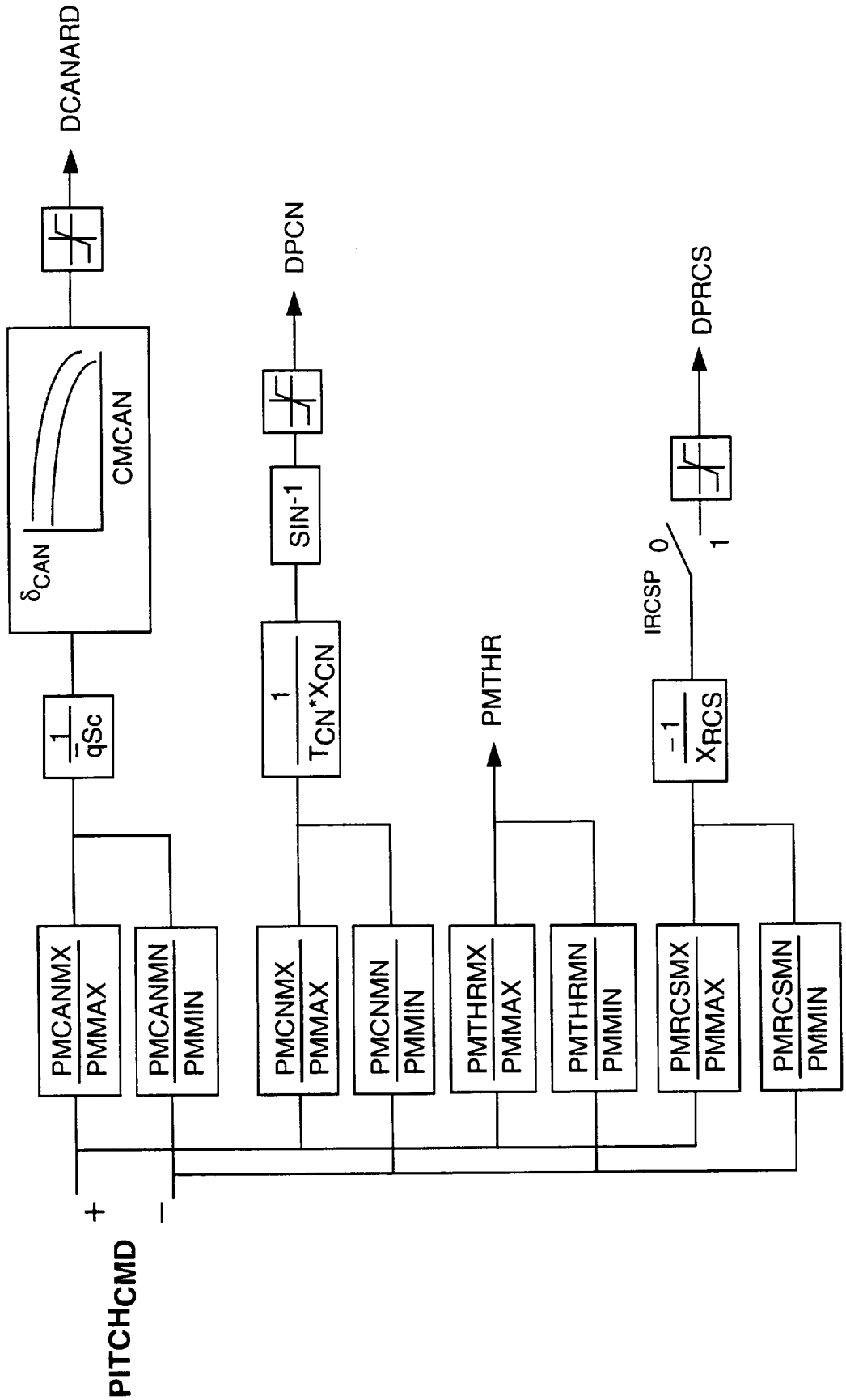

Figure 24. Pitch control selector.

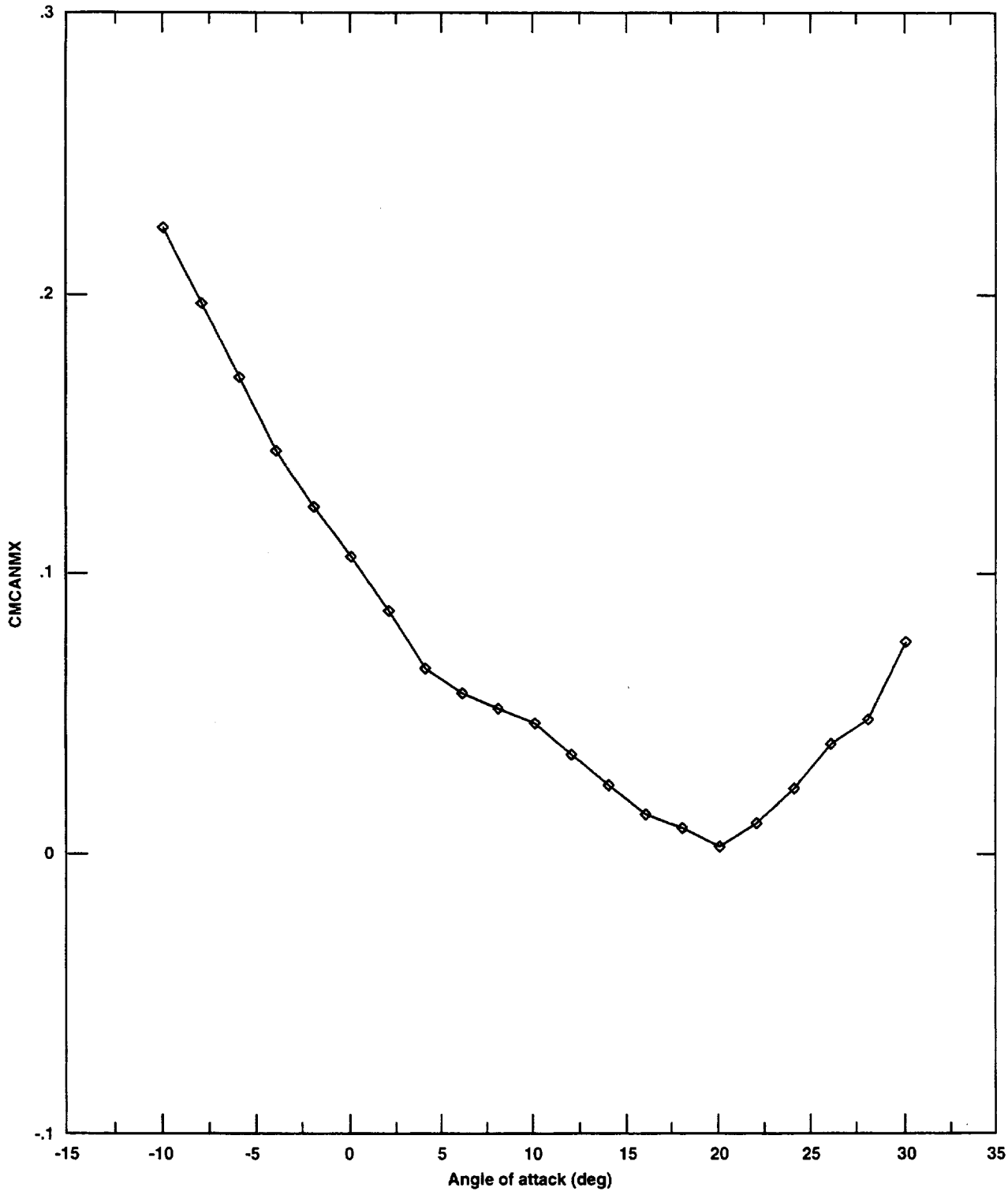

Figure 25. Maximum canard nose-up pitching moment coefficient as a function of angle of attack.

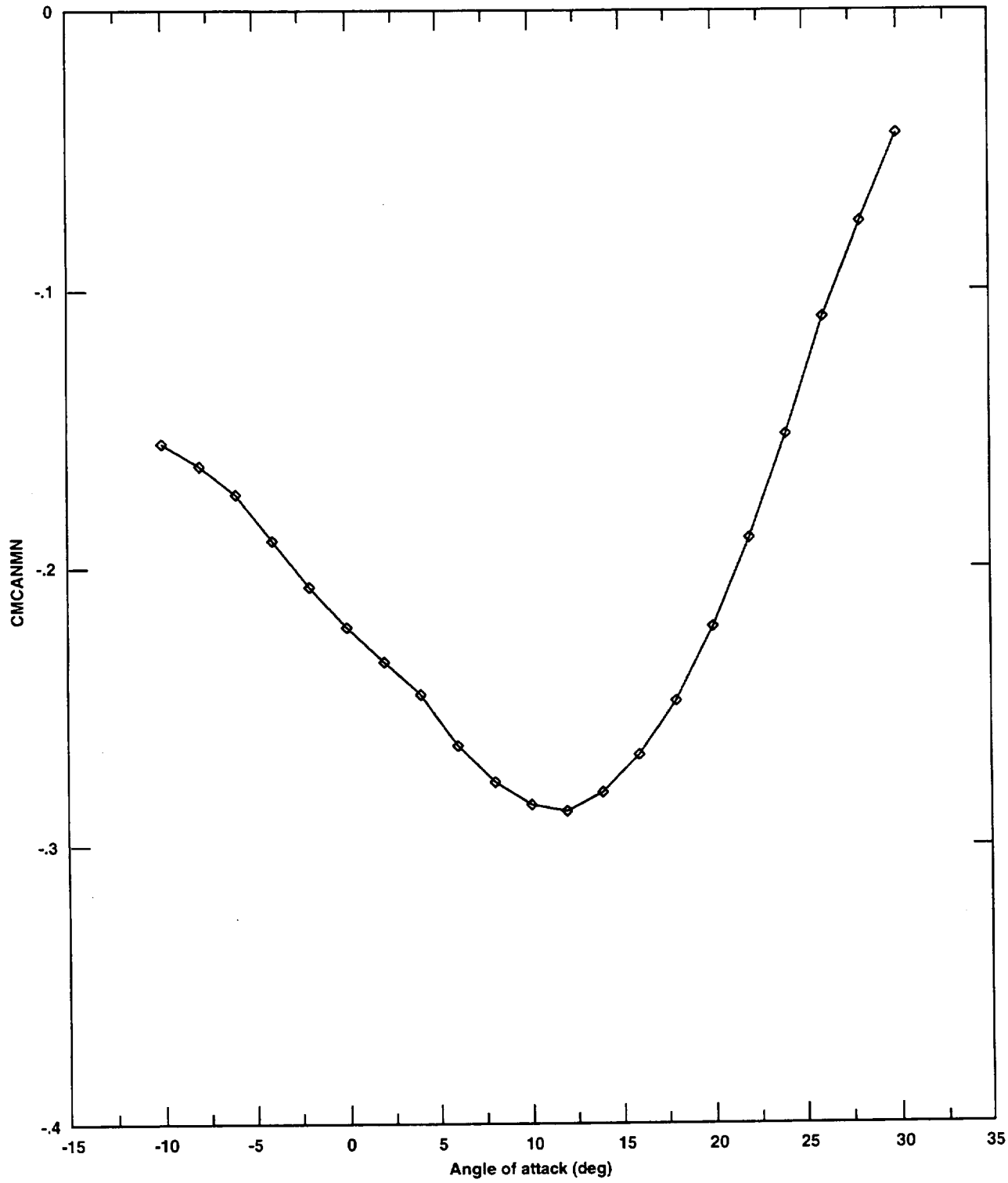

Figure 26. Maximum canard nose-down pitching moment coefficient as a function of angle of attack.

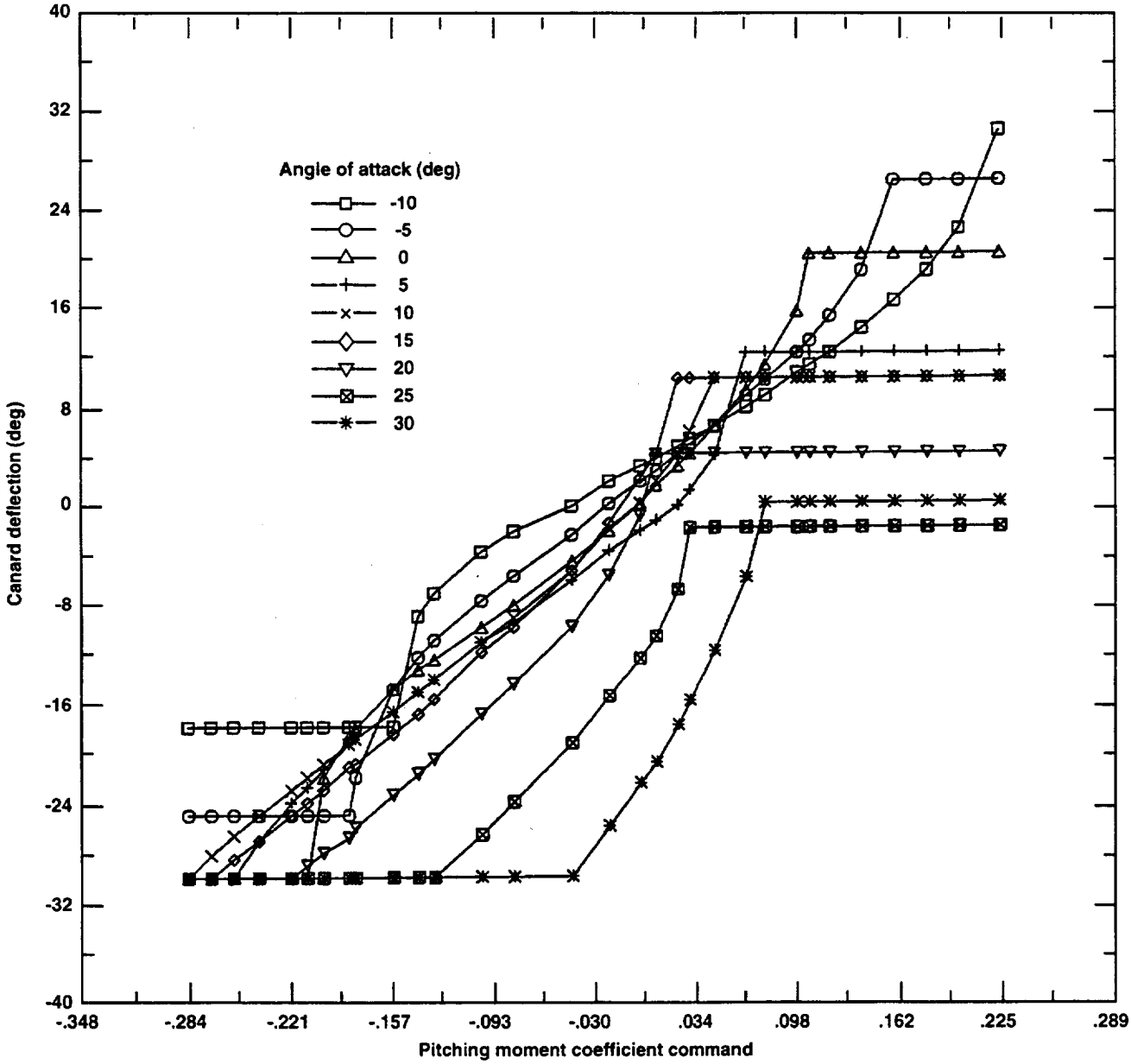

Figure 27. Inverse relationship of canard deflection to pitching moment coefficient for various angles of attack.

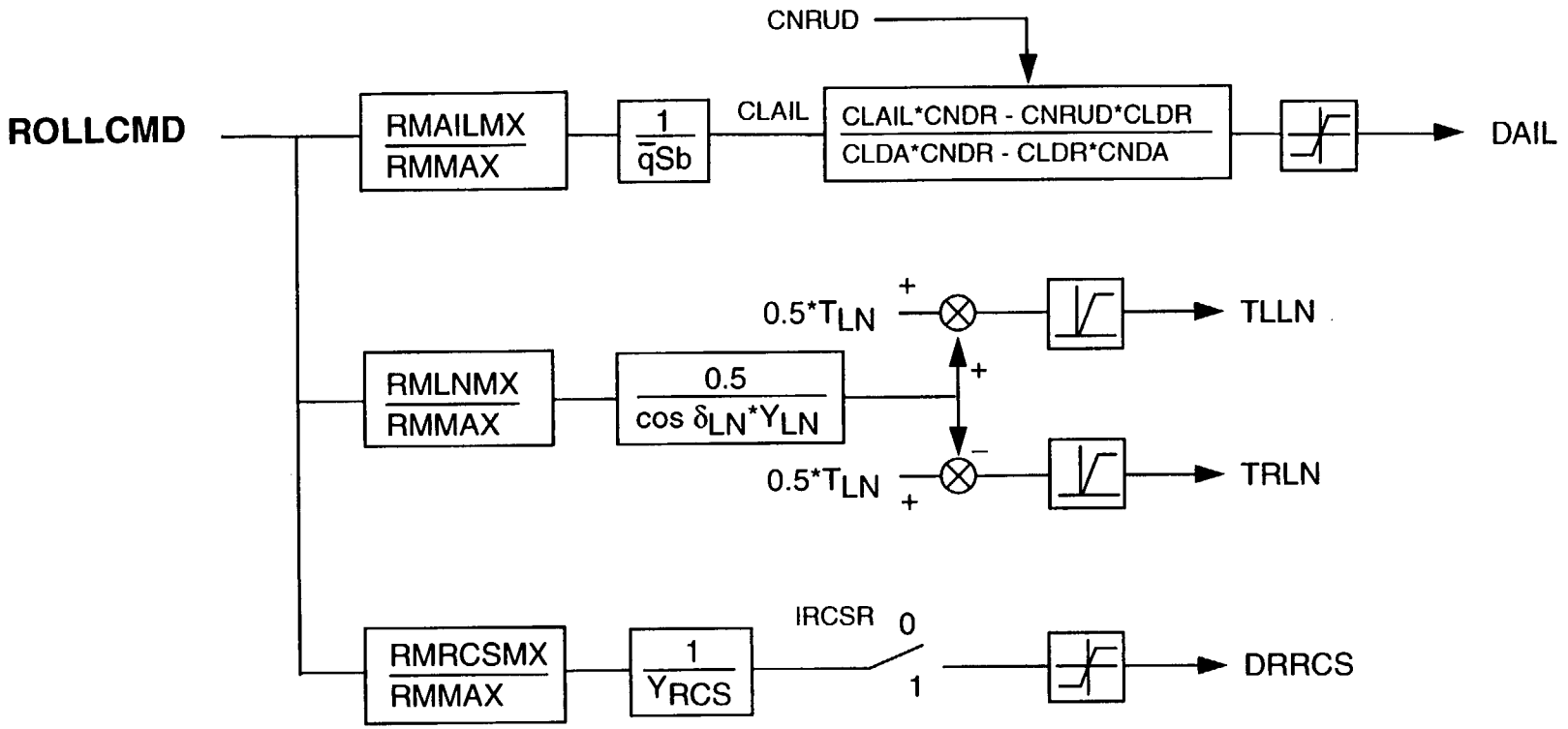

Figure 28. Roll control selector.

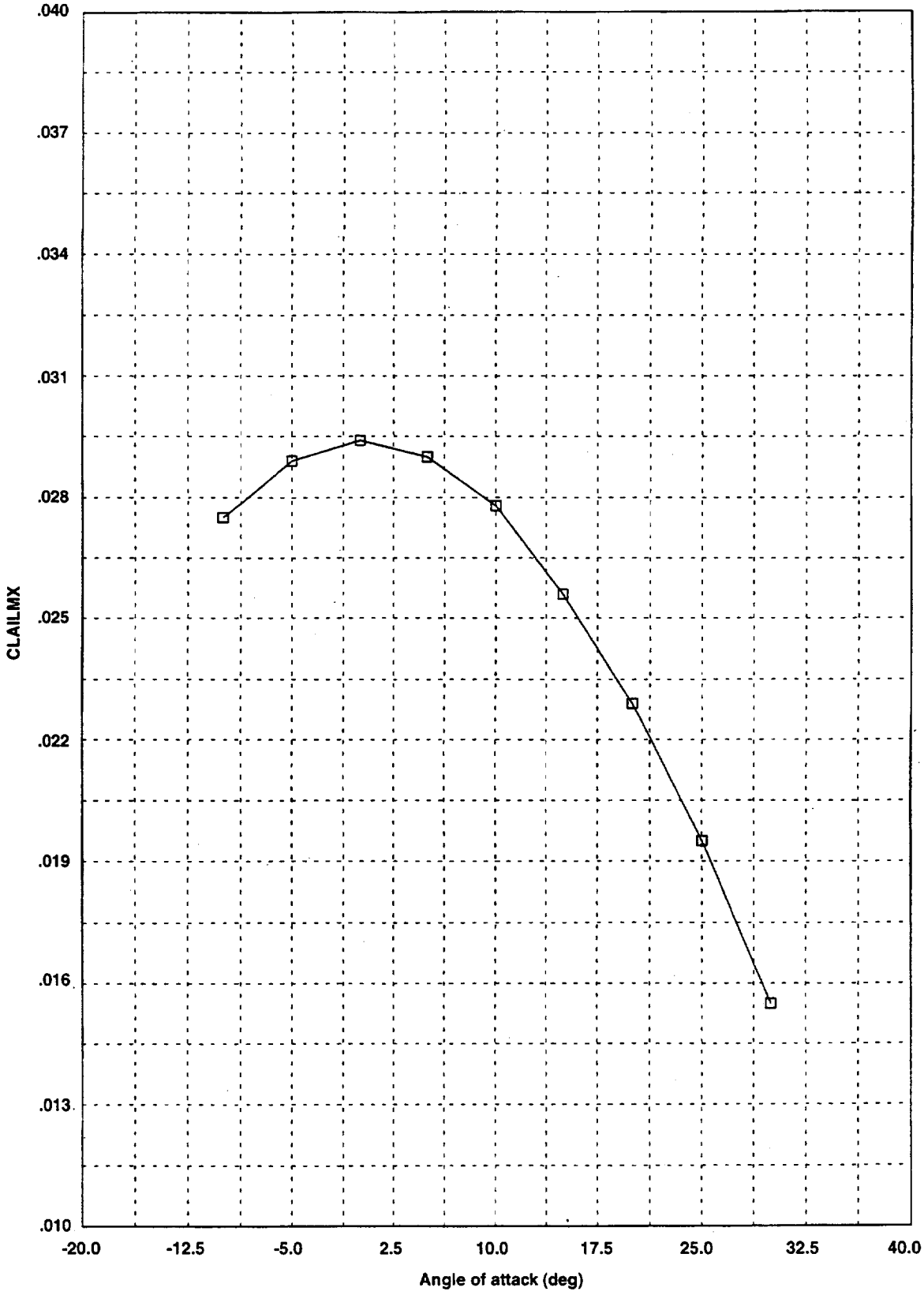

Figure 29. Maximum aileron rolling moment coefficient as a function of angle of attack.

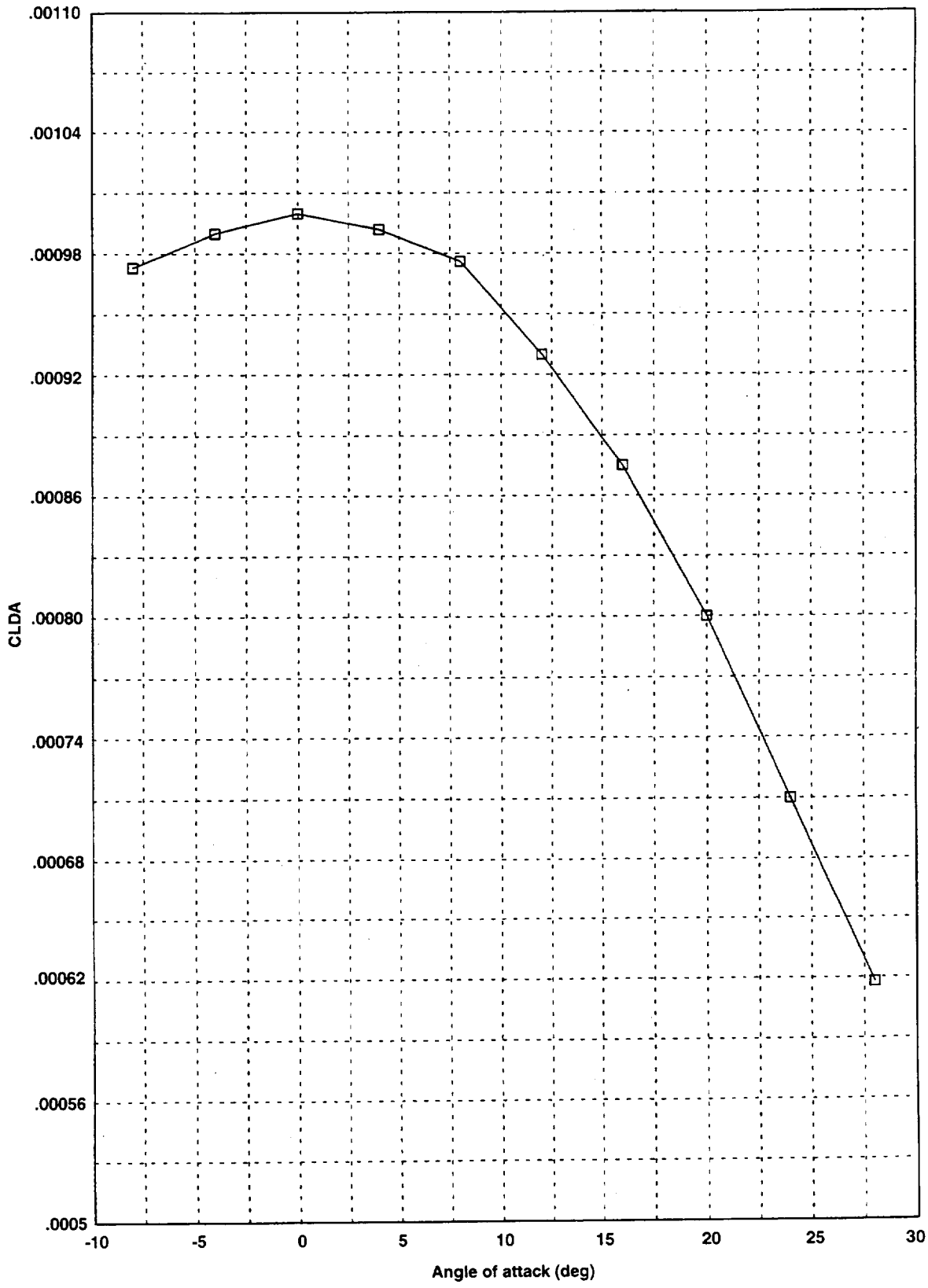

Figure 30. Derivative of rolling moment coefficient with aileron deflection as a function of angle of attack.

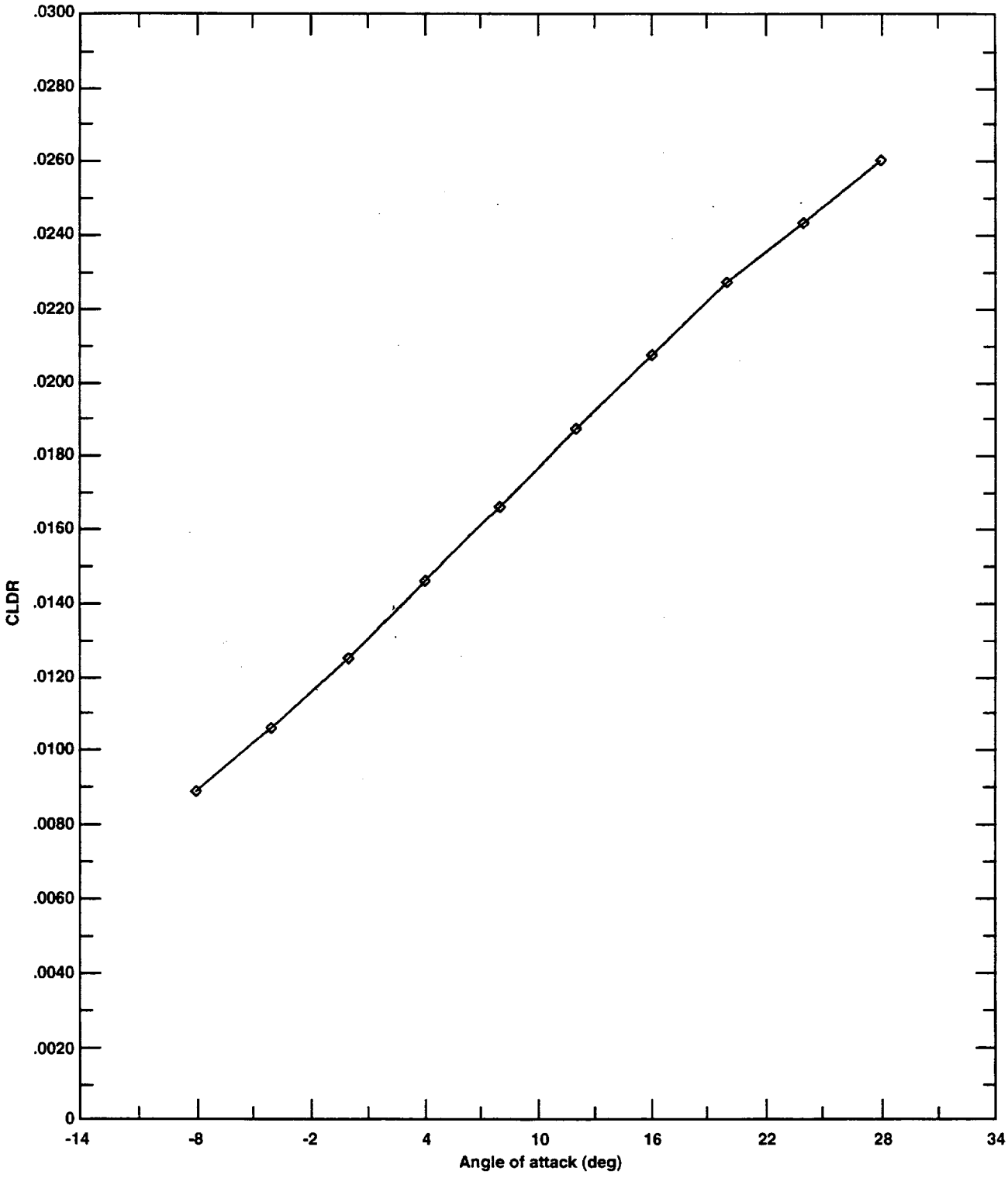

Figure 31. Derivative of rolling moment coefficient with rudder deflection as a function of angle of attack.

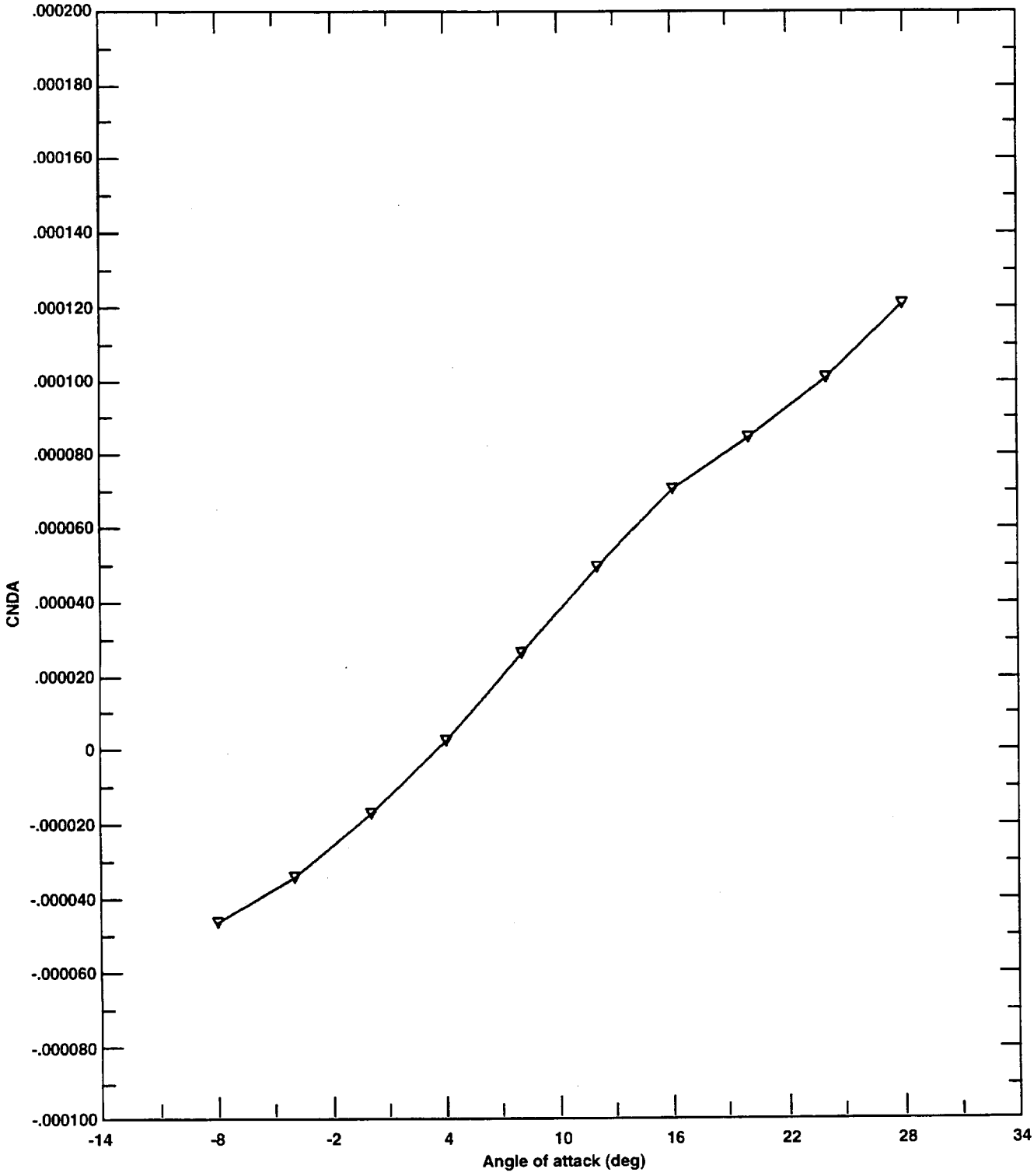

Figure 32. Derivative of yawing moment coefficient with aileron deflection as a function of angle of attack.

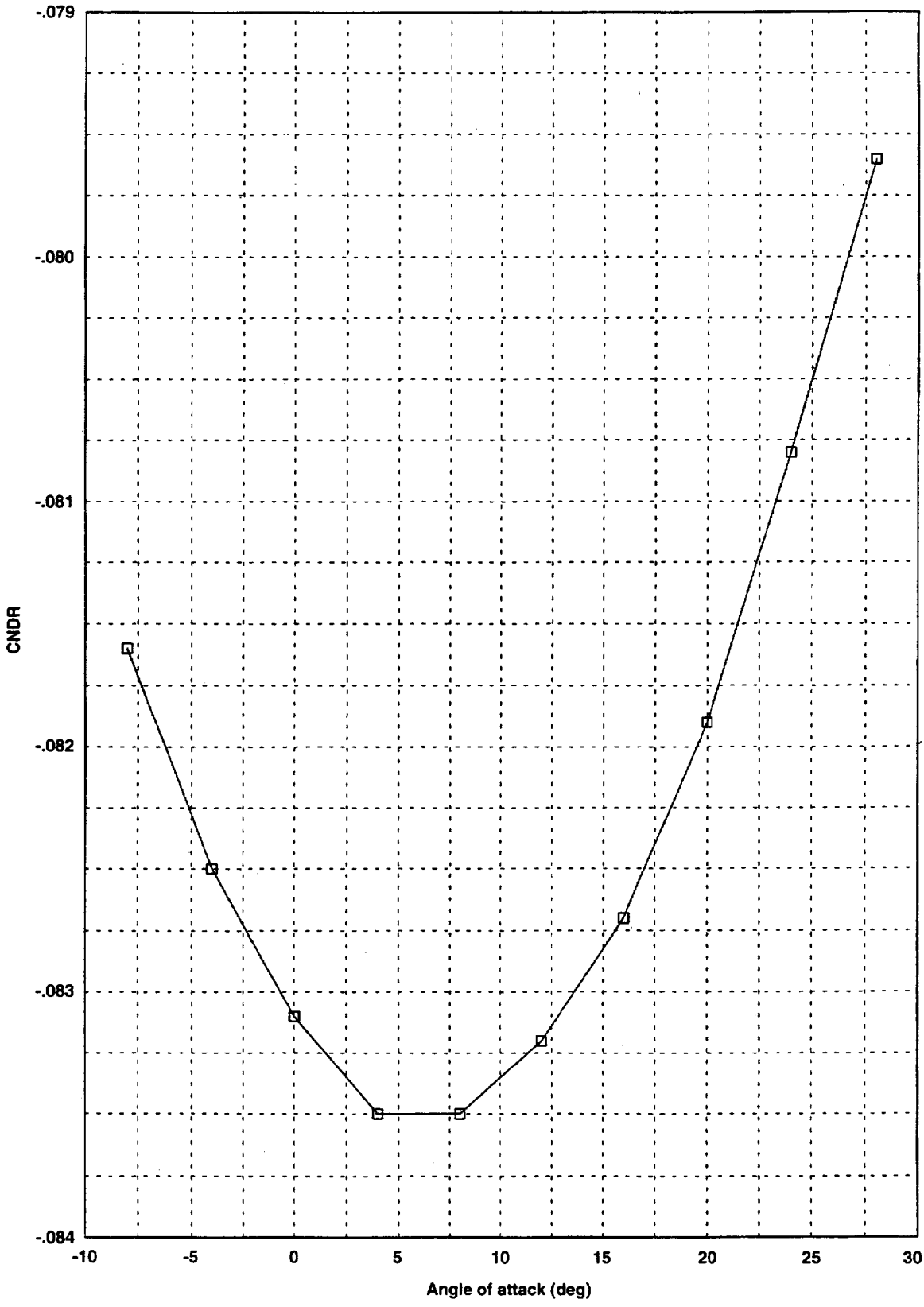

Figure 33. Derivative of yawing moment coefficient with rudder deflection as a function of angle of attack.

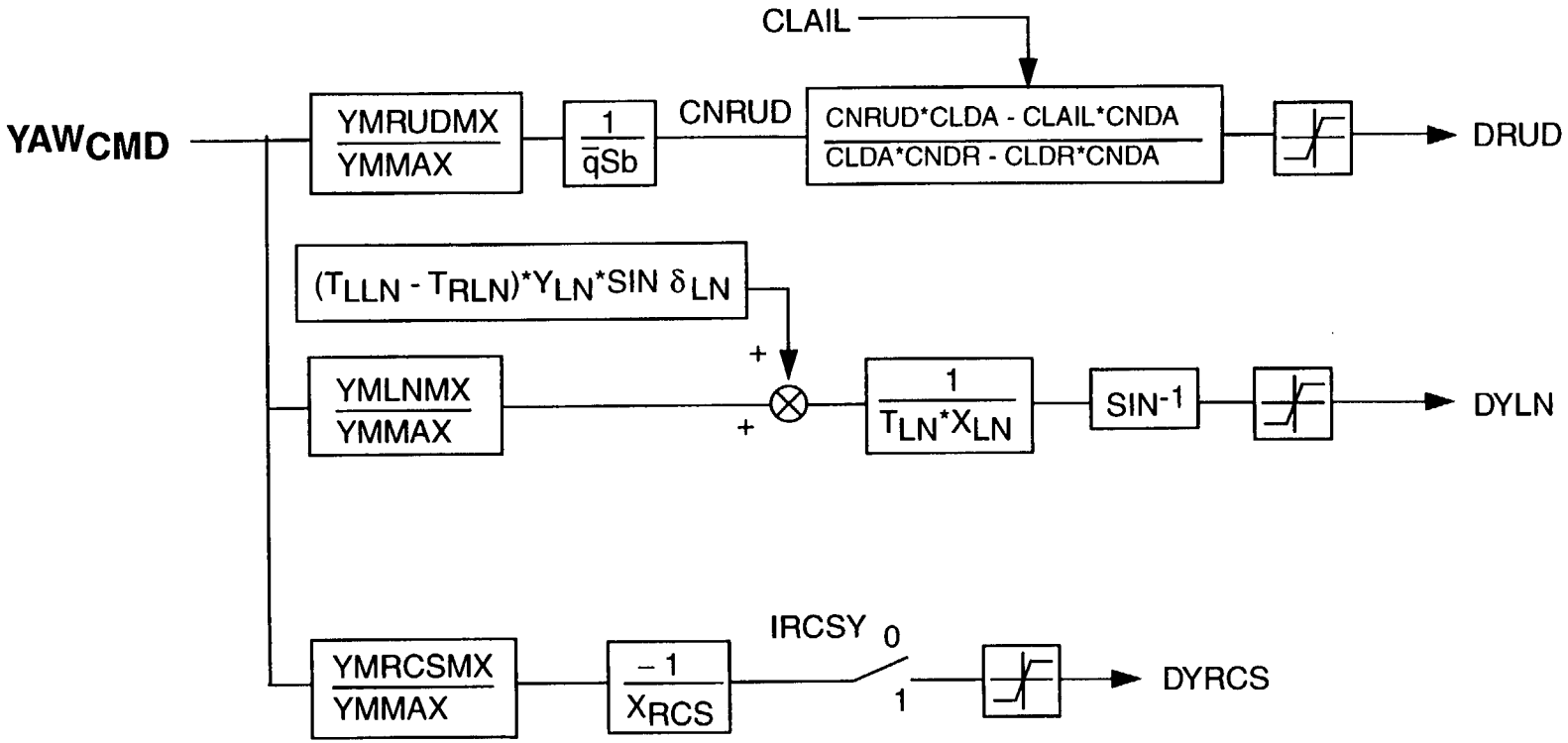

Figure 34. Yaw control selector.

REPORT DOCUMENTATION PAGE

Form Approved
OMB No. 0704-0188

1. AGENCY USE ONLY *(Leave blank)*	2. REPORT DATE	3. REPORT TYPE AND DATES COVERED
	October 1997	Technical Memorandum

4. TITLE AND SUBTITLE

Revised Simulation Model of the Control System, Displays, and Propulsion System for an ASTOVL Lift Fan Aircraft

5. FUNDING NUMBERS

581-50-22

6. AUTHOR(S)

James A. Franklin

7. PERFORMING ORGANIZATION NAME(S) AND ADDRESS(ES)

Ames Research Center
Moffett Field, CA 94035-1000

8. PERFORMING ORGANIZATION REPORT NUMBER

A-977189

9. SPONSORING/MONITORING AGENCY NAME(S) AND ADDRESS(ES)

National Aeronautics and Space Administration
Washington, DC 20546-0001

10. SPONSORING/MONITORING AGENCY REPORT NUMBER

NASA TM-102208

11. SUPPLEMENTARY NOTES

Point of Contact: James A. Franklin, Ames Research Center, MS 211-2, Moffett Field, CA 94035-1000
(650) 604-6004

12a. DISTRIBUTION/AVAILABILITY STATEMENT

Unclassified — Unlimited
Subject Category 08

12b. DISTRIBUTION CODE

13. ABSTRACT ***(Maximum 200 words)***

This report describes revisions to a simulation model that was developed for use in piloted evaluations of takeoff, transition, hover, and landing characteristics of an advanced short takeoff and vertical landing lift fan fighter aircraft. These revisions have been made to the flight/propulsion control system, head-up display, and propulsion system to reflect recent flight and simulation experience with short takeoff and vertical landing operations. They include nonlinear inverse control laws in all axes (eliminating earlier versions with state rate feedback), throttle scaling laws for flightpath and thrust command, control selector commands apportioned based on relative effectiveness of the individual controls, lateral guidance algorithms that provide more flexibility for terminal area operations, and a simpler representation of the propulsion system.

The model includes modes tailored to the phases of the aircraft's operation, with several response types which are coupled to the aircraft's aerodynamic and propulsion system effectors through a control selector tailored to the propulsion system. Head-up display modes for approach and hover are integrated with the corresponding control modes. Propulsion system components modeled include a remote lift fan and a lift-cruise engine. Their static performance and dynamic responses are represented by the model. A separate report describes the subsonic, power-off aerodynamics and jet induced aerodynamics in hover and forward flight, including ground effects.

14. SUBJECT TERMS	15. NUMBER OF PAGES
STOVL, Integrated flight/propulsion controls, Simulation	63
	16. PRICE CODE: A04

17. SECURITY CLASSIFICATION OF REPORT	18. SECURITY CLASSIFICATION OF THIS PAGE	19. SECURITY CLASSIFICATION OF ABSTRACT	20. LIMITATION OF ABSTRACT
Unclassified	Unclassified		